110
9/19/88 JS(6)

DR#0562-2

DOE/MC/21179-2564
(DE88001063)

Energy

FOSSIL

Rock Matrix and Fracture Analysis of Flow in Western Tight Gas Sands

Annual Report
Phase III

V. Dandge
M. Graham
B. Gonzales
D. Coker

December 1987

Work Performed Under Contract No.: DE-AC21-84MC21179

For
U.S. Department of Energy
Office of Fossil Energy
Morgantown Energy Technology Center
Morgantown, West Virginia

By
New Mexico Petroleum Recovery Research Center
New Mexico Institute of Mining and Technology
Socorro, New Mexico

DISCLAIMER

This report was prepared as an account of work sponsored by an agency of the United States Government. Neither the United States Government nor any agency Thereof, nor any of their employees, makes any warranty, express or implied, or assumes any legal liability or responsibility for the accuracy, completeness, or usefulness of any information, apparatus, product, or process disclosed, or represents that its use would not infringe privately owned rights. Reference herein to any specific commercial product, process, or service by trade name, trademark, manufacturer, or otherwise does not necessarily constitute or imply its endorsement, recommendation, or favoring by the United States Government or any agency thereof. The views and opinions of authors expressed herein do not necessarily state or reflect those of the United States Government or any agency thereof.

DISCLAIMER

Portions of this document may be illegible in electronic image products. Images are produced from the best available original document.

DISCLAIMER

This report was prepared as an account of work sponsored by an agency of the United States Government. Neither the United States Government nor any agency thereof, nor any of their employees, makes any warranty, express or implied, or assumes any legal liability or responsibility for the accuracy, completeness, or usefulness of any information, apparatus, product, or process disclosed, or represents that its use would not infringe privately owned rights. Reference herein to any specific commercial product, process, or service by trade name, trademark, manufacturer, or otherwise does not necessarily constitute or imply its endorsement, recommendation, or favoring by the United States Government or any agency thereof. The views and opinions of authors expressed herein do not necessarily state or reflect those of the United States Government or any agency thereof.

This report has been reproduced directly from the best available copy.

Available from the National Technical Information Service, U. S. Department of Commerce, Springfield, Virginia 22161.

Price: Printed Copy A06
Microfiche A01

Codes are used for pricing all publications. The code is determined by the number of pages in the publication. Information pertaining to the pricing codes can be found in the current issues of the following publications, which are generally available in most libraries: *Energy Research Abstracts (ERA); Government Reports Announcements* and Index *(GRA* and I); *Scientific and Technical Abstract Reports (STAR);* and publication NTIS-PR-360 available from NTIS at the above address.

DOE/MC/21179-2564
(DE88001063)
Distribution Category UC-132

Rock Matrix and Fracture Analysis of Flow in Western Tight Gas Sands

Annual Report
Phase III

V. Dandge
M. Graham
B. Gonzales
D. Coker

Work Performed Under Contract No.: DE-AC21-84MC21179

For
U.S. Department of Energy
Office of Fossil Energy
Morgantown Energy Technology Center
P.O. Box 880
Morgantown, West Virginia 26507-0880

By
New Mexico Petroleum Recovery Research Center
New Mexico Institute of Mining and Technology
Socorro, New Mexico 87801

December 1987

TABLE OF CONTENTS

LIST OF TABLES iv

LIST OF FIGURES v

ACKNOWLEDGEMENTS viii

EXECUTIVE SUMMARY 1

Background 1

Project Tasks - Phase III 1

Advanced Core Analysis 1
Natural Fractures in Tight Sandstones 1

TASK 1 ADVANCED CORE ANALYSIS 2

Diagenesis of MWX Sandstones - Types and Effects of Secondary Pores . . 3
Cements 5
Carbonate 5
Quartz 5
Clays 5
Diagenetic Controls on Reservoir Characteristics 6

Correlation of Pressure Sensitivity With Depositional Environment 6

Resin Injection for Visible, UV Reflectance, and Electron Microscopy . . . 8
Effect of Confining Pressure on Pore Structure 9

Clay Analysis 9
Procedure 9
Results 10

TASK 2 FLOW ALONG AND ACROSS FRACTURES 10

Background 10

Results 12

Effect of Acetic Acid Treatment on Mineralized Fractures 12

TASK 3 CHEMICAL ALTERATION 12

Background 12

Sample Preparation 22

Results of Chemical Treatments 24

Summary of Chemical Treatment Study 47

TASK 4 EFFECT OF WATER ON GAS PRODUCTION 47

Introduction 49
Preserved Cores 49
Permeability Measurements 49
Experimental 49
Absolute Brine Permeabilities of Preserved and Dried Cores 51
Results 51
Absolute Permeabilities 51
Relative Permeability to Gas 51
Desorption-Adsorption Isotherms 57
Experimental 57
Results 57
Moisture Content of Preserved Cores 57
Experimental 57
Results 57
Electrical Resistivity of Tight Sands 62

SUMMARY 62

OBJECTIVES FOR PHASE IV 71

Task 1 Advanced Core Analysis 71
Task 2 Gas Flow in Mineralized Fractures 72
Task 3 Changes in Matrix Properties after Chemical Treatment 72
Task 4 Properties of Tight Sands Related to Water Content 72
Electrical Resistivities 72
Capillary Pressure Measurements 72

REFERENCES 73

APPENDIX 75

LIST OF TABLES

Table 1. Fractured Samples and Work Completed on Mineralized Fractures and Neighboring Matrix 13

Table 2. Comparison of Permeabilities for Fractured Core and Neighboring Matrix 14

Table 3. Relative Permeability Data for Fractured Core 17

Table 4. Effect of Treatment of Mineralized Fracture With Acetic Acid 20

Table 5. Chemicals Used in Treatments of MWX Matrix Samples 23

Table 6. Core Properties Before and After Chemical Treatments 26

Table 7. Ratios of Treated to Untreated Core Properties 27

Table 8. Summary of Tests Performed on Multi-Well Preserved Core Samples 50

Table 9. Initial Moisture Content 61

LIST OF FIGURES

Figure 1.	Diagram showing depositional and diagenetic facies, sample intervals and selected diagenetic features for Mesaverde sandstones at MWX (diagenesis data from unpublished reports by Bendix Field Engineering Corporation)	4
Figure 2.	Permeability at 5000 psi confining pressure vs. permeability at 500 psi confining pressure.	7
Figure 3.	Relative proportions of clay types from x-ray diffraction for five geologic zones	11
Figure 4.	Horizontal permeability vs. confining pressure for fractured and matrix samples (flow across mineralized fracture)	15
Figure 5.	Vertical permeability vs. confining pressure for fractured and matrix samples (flow along mineralized fracture).	16
Figure 6.	Horizontal relative permeability to gas for flow across a mineralized fracture for MWX1 29-7B H*	18
Figure 7.	Effect of confining pressure on gas relative permeabilities for MWX1 29-7B H*	19
Figure 8.	Variation of vertical permeability flow along fracture with confining pressure before and after treatment of a fractured sample with acetic acid	21
Figure 9.	Apparatus used to flush cores with reagents	25
Figure 10a.	Changes in permeability vs. confining pressure for various chemical treatments of a coastal core (hydrochloric acid)	28
Figure 10b.	Changes in permeability vs. confining pressure for various chemical treatments of a coastal core (acetic acid)	29
Figure 10c.	Changes in permeability vs. confining pressure for various chemical treatments of a coastal core (buffered acetic acid).	30
Figure 10d.	Changes in permeability vs. confining pressure for various chemical treatments of a coastal core (sodium hydroxide).	31
Figure 10e.	Changes in permeability vs. confining pressure for various chemical treatments of a coastal core (sodium carbonate)	32
Figure 10f.	Changes in permeability vs. confining pressure for various chemical treatments of a coastal core (EDTA)	33
Figure 11a.	Changes in permeability vs. confining pressure for various chemical treatments of a fluvial core (hydrochloric acid)	34

Figure 11b. Changes in permeability vs. confining pressure for various chemical treatments of a fluvial core (acetic acid). 35

Figure 11c. Changes in permeability vs. confining pressure for various chemical treatments of a fluvial core (buffered acetic acid). 36

Figure 11d. Changes in permeability vs. confining pressure for various chemical treatments of a fluvial core (sodium hydroxide) . . 37

Figure 11e. Changes in permeability vs. confining pressure for various chemical treatments of a fluvial core (sodium carbonate) . . 38

Figure 11f. Changes in permeability vs. confining pressure for various chemical treatments of a fluvial core (EDTA) 39

Figure 12. Log-log plots of permeability vs. confining pressure for a coastal sample (changes in slope indicate relative changes in pressure sensitivity) 40

Figure 13. Log-log plots of permeability vs. confining pressure for a fluvial sample (changes in slope indicate relative changes in pressure sensitivity) 41

Figure 14. Porosity after chemical treatment vs. orginial porosity. . . 42

Figure 15. Slope of log K vs. log P after chemical treatment vs. original slope 44

Figure 16. Effect of hot sodium hydroxide treatment on K vs. P relationship 45

Figure 17. Effect of oxalic acid treatment on K vs. P relationship. . . 46

Figure 18. Surface areas from nitrogen adsorption before and after chemical treatment 48

Figure 19. Changes in P vs. K relationship for preserved and dried cores (MWX3 42-4). 52

Figure 20. Increase in permeability caused by drying (MWX1 33-10) . . . 53

Figure 21. Increase in permeability caused by drying (MWX3 58-11) . . . 54

Figure 22. Relative permeability to gas for preserved and previously dried core (MWX3 42-4) 55

Figure 23. Relative permeability to gas for preserved and previously dried core (MWX1 33-10). 56

Figure 24. Desorption isotherms for preserved and oven-dried cores (MWX1 33-10) 58

Figure 25. Adsorption hysteresis for dried and preserved cores (MWX1 33-10) 59

Figure 26. Adsorption hysteresis for preserved and oven-dried core (MWX3 42-4) 60

Figure 27. Water loss for various core preservation methods.[21] 63

Figure 28. Formation factor vs. permeability (Klinkenberg corrected) for MWX1 10-13 64

Figure 29. Formation factor vs. permeability (Klinkenberg corrected) for MWX3 64-29 65

Figure 30. Formation factor vs. permeability (Klinkenberg corrected) for MWX1 22-20 66

Figure 31. Formation factor vs. permeability (Klinkenberg corrected) for MWX1 13-15 67

Figure 32. Formation factor vs. permeability (Klinkenberg corrected) for samples from Well: S.F.O.T. Unit #1.[22] 68

Figure 33. Formation factor vs. permeability (Klinkenberg corrected) for samples from Well: B.F. Phillips Unit #1.[22] 69

Figure 34. Formation factor vs. permeability (Klinkenberg corrected) for samples from Well: Sam Hughes Unit #1.[22] 70

ACKNOWLEDGEMENTS

The assistance of Allan Sattler of Sandia Laboratories in the selection and provision of cores used in this study and Vijaya Dandge and Mary Graham in performing the laboratory work is greatly appreciated. George Austin of the New Mexico Bureau of Mines and Mineral Resources kindly provided advice on procedures for analysis of clays which was performed by Kent Cadie.

EXECUTIVE SUMMARY

BACKGROUND

Tight gas sands are a vast future source of natural gas. These sands are characterized as having very low porosity and permeability. The main resource development problem is efficiently extracting the gas from the reservoir. Future production depends on a combination of gas price and technological advances. Gas production can be enhanced by fracturing. Studies have shown that many aspects of fracture design and gas production are influenced by properties of the rock matrix. Computer models for stimulation procedures require accurate knowledge of flow properties of both the rock matrix and the fractured regions. In the proposed work, these properties will be measured along with advanced core analysis procedures aimed at understanding the relationship between pore structure and properties.

The objective of this project is to develop reliable core analysis techniques for measuring the petrophysical properties of tight gas sands. Recent research has indicated that the flow conditions in the reservoir can be greatly enhanced by the presence of natural fractures, which serve as a transport path for gas from the less permeable matrix. The study is mainly concerned with the dependence of flow in tight gas matrix and healed tectonic fractures on water saturation and confining pressure. This dependency is to be related to the detailed pore structure of tight sands as typified by cores recovered in the Multi-Well experiment.

PROJECT TASKS - PHASE III

Advanced Core Analysis

Investigation of the pore structure of matrix samples recovered from the MWX field laboratory demonstrate the importance of environment and diagenetic history. At any given level of permeability, cores from a fluvial environment are about 3 times more pressure sensitive than cores of shoreline/marine origin. Coastal sandstones are of intermediate sensitivity.

A recently reported surface staining technique for examination of pore structure by UV reflectance microscopy has been found ideal for examination of low permeability gas sands. Only a thin surface slice of a 30 μm thick thin section is examined by this technique. Fine details of microporosity and sheet pores at grain boundaries which largely control the flow and pressure sensitivity of these sands are revealed in fine detail. Examination of cores in which resin was set up at high confining pressure (5000 psi) indicates that sheet pores at grain boundaries are reduced in thickness.

Clay analyses are reported for 35 MWX samples, together with water desorption/adsorption isotherms and BET surface areas. Distribution of clay types in coastal sandstones is fairly uniform, whereas fluvial sandstones show considerable variability.

Natural Fractures in Tight Sandstones

Natural fractures play a dominant role in production from tight sands. The most readily detected fractures in whole core samples are mineralized, the majority being filled by calcite. Further permeability vs. confining pressure measurements have been

made for cores with mineralized fractures lying either along or perpendicular to this direction of flow. For the most recent core to be tested, permeability for a core containing a mineralized fracture along the direction of flow had somewhat lower permeability than that of the neighboring matrix. The effect of confining pressure on relative permeabilities for a core containing mineralized fractures is also reported. After flowing 20% acetic acid through a core having a mineralized fracture (running in the direction of flow) permeability at 5000 psi confining pressure was increased by almost four orders of magnitude.

The effect of chemical treatment (six chemicals in all ranging from strong base to strong acid) on the permeability and pressure sensitivity of fluvial and shoreline matrix samples from the MWX has been investigated. The objective of this work was to determine which minerals occupy key positions in the pore structure with respect to permeability and pressure sensitivity. Results showed the likely importance of quartz overgrowths with respect to pressure sensitivity. Removal of carbonate cements by acid treatment resulted in significant increase in permeability for the fluvial sample.

The effect of drying on MWX cores has been assessed by comparing absolute permeabilities to water, relative permeabilities to gas, and desorption/adsorption isotherms, for preserved (undried) and dried cores. Permeabilities of the dried cores were higher than those of the fresh cores with differences in permeability to gas being greater at higher water saturations and overburden pressures. Core analysis measurements on tight sands should, where possible, be performed on preserved (undried) cores. Measurements of water saturation in MWX preserved cores (wrapped in Saran wrap and aluminum foil followed by coating with seal peel) showed that the method was far from reliable as a means of preserving water content. It is recommended that improved techniques which have been developed recently should be applied to preservation of low permeability gas sands.

TASK 1 ADVANCED CORE ANALYSIS

Matrix properties are important even in fractured wells and formations since they determine the rate of gas flow into the fractures. Cores have been tested from the fluvial, coastal, and paludal zones of the Mesaverde. Special attention is being given to the effect of overburden pressure on pore structure as it relates to permeability, relative permeability, and electrical properties.

Work performed under Task 1 of Phase III was as follows:

(a) An account of the diagenetic history of MWX sandstones as it relates to pore structure.

(b) Test for correlations between pressure sensitivity and diagenetic history for at least 30 samples.

(c) Further development of low viscosity resin formulations containing visible and UV dye for impregnation of tight sands. This work has been applied to examination of the effect of overburden pressure on pore structure through UV reflectance microscopy.

(d) Clay analyses.

DIAGENESIS OF MWX SANDSTONES - TYPES AND EFFECTS OF SECONDARY PORES

The deposits of four distinct siliciclastic paleoenvironments in the Mesaverde Group have been penetrated by MWX wells. Three of these paleoenvironments are part of a progradational sequence[1,2] that includes, in ascending order, (1) marine/shoreline deposits; (2) delta plain, coastal, and paludal deposits and (3) meanderbelt fluvial deposits. Marine-influenced paralic sandstones and mudstones cap the progradational sequence and appear to be associated with the Lewis transgression.[1] These paralic deposits do not contain significant gas resources in the MWX wells, and will not be discussed here. The sedimentologic characteristics of the Mesaverde progradational sequence are described in detail by Lorenz.[1,2]

Two generalized diagenetic facies can be delineated in the sandstones of the Mesaverde progradational sequence. We term the lowest of these the marine facies. This facies includes sandstones deposited in shoreline/marine, paludal and coastal environments and is characterized by the presence of widespread, early diagenetic carbonate and high dolomite/calcite ratios (see Fig. 1). Sandstones deposited in nearshore areas (paludal, coastal) are included in the marine facies because the nature and distribution of carbonate cements in these rocks are generally similar to those of the underlying shoreline/marine sandstones. The inclusion of coastal and paludal sandstones in the marine facies presumably reflects the diagenetic role of seawater during shallow burial of the nearshore deposits. In contrast, rocks of the overlying continental diagenetic facies are characterized by patchy, local development of early carbonate cements that developed during meteoric diagenesis. Dolomite is minor in the continental diagenetic facies. Differences in style and extent of paleoenvironment-controlled early carbonate cements and quartz are the most important factors in the contrasting reservoir characteristics of Mesaverde sandstones at MWX. The contact between the two diagenetic facies is gradational, and occurs at a depth of about 6000 ft.

A generalized diagenetic history for MWX sandstones was derived using the following methods: (1) petrographic examination of over 500 thin sections; (2) preparation of polystyrene pore casts from selected sandstones, and (3) examination and photography of rock chips and pore casts with the scanning electron microscope. Particular attention was given to the nature and distribution of fractures and primary and secondary pores. Modal mineralogic data were derived from unpublished petrographic analyses reported by D.R. Allen, R.D. Dayvault, M.L. Dixon, M.O. Eatough, M.J. Eatough, L.M. Fukui and R.D. Hopping of Bendix Field Engineering Laboratory.

Sandstones of the Mesaverde progradational sequence at MWX exhibit a wide range of compositions. Feldspar content of the continental diagenetic facies is generally higher than that of the marine facies. The more arkosic nature of sandstones in the continental facies is the result of two factors: (1) continental sandstones are typically coarser than the marine sandstones, thus abrasional removal of feldspars was less complete in the continental deposits; (2) destruction of feldspars by calcitization is more widespread in marine sandstones. Lithic fragments are dominantly of sedimentary origin, although subordinate metamorphic and volcanic detritus are also present. Labile rock fragments are commonly deformed to produce pseudomatrix.

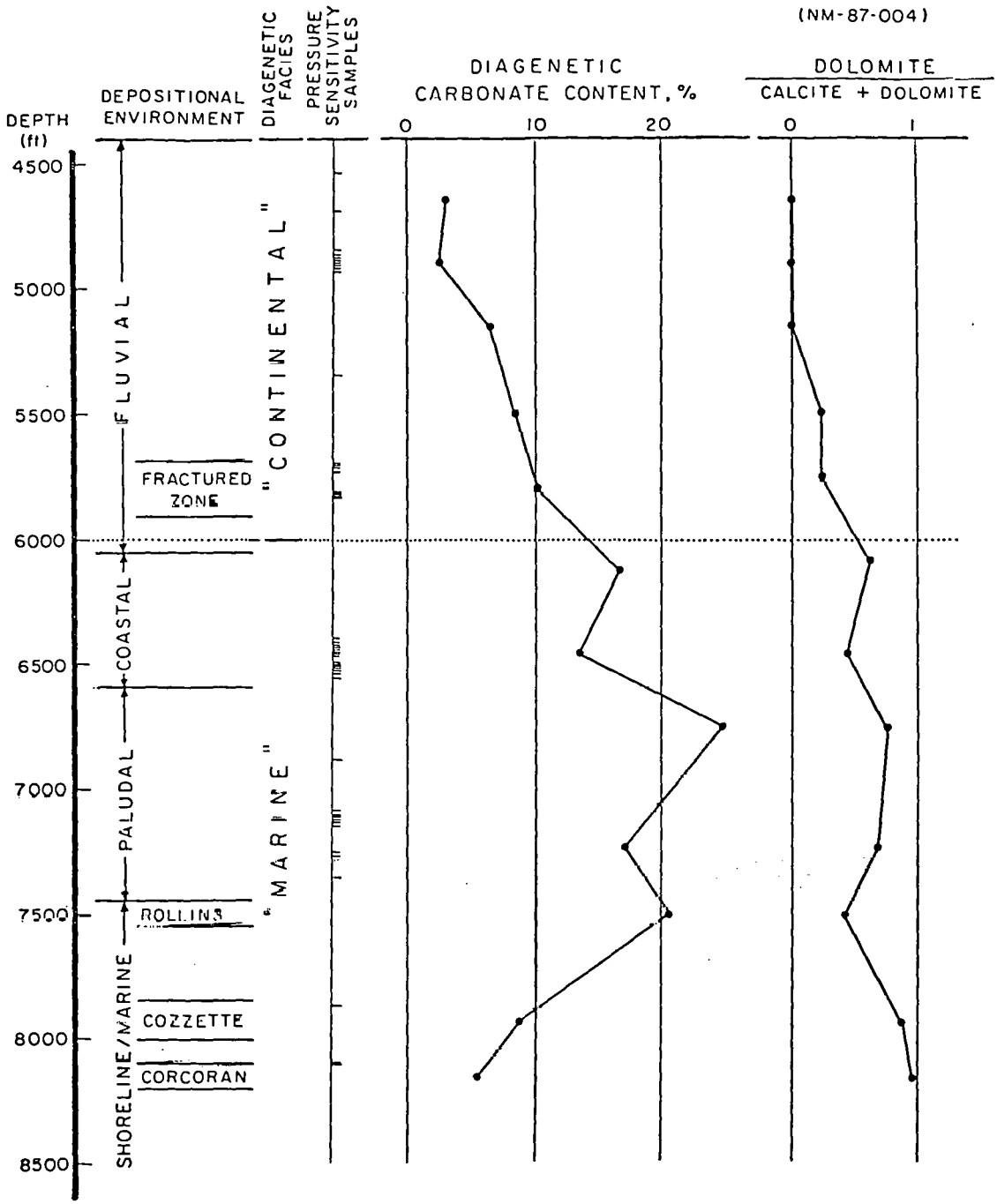

Figure 1. Diagram showing depositional and diagenetic facies, sample intervals and selected diagenetic features for Mesaverde sandstones at MWX (diagenesis data from unpublished reports by Bendix Field Engineering Corporation).

Cements

Carbonate

Carbonate cements are best developed in the marine diagenetic facies, presumably due to availability of seawater to the marine and nearshore sediments. Except for sparse, pore-rimming chlorite in some fluvial sandstones and minor early dolomite in a few coastal sandstones,[3] calcite cement was the first to form. It developed early in the burial history of the host sandstones, as shown by the common loosely packed nature of calcite-cemented detrital grains. Diagenetic calcite in Mesaverde sandstones at MWX is sparry and commonly occurs as large, poikilotopic crystals which are typical of early formed concretions and phreatic carbonates in many clastic units. Detrital feldspar grains are commonly replaced by calcite, especially in non-fluvial sandstones.

Dolomite occurs as pore-fill and as a replacement of detrital grains. It is the dominant carbonate mineral in sandstones of the lower portion of the Mesaverde progradational sequence (Fig. 1). Most dolomite formed during late diagenesis and commonly appears as a replacement product of earlier calcite.

Quartz

Following early diagenetic calcite, quartz was the next cement to form in the Mesaverde sandstones at MWX. Authigenic quartz is present in nearly all of these sandstones, and occurs dominantly as simple, syntaxial overgrowths. Mean content of quartz cements in MWX sandstones is about 5 percent.

Several lines of evidence indicate that authigenic quartz post-dated the development of calcite cements in the Mesaverde progradational sequence:

1. Detrital grains in calcite-cemented sandstones typically are less compacted than those in quartz-cemented sandstones; such packing differences were occasionally noted between adjacent areas within individual thin sections.

2. Where authigenic quartz has replaced earlier calcite cement, remnants of the earlier cement are locally present beneath and within quartz overgrowths.

3. Development of quartz overgrowths is commonly inhibited only along those surfaces of detrital grains where calcite or early clay cements are present.

Authigenic quartz is an important modifier of porosity. Where well-developed, quartz overgrowths almost completely occlude primary porosity, leaving only sheet-like pores between adjacent overgrowths. Authigenic quartz is not present in secondary pores, indicating that quartz cementation preceded dissolution of calcite and feldspar.

Clays

With the exception of rare early chlorite in some fluvial sandstones, clay minerals were the last major cements to form in the Mesaverde sandstones at MWX. Diagenetic clays consist dominantly of kaolinite, illite, illite-smectite, and chlorite. These clays are present in both primary and secondary pores.

Diagenetic Controls on Reservoir Characteristics

Both primary and secondary pores occur in Mesaverde sandstones at MWX, although secondary porosity dominates volumetrically. Primary pores typically appear as remnant porosity between pore-filling cements and as circumgranular cracks beneath authigenic minerals. With the exception of local, clay-lined intergranular areas in a few fluvial sandstones, primary pores in sandstones at MWX generally exhibit high-aspect geometries. These sheet-like primary pores exert important influences on the reservoir characteristics of Mesaverde sandstones, and provide a connecting network between the larger, volumetrically dominant secondary pores.

Secondary pores are of two major types. Dissolution porosity in detrital feldspars is mostly restricted to the continental diagenetic facies, where calcitization of unstable feldspar grains during calcite cementation was incomplete. Secondary porosity after calcite predominates in the marine diagenetic facies, but is also present to a lesser extent in the continental facies. Calcite dissolution porosity occurs within areas of intergranular cement and within calcitized detrital grains. Bituminous residues are locally present within dissolved feldspars of some fluvial sandstones, but not within secondary porosity after calcite. These relationships constrain the relative timing of hydrocarbon migration, and indicate that dissolution of feldspar and calcite did not occur simultaneously.

Polystyrene casts of pore space were prepared by saturating a core with styrene monomer which is subsequently polymerized. Casts of pore space were recovered after dissolving the rock matrix by chemical treatment. Examination of polystyrene pore casts using the scanning electron microscope often enables identification of minerals that were precursor to secondary porosity. Casts of dissolved feldspars typically exhibit irregular, detrital morphologies. Casts of secondary pores after calcite are commonly euhedral, mimicking the crystal habit of earlier intergranular cements and replacement products.

CORRELATION OF PRESSURE SENSITIVITY WITH DEPOSITIONAL ENVIRONMENT

A characteristic feature of most tight sandstones is their unusually high sensitivity of permeability (characterized by the ratio of $K_{\infty,500}/K_{\infty,5000}$ for first unloading) to overburden pressure. Extensive investigation has been undertaken to relate this pressure sensitivity to other measurable physical properties for a variety of rock types.[4] In examining the pressure role of diagenetic history, recent work was focussed on cores recovered from the Multi-Well experiment. It has been found that pressure sensitivity varies systematically in sandstones of the Mesaverde progradational sequence. Permeabilities of the tested samples ranged from about .001 to 50 μ darcies at 500 psi confining pressure. A plot of $K_{\infty,5000}$ vs. $K_{\infty,500}$ (Fig. 2) shows that at any given level of permeability, pressure sensitivity increases upward stratigraphically. The fluvial sandstones exhibit about three times the pressure sensitivity of the shoreline/ marine and paludal rocks. Coastal sandstones display intermediate values of sensitivity to overburden pressure.

Pressure sensitivity is thought to result from the effects of nearly elastic sheet-pore closure in the host sandstones.[5] The upsection increase in pressure sensitivity in the Mesaverde sandstones may result from several factors:

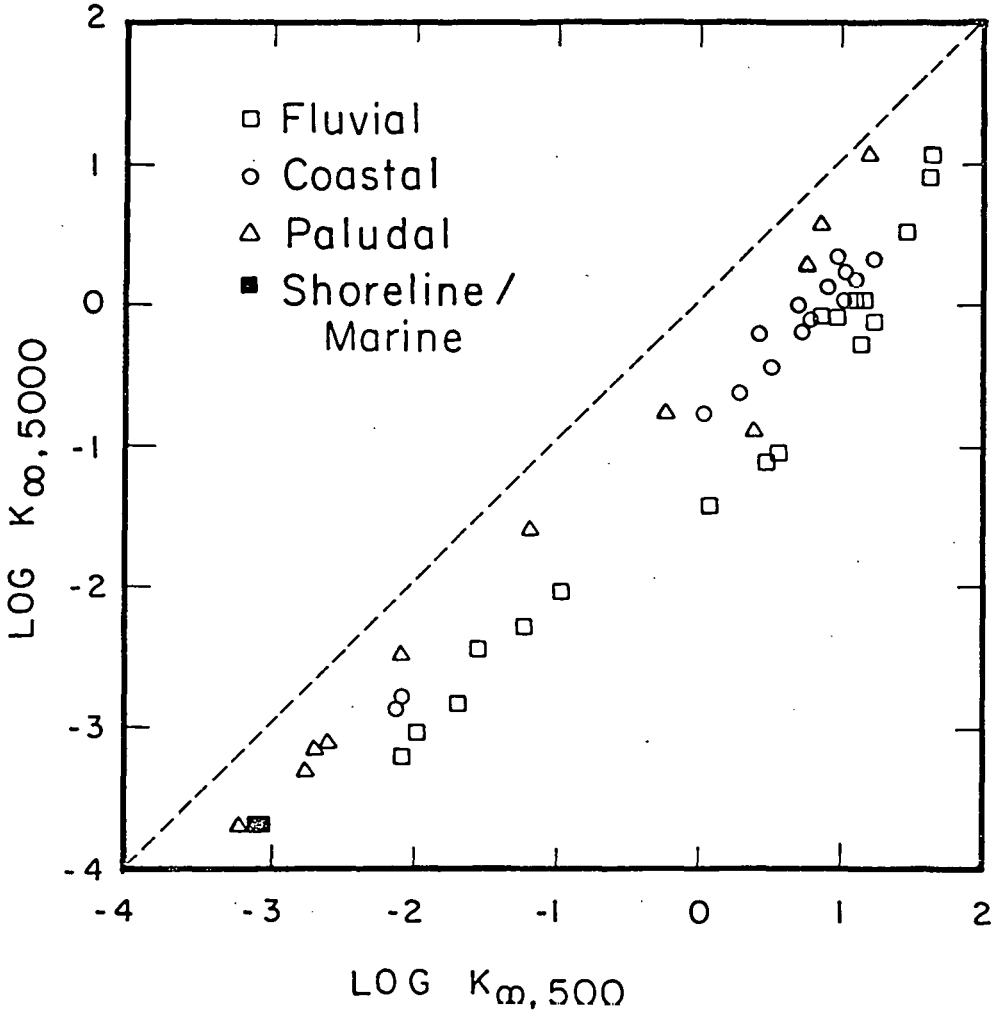

Figure 2. Permeability at 5000 psi confining pressure vs. permeability at 500 psi confining pressure.

1. The overall upward increase in grain size of sandstones in the Mesaverde progradational sequence may yield a corresponding increase in pressure sensitivity, due to the greater area of individual sheet pores in the coarser sandstones.

2. The more widely spaced, discontinuous nature of dissolution porosity in the fluvial diagenetic facies may allow more opportunity for sheet-pore closure due to overburden in these rocks.

3. The upsection increase in quartz cements (and, hence, sheet pores between overgrowths) may cause greater sensitivity to overburden pressure in the upper portions of the Mesaverde progradational sequence.

Initial reagent-treatment results (described in this report under Task 3) suggest that quartz cements may be an important factor in pressure sensitivity.

RESIN INJECTION FOR VISIBLE, UV REFLECTANCE, AND ELECTRON MICROSCOPY

Considerable progress has been made in preparation of thin sections for which pore structure can be examined by both conventional transmitted light and UV reflectance microscopy. We have applied a technique recently reported by Ruzyla and Jezek[6] to tight gas sands. In this technique, which was brought to our attention by Michael Holland, conventional thin sections are prepared after impregnation with blue-dyed epoxy resin. The surface of the thin section is then cleaned and contacted with a fluorescent dye which diffuses for a short distance into the resin within a few minutes. The excess dye is washed off with isopropyl alcohol. The resulting thin sections can then be examined by both transmitted and UV reflectance either alone or in combination. Fine details of microporosity and sheet pores at grain boundaries are clearly revealed by UV reflectance.

Advantages to the technique noted by Ruzyla and Jezek are:

1. It can be applied to both thin sections and polished thick sections.

2. Fluorescent dye does not need to be mixed with the epoxy resin. (We had experienced problems in obtaining a satisfactory formulation for work in tight sands.)

3. It can be applied to any existing epoxy-impregnated sample. (If the thin section has a cover slip it must be removed.)

4. It gives improved characterization of reservoir pore systems. Small pore systems (microporosity) can be recognized. (In tight sands, adsorption isotherms show that about 25% of the pore space is in pores of less than 200 Å diameter.)[7,8]

5. Pore space differentiated with fluorescent dye can be quantified by image analysis.

6. Areas of plucked grains are apparent from differences in transmitted light and UV reflectance images.

A distinct advantage of the technique, especially with respect to tight gas sands, is that the diffusion distance for the fluorescent dye is probably of the order of a few microns. Thus the image is very close to a mathematical 2-dimensional image of the section rather than being 30 μ in thickness. Internal imaging and reflectance is reduced to give much clearer delineation of pore space than that given when UV dye occupies all of the pore space of the thin section as in the technique described by Gies.[9] This is especially important in any attempt to characterize the pore space of tight gas sands by image analysis.

The present working hypothesis of the cause of pressure sensitivity is that elastic opening and closing of sheet pores at grain boundaries is largely responsible for the observed pressure sensitivity.[5] The sheet pores are on the order of 0.1 - 0.2 microns in thickness and would be difficult to measure directly. We have therefore experimented with the length of time in which the thin section is left in contact with the fluorescent dye. The thin section was first contacted with the dye for 30 sec. and the UV reflectance image was photographed before subjecting the thin section to further exposure. As the time of exposure was increased, the amount of revealed porosity including the sheet pore structure also increased. Assuming that the widest sheet pores are revealed first by this method, a map showing the more permeable sheet-pore pathways can be prepared using this technique.

Effect of Confining Pressure on Pore Structure

Five samples have been impregnated with resin and subjected to 5000 psi confining pressure before curing. Thin sections of these and of duplicate samples not subjected to confining pressure were surface-stained with Hi-Brite Yellow UV dye. The staining was done in timed intervals so that development of the pore space viewed by UV reflectance could be recorded as a series of photomicrographs. The bigger pore spaces and cemented areas took up the stain within 5-10 seconds. With subsequent exposure these areas changed from green to bright yellow. The smaller pores were visible within 30 seconds but not totally developed. Depending on the sample, additional improvements in the image were sometimes seen after immersing the sample in the dye for as long as eight minutes. Others did not seem to show much further change after being immersed only two minutes. Qualitative differences in pore structure for confined and unconfined samples have been observed but further observation and improved methods of comparison are needed to confirm them. This work will be given priority in Phase IV.

CLAY ANALYSIS

Procedure

Clay samples were prepared from Multi-Well cores by the following procedure as recommended by Dr. George Austin of the New Mexico Bureau of Mines and Mineral Resources. Core samples of 20-25 grams were crushed and dispersed in deionized distilled water. Various precautions were taken to ensure that the sample did not flocculate at any stage of the procedure. After allowing the sample to stand for ten minutes, an eye dropper was used to withdraw from the surface a sample of sufficient size to cover a glass slide. Samples, generally prepared two at a time, were allowed

to air dry. This procedure gives samples which are strongly oriented to the slide surface and give intense basal x-ray reflection.

The slide was then examined with an x-ray diffractometer at 2° 2θ/minute from 2°(2θ) to 3°(2θ) with monochromatic or Ni-filtered Cu radiation. Results for the Multi-Well samples revealed a mixture of clay minerals. Further identification was aided by the routine procedures of heat treatment at 375°C for 30 minutes, and by treatment overnight in a closed container containing ethylene glycol.

Results

Results of the x-ray scans are presented in the Appendix. Peak height intensities were analyzed to obtain the relative amounts of clay as listed for each sample. Desorption isotherms and BET surface areas, both of which are strongly related to microstructure of pore space, are included for each sample.

Because relationship between pressure sensitivity and depositional facies exists (Fig. 2), clay contents were also tabulated according to depositional facies. Results are shown in Fig. 3 as relative proportions of illite, mixed layer clay, kaolinite and chlorite. Paludal and coastal intervals have illite and mixed layer clays in fairly similar proportions. Much more spread in results was found for the fluvial samples. Thus, from initial examination of these results and some preliminary results for shoreline/marine samples, there is no distinct trend in clay content that relates to change in pressure sensitivity with depositional environment. Because pressure sensitivity is related to sheet pores, the lack of correlation with clay content is not surprising. Clays may still be important as proppants in sheet pores, whereby they affect crack-closing and elastic properties of the rock. Swelling and dispersion of clays also provide a possible explanation for the large differences in brine and gas permeabilities commonly observed for tight sandstones.[10]

TASK 2 FLOW ALONG AND ACROSS FRACTURES

BACKGROUND

Production from some MWX low permeability gas sands is much higher than would be expected from properties of the rock matrix.[11] The presence of tectonic fractures is often cited as a key factor in such behavior for both fractured and unfractured wells. Vertical fractures are common in some of the cores recovered in the Multi-Well project.[12] By far the majority of these fractures are filled with calcite cement.

In work under Task 2, flow measurements are being made along and across selected mineralized fractures as a function of overburden pressure. Comparative measurements have also been made on unfractured neighboring zones of a given whole core sample. The effect of water content on permeabilities in fractured systems has also been determined. Chemical treatments of mineralized fractures demonstrate that permeability to gas along the fracture can be increased by several orders of magnitude. This work will largely complete previous work on natural fractures performed under Phases I and II.

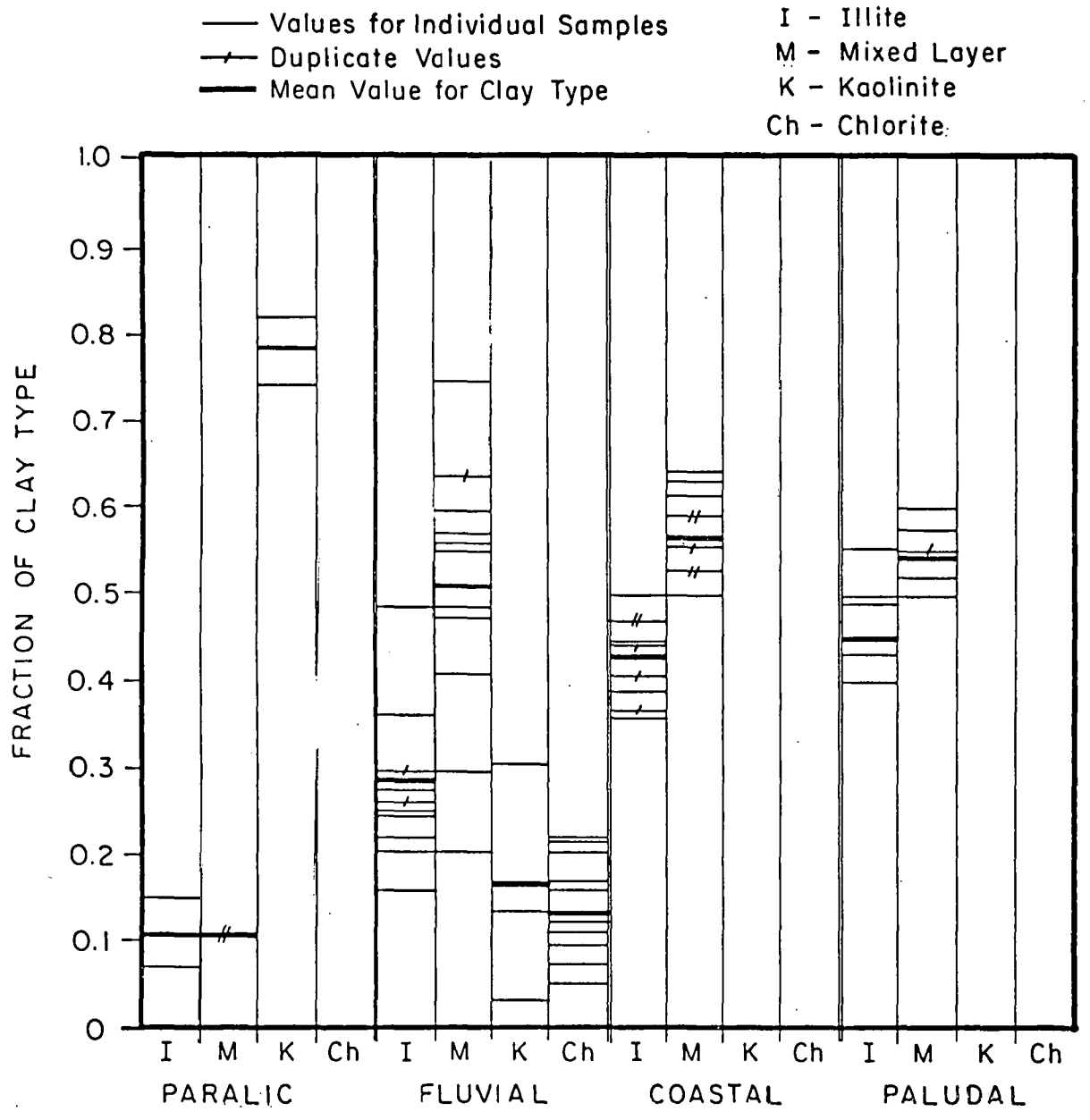

Figure 3. Relative proportions of clay types from x-ray diffraction for five geologic zones.

RESULTS

An updated summary of measurements related to cores containing mineralized fractures that have been completed to date is given in Table 1.

In Phase III, the effect of confining pressure on fractures and neighboring matrix was studied for MWX3 Q-CO, a coastal sand recovered from 6459.2-6460.0 ft. Results are presented in Table 2. Permeability along a horizontal core plug containing the fracture was less than for a horizontal plug taken from the neighboring matrix indicating that the fracture permeability may be less than the matrix (Fig. 4). However, vertical permeability along the fracture was higher than the matrix for a plug cut along the axis of the whole core. The pressure sensitivity ($K_{\infty,500}/K_{\infty,5000}$) of this core was distinctly less than for the matrix (see Fig. 5).

Relative permeabilities to nitrogen gas were determined for MWX1 29-7B H* (see Table 1) for gas flow across the fracture. Measurements were made at five levels of water saturation. Results are given in Table 3 and Fig. 6. Relative permeabilities were increasingly sensitive to confining pressure at any given level of water saturation (see Fig. 7).

EFFECT OF ACETIC ACID TREATMENT ON MINERALIZED FRACTURES

Although mineralized fractures are not greatly different in permeability from the matrix, large increase in permeability along the fracture can be effected by acid treatment. The effect of acetic acid on mineralized fractures was studied for three samples: MWX1 29-31 V* (along the fracture); MWX1 29-7B H* and MWX3 Q-CO H* (both across the fracture). The samples were treated with about 2 cc of 20% acetic acid. After treatment MWX1 29-7B H* as well as MWX3 Q-CO H* fell apart at the fracture.

Permeabilities before and after acid treatment were measured for MWX1 29-31 V*. Porosity and BET surface area were also measured for the treated plug. Results are given in Table 4. The effect of confining pressure on permeability before and after the treatment is shown in Fig. 8. Acetic acid treatment increased the permeability at high confining pressure by almost four orders of magnitude with only small changes in porosity and surface area. Pressure sensitivity was decreased from 13 to 1.5 (see Table 4 and Fig. 8).

It is possible that acid treatment can be used to increase gas production. Mineralized fractures are a plane of weakness within a core. Because the planes of these ancient fractures are normal to the present day direction of least principal stress it is feasable that induced hydraulic fracturing will part the sandstone along these planes. Acid treatment is therefore a possible alternative or supplement to use of proppants for maintaining fracture conductivity.

TASK 3 CHEMICAL ALTERATION

BACKGROUND

Chemical alteration of various mineralogical components and resultant effects on permeability are being investigated. Experiments include the use of various reagents, including strong and weak acids and bases, and chelating agents. The objective of

Table 1

Fractured Samples and Work Completed on Mineralized Fractures and Neighboring Matrix

Well	ID	Depth (ft)	Geologic Zone	Gas Permeability				Relative Permeability				Acid Treatment				BET Surface Area			
				V*	V	H*	H	V*	V	H*	H	V*	V	H*	H	V*	V	H*	H
MWX-1	13-18	4846.5-4847.0	FM	x	x	x	x	x	x			x				x	x	x	x
MWX-1	16-11	5034.8-5035.2	FM																
MWX-1	21-4A	5271.6-5272.0	FP	x	x											x	x		
MWX-1	29-31	5730.9-5731.2	FP	x	x	x	x	x				x				x	x	x	x
MWX-1	29-7B	5733.2-5733.6	FP	x	x	x	x	x		x				x		x	x	x	x
MWX-1	34-10	6002.3-6002.5	CO	x	x	x	x												
MWX-1	38-27	6192.6-6193.0	CO	x	x	x	x									x	x	x	x
MWX-1	O-FP	5735.8-5736.0	FP																
MWX-2	P-FP	5764.0	FP																
MWX-3	Q-CO	6459.2-6460.0	CO	x	x	x	x							x		x	x	x	x

CO = Coastal
FM = Fluvial (meander belts)
FP = Fluvial (point bars)

V* = vertical; cored along the fracture
V = vertical; matrix
H* = horizontal; cored across the fracture
H = horizontal; matrix

Table 2

Comparison of Permeabilities for Fractured Core and Neighboring Matrix.

MWX-3 Q-CO [6459.2-6460.0 ft.]

Core	Porosity (%)	BET Surface Area (m^2/g)	First Unloading		$\frac{K_{\infty(500)}}{K_{\infty(5000)}}$
			$K_{\infty(500)}$	$K_{\infty(5000)}$	
V*	8.39	2.70	16.90	5.20	3.25
V	8.89	3.00	10.90	2.05	5.32
H*	8.47	2.97	18.58	2.38	7.81
H	8.81	3.16	25.16	3.64	6.91

V* = Vertical; cored along the fracture
V = Vertical; matrix
H* = Horizontal; cored along the fracture
H = Horizontal; matrix

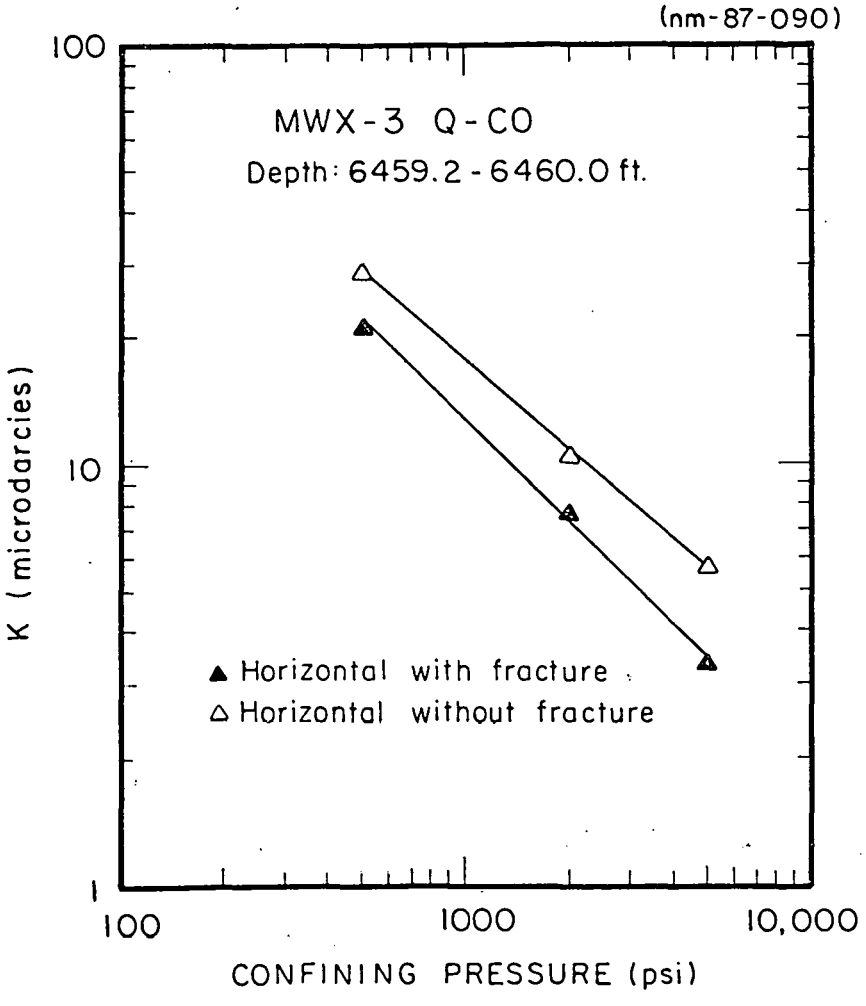

Figure 4. Horizontal permeability vs. confining pressure for fractured and matrix samples (flow across mineralized fracture).

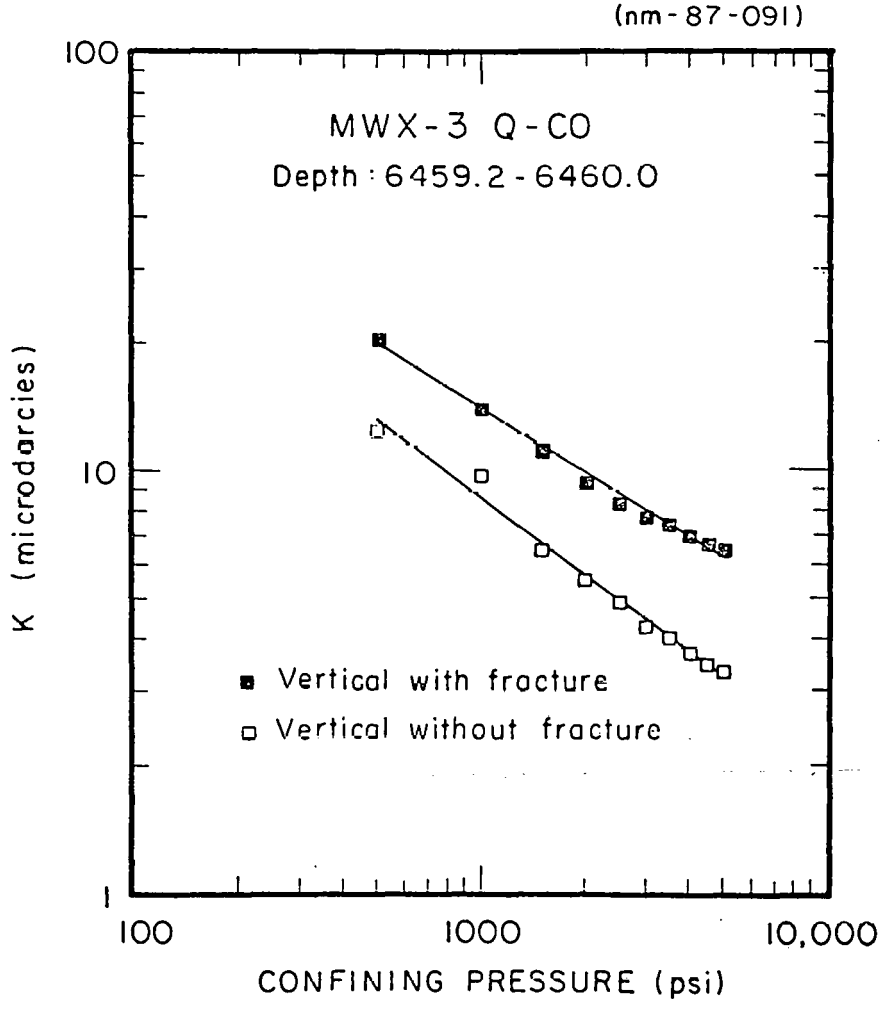

Figure 5. Vertical permeability vs. confining pressure for fractured and matrix samples (flow along mineralized fracture).

Table 3

Relative Permeability Data for Fractured Core.

MWX-1 29-7B H* [5733.2-5733.6 ft.]

Water Saturation (%)		First Unloading		$K_{\infty(500)}$
Initial	Final	$K_{\infty(500)}$ μd	$K_{\infty(5000)}$ μd	$K_{\infty(5000)}$
60.0	58.7	0.316†	0.000025†	1264
42.6	41.8	2.33	0.0039	597.4
30.0	29.8	5.71	0.088	64.89
15.6	15.6	10.15	0.38	26.71
0	0	11.8	1.24	9.52

†Not K_{∞} values.

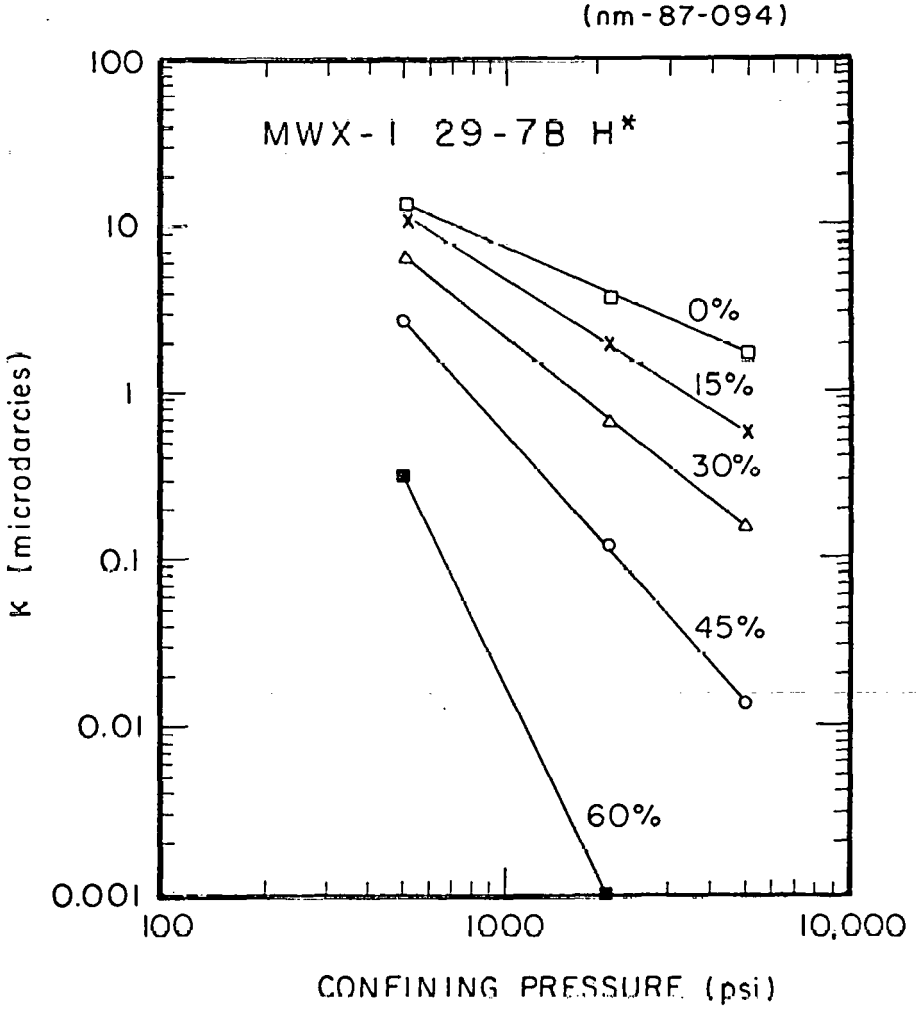

Figure 6. Horizontal relative permeability to gas for flow across a mineralized fracture for MWX1 29-7B H*.

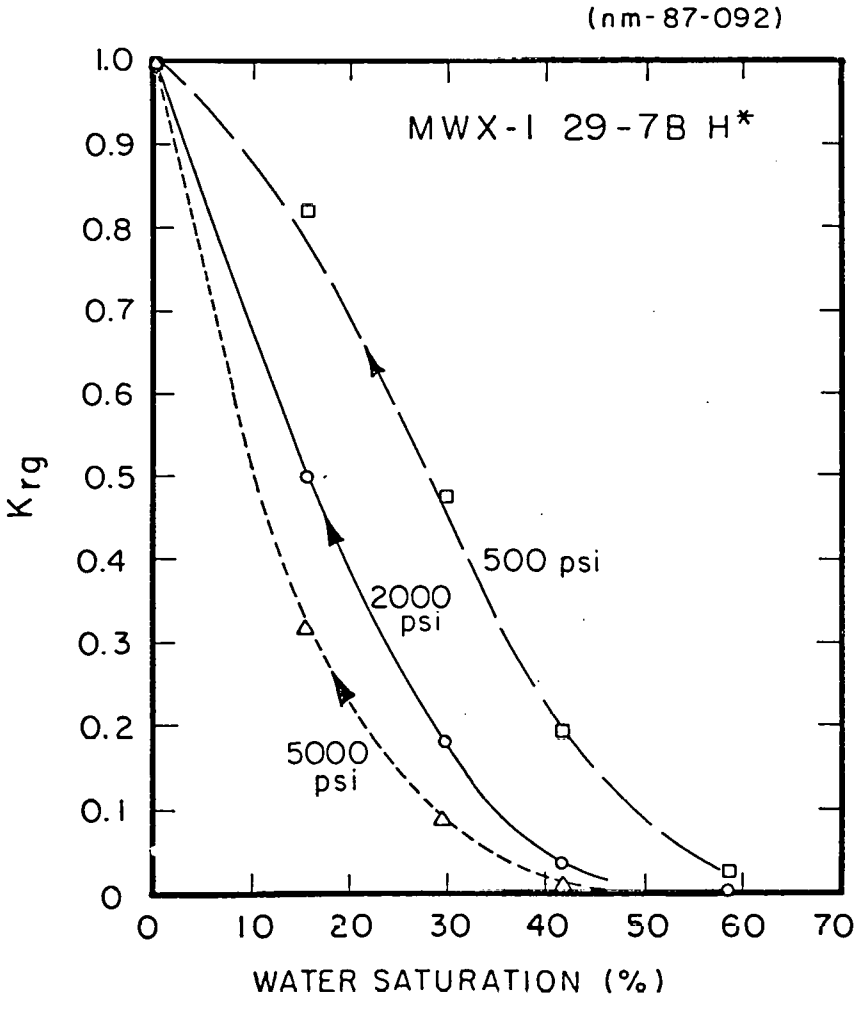

Figure 7. Effect of confining pressure on gas relative permeabilities for MWX1 29-7B-H*.

Table 4

Effect of Treatment of Mineralized Fracture With Acetic Acid.

MWX-1 29-31 V* [5730.9-5731.2 ft.]

Sample	Porosity (%)	BET Surface Area (m^2/g)	$K_{\infty(500)}$ (md)	$K_{\infty(5000)}$ (md)	$\frac{K_{\infty(500)}}{K_{\infty(5000)}}$
Untreated	7.01	1.14	0.017	0.0013	13.08
Treated	7.29	1.21	17.59†	11.45†	1.54

†Not K_∞ values.

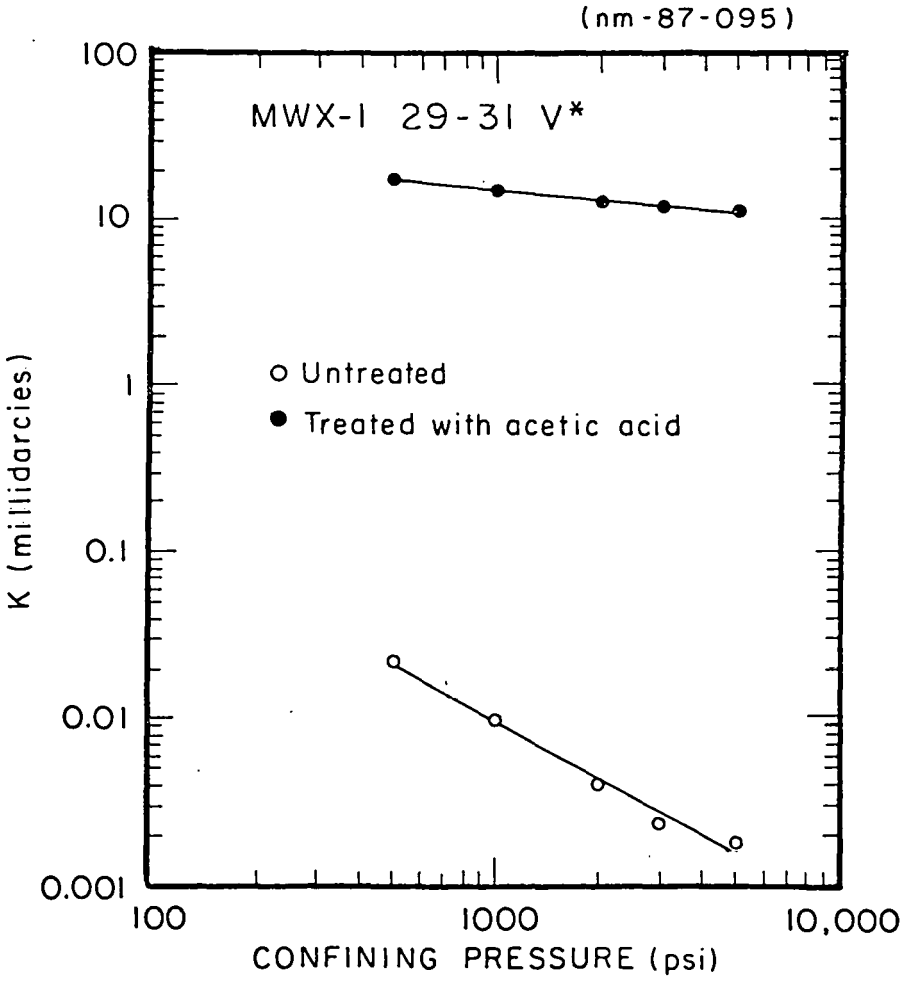

Figure 8. Variation of vertical permeability flow along fracture with with confining pressure before and after treatment of a fractured sample with acetic acid.

this work is to determine which features of pore structure contribute to permeability and pressure sensitivity and to explore new possibilities for chemical stimulation of low permeability gas sands.

Six reagents were chosen to cover a broad range of acids, bases and complexing agents. Table 5 lists these chemicals and the solution concentrations. Properties and some possible effects of these reagents are as follows:

1. Hydrochloric acid (HCl) is a strong mineral acid which will not precipitate metal ions other than silver and lead at reasonable concentrations. It will react with all metal oxides, hydroxides, carbonates, and silicates, although some silicates require long times, high temperatures, and high concentration for complete decomposition. It seems likely that formation of an insoluble sheath of silica around grains of silicate minerals impedes the reaction. The cost of hydrochloric acid is very low in comparison with other chemical reagents.

2. Acetic acid. Aqueous solutions of acetic acid (CH_3COOH) will react at reasonable rates only with metal oxides, hydroxides, and carbonates. Its metallic salts are highly soluble in water. Its low reactivity with silicate minerals might be advantageous in several ways. Consumption of acid by reaction with silicates does not lead to a significant reduction of volume of the reacting grains since the silica remains. Attack on silicates might be harmful if gelatinous silica swells into the pore spaces or becomes mobilized.

3. Buffered acetic acid. Buffering should further reduce the rate of decomposition of clays, feldspars, and other aluminosilicates, but perhaps not greatly retard the dissolution of carbonates. There is some evidence that dissolution of strontianite and probably other Group IIA carbonates shows general acid catalysis.[13] The rate component due to the general acid (acetic) would not be affected by the reduction in proton concentration.

4. Sodium hydroxide (NaOH) dissolves quartz and aluminosilicates which are the major constituents of sandstone. It has no effect on the carbonates of calcium, magnesium, and iron. The possibility of dissolving clays lodged in the pores is particularly attractive. Reaction with chert would probably be a chief mode of consumption.

5. Sodium carbonate (Na_2CO_3) would have an action like that of sodium hydroxide, but would be weaker and slower. It is possible that it might show more selectivity among mineral grains.

6. EDTA will form very stable complexes with the ions of calcium, magnesium and iron. It is conceivable therefore that a significant dissolution might be achieved at ordinary pH. The reagent is moderately expensive, but its inclusion in a research study is certainly justified.

SAMPLE PREPARATION

For the full suite of chemical treatment tests, six core plugs were cut from each of two whole cores from MWX3, one from the coastal and the other from the fluvial

Table 5

Chemicals Used in Treatments of MWX Matrix Samples

Treatment #		Plug #
1	6 M HCl	2
2	1 M Acetic acid	1
3	1 M Buffered acetic acid	6
4	10 % NaOH	4
5	10 % Na_2CO_3	3
6	10 % EDTA	5

zone. Each plug was dried to constant weight at 110°C. The plugs were then saturated with distilled water to measure porosity. Permeability to gas was measured at confining pressures of 5000, 2000 and 500 psi. At the 500 and 5000 psi levels, Klinkenberg permeabilities were determined. The surface area of each sample was determined by the BET single point method. One cm long samples were cut from one end of each plug for thin-section preparation.

After completion of the preliminary series of tests, each plug was treated with one of the chosen chemical reagents in the apparatus shown schematically in Fig. 9. The cores were flushed with about 20 pore volumes (10 ml), of liquid using nitrogen gas to drive the process. Following treatment, the cores were flushed with distilled water, dried at 110°C, and the porosity, permeability, and surface area measurements were repeated. Again, a piece of one end of each plug was removed for examination in thin-section.

In addition to the full suite tests, two coastal samples, prepared as described above, were treated with hot (67°C) sodium hydroxide and one sample was tested with oxalic acid, one of the dicarboxylic acids which may be important in diagenetic processes.[14]

RESULTS OF CHEMICAL TREATMENTS

Results of the full suite of chemical tests are summarized in Table 6 for plugs from two whole cores. MWX3 64-29 is from the coastal zone and MWX3 63-13 is fluvial in origin.

Table 7 further compares the data from Table 6, giving the ratios of each measurement, after treatment, to the same quantity measured before the core plugs were exposed to the various chemical agents. The permeabilities as a function of confining pressure are shown in Figs. 10a-f for MWX3 64-29 and Figs. 11a-f for MWX3 63-16.

Included in Tables 6 and 7 are the slopes of log-log plots of permeability vs. confining pressure. Figs. 12a-f and 13a-f show the same data as in Figs. 10 and 11, plotted in log-log format. We find consistent linear trends for the Multi-Well samples from 500 to 5000 psi confining pressures. The slopes of the lines are related to pressure sensitivity: flatter for less sensitive and steeper for more sensitive samples. Slopes of the linear least-squares fits to the data (see Table 6), are plotted as solid and dashed lines in Figs. 12 and 13.

Changes in the pore volume resulting from chemical treatment are shown in Fig. 14. The weakly acidic buffered acetic acid and the weak base, sodium carbonate, had only minor effects on either sample. EDTA consistently increased porosity, as did both HCl and acetic acid. Sodium carbonate decreased porosity slightly for the fluvial sample and increased it about 10% for the coastal sample.

Changes in porosity do not correlate in any simple way with changes either in permeability or pressure sensitivity. For that matter, the relationship between changes in magnitude of permeability and pressure sensitivity are complex as well. NaOH, which has only a minor effect on porosity, increased the permeability of the coastal sample by 3.43 times at 500 psi and 6.75 times at 5000 psi (Table 7). At the same time, pressure sensitivity, as measured by the change in slope of logarithmic

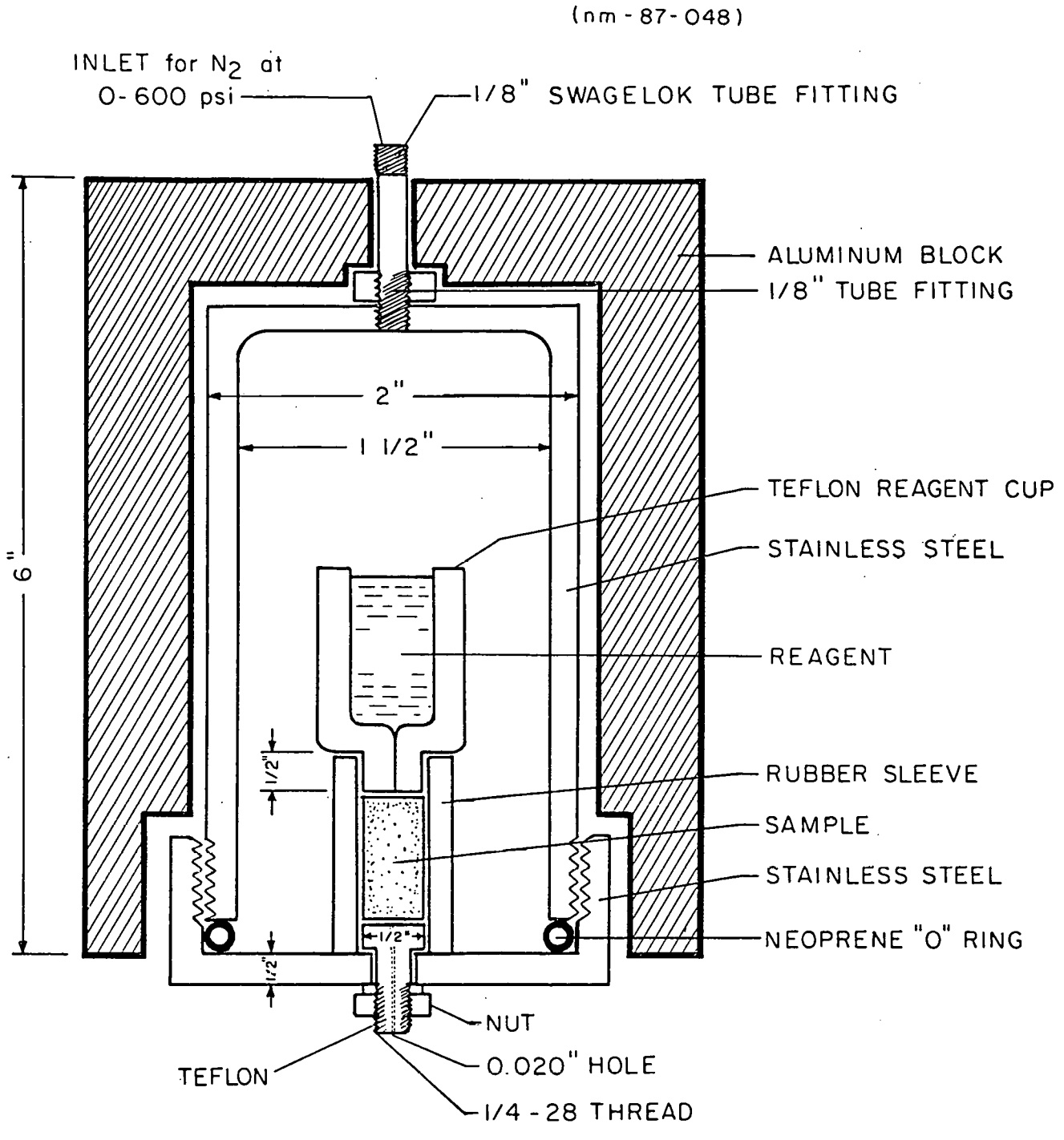

Figure 9. Apparatus used to flush cores with reagents.

Table 6

Core Properties Before and After Chemical Treatments

Core	Treatment	Porosity (%)		BET Surface Area (m^2/g)		Permeability (μd) at 500 psi		Permeability (μd) at 5000 psi		Slope	
		before	after	before	after	before	before	after	after	before	after
MWX3 64-29	HCl	8.30	9.71	2.98	3.43	10.81	2.33	13.30	3.16	-0.555	-0.559
	HAc	8.20	9.59	2.79	2.91	11.50	2.29	14.40	3.21	-0.584	-0.568
	HAc-buf	8.17	8.48	3.35	4.08	10.89	2.35	11.70	2.17	-0.592	-0.646
	NaOH	8.16	8.93	3.09	4.99	11.02	2.46	37.80	16.60	-0.562	-0.347
	Na_2CO_3	7.88	7.98	3.16	2.41	11.12	1.65	11.50	2.02	-0.707	-0.667
	EDTA	8.31	11.32	3.22	4.02	10.97	2.20	23.60	3.96	-0.596	-0.678
MWX3 63-16	HCl	7.33	9.80	3.71	4.99	9.04	1.03	22.07	2.97	-0.799	-0.763
	HAc	7.32	9.87	3.76	3.12	9.90	1.12	23.98	1.94	-0.811	-0.920
	HAc-buf	7.12	6.77	3.21	3.13	7.04	1.12	9.05	0.96	-0.667	-0.838
	NaOH	7.19	6.95	3.43	3.01	7.19	1.00	7.06	1.76	-0.764	-0.523
	Na_2CO_3	7.11	6.82	3.46	2.79	6.69	1.11	7.80	1.24	-0.671	-0.643
	EDTA	7.13	8.17	3.40	2.98	7.82	0.98	13.30	1.45	-0.766	-0.882

Table 7

Ratios of Treated to Untreated Core Properties

Core	Treatment	Porosity	Surface Area	$K_{\infty,500}$	$K_{\infty,5000}$	Slope
MWX3 64-29	HCl	1.17	1.15	1.23	1.36	1.01
	HAc	1.17	1.04	1.25	1.40	0.97
	HAc-buf	1.04	1.22	1.07	0.92	1.09
	NaOH	1.09	1.61	3.43	6.75	0.62
	Na_2CO_3	1.01	0.76	1.03	1.22	0.94
	EDTA	1.36	1.25	2.15	1.80	1.14
MWX3 63-16	HCl	1.34	1.35	2.44	2.88	0.95
	HAc	1.35	0.83	2.42	1.73	1.13
	HAc-buf	0.95	0.98	1.29	0.86	1.26
	NaOH	0.97	0.88	0.98	1.76	0.68
	Na_2CO_3	0.96	0.81	1.17	1.12	0.96
	EDTA	1.15	0.88	1.70	1.48	1.15

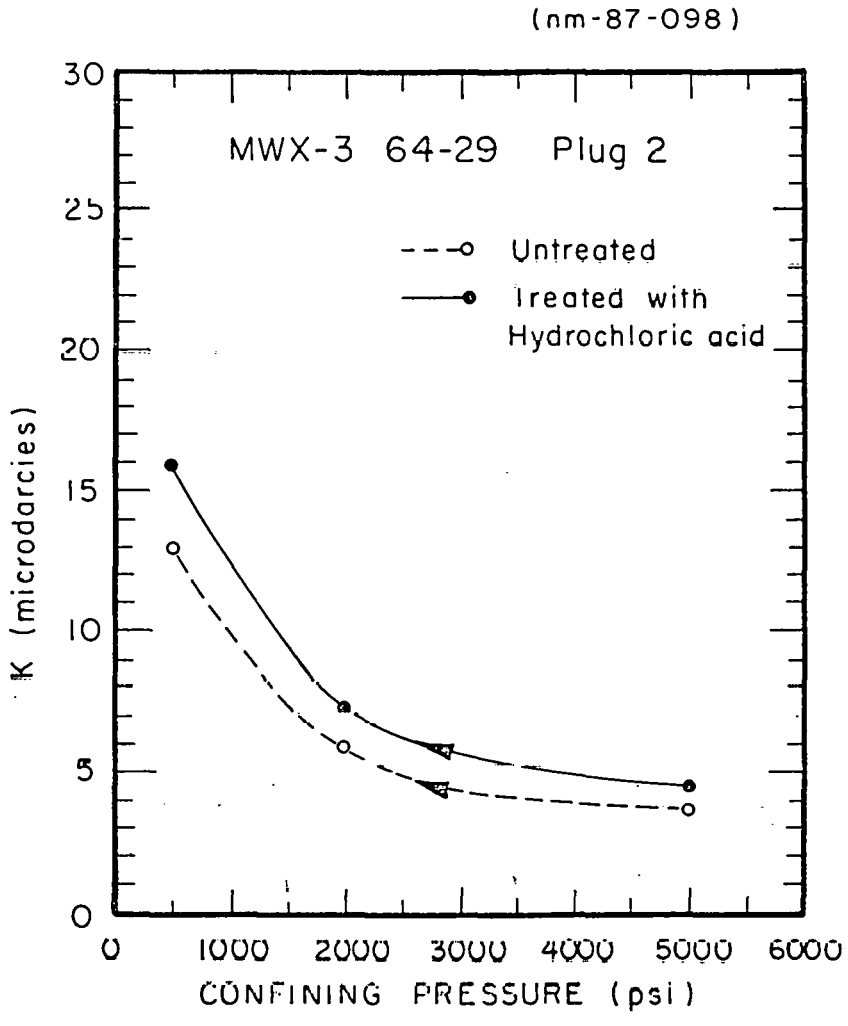

Figure 10a. Changes in permeability vs. confining pressure for various chemical treatments of a coastal core (hydrochloric acid).

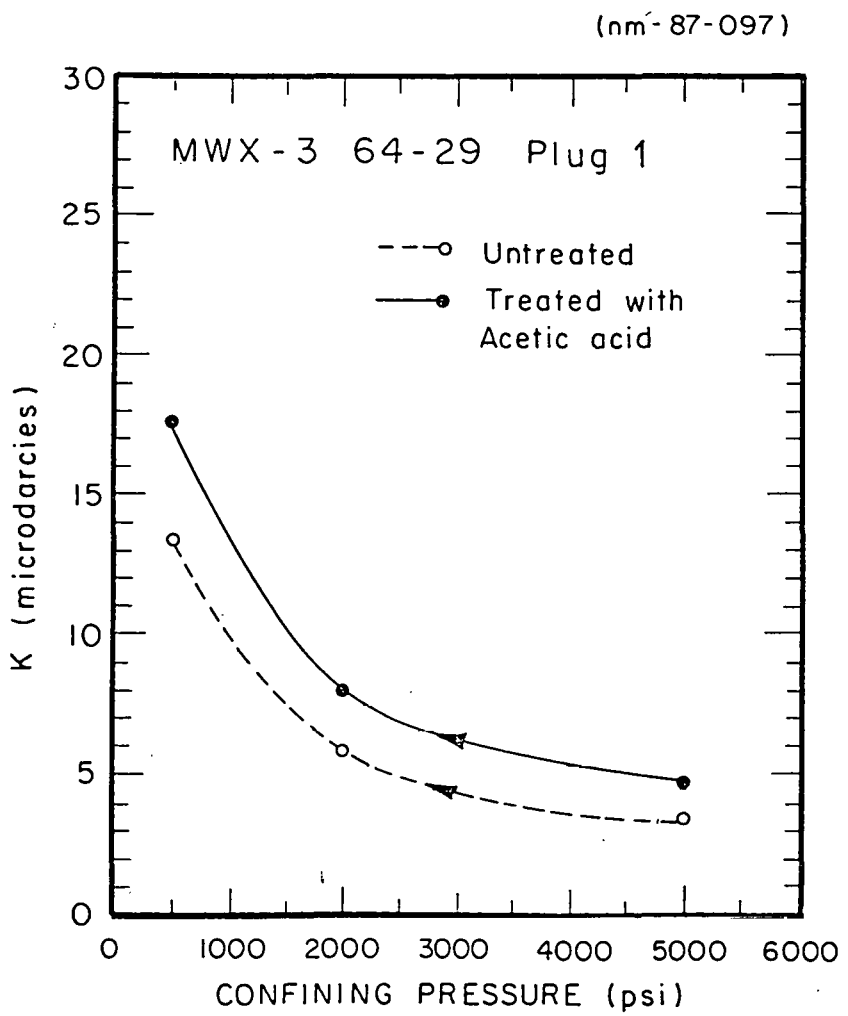

Figure 10b. Changes in permeability vs. confining pressure for various chemical treatments of a coastal core (acetic acid).

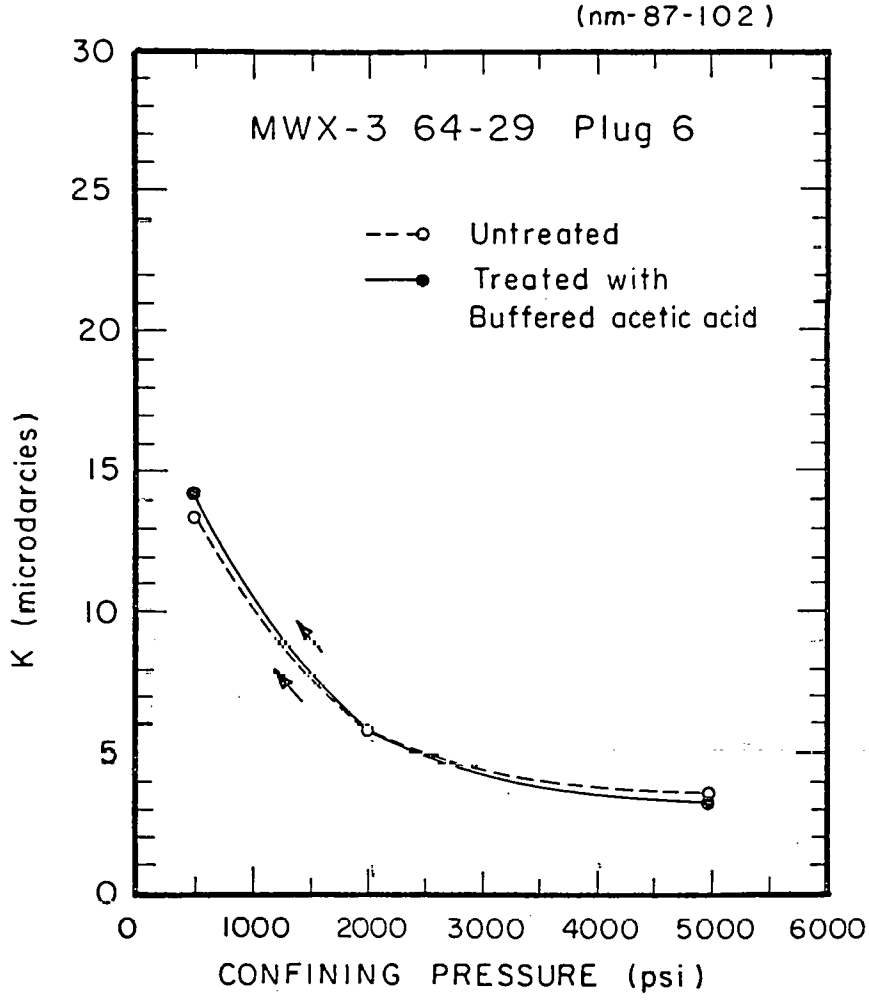

Figure 10c. Changes in permeability vs. confining pressure for various chemical treatments of a coastal core (buffered acetic acid).

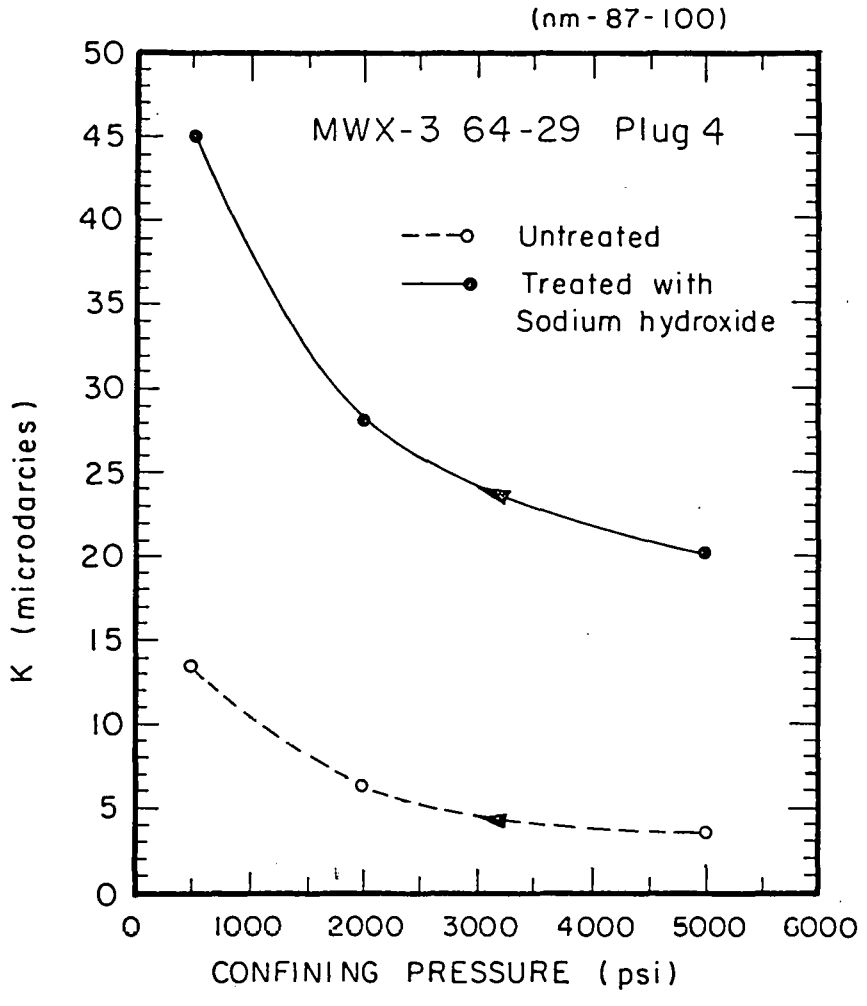

Figure 10d. Changes in permeability vs. confining pressure for various chemical treatments of a coastal core (sodium hydroxide).

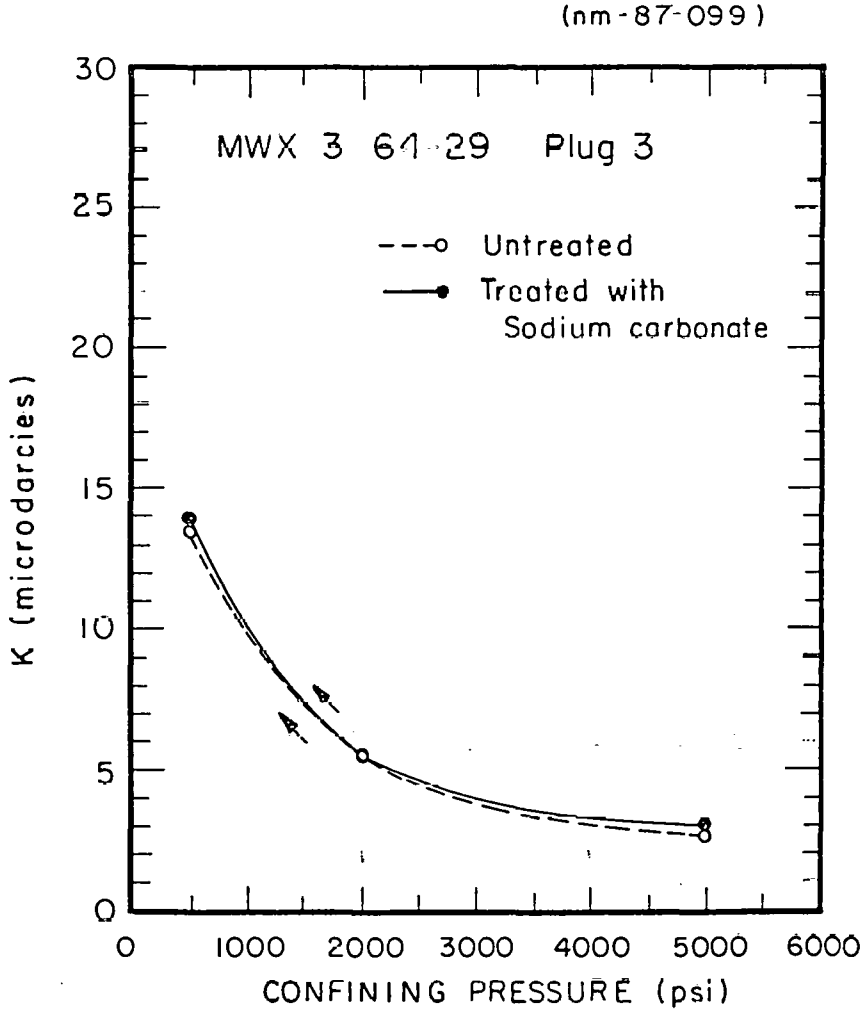

Figure 10e. Changes in permeability vs. confining pressure for various chemical treatments of a coastal core (sodium carbonate) .

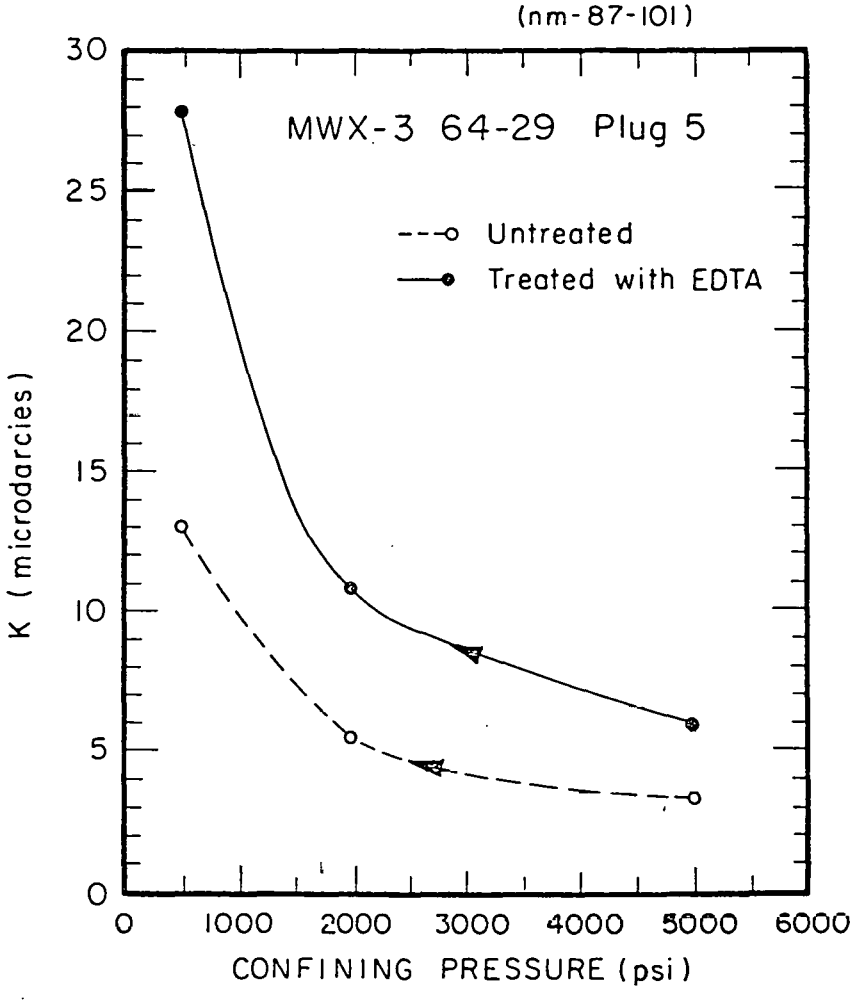

Figure 10f. Changes in permeability vs. confining pressure for various chemical treatments of a coastal core (EDTA).

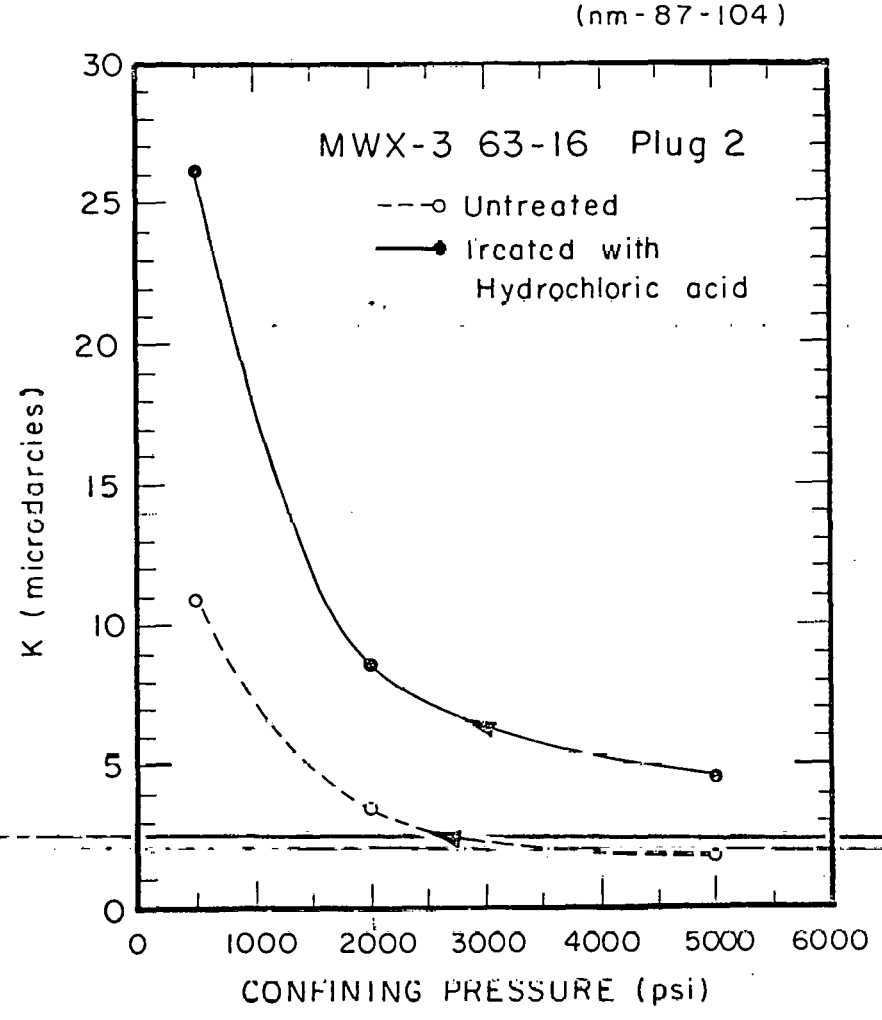

Figure 11a. Changes in permeability vs. confining pressure for various chemical treatments of a fluvial core (hydrochloric acid) .

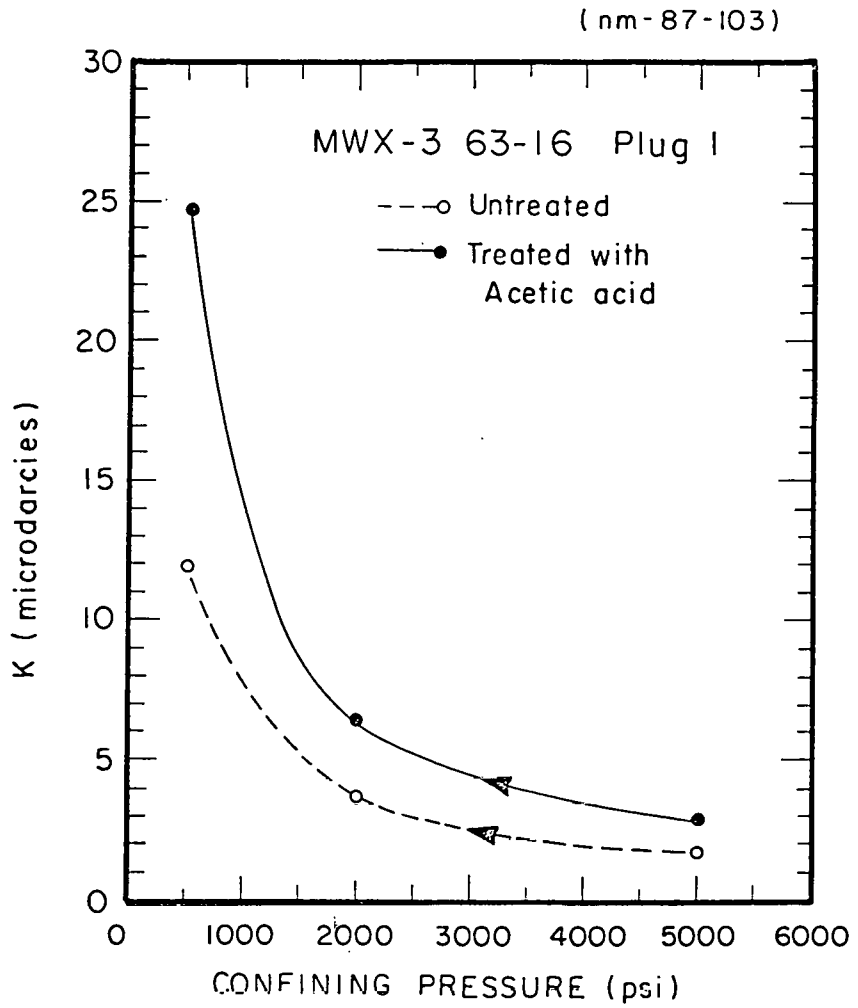

Figure 11b. Changes in permeability vs. confining pressure for various chemical treatments of a fluvial core (acetic acid).

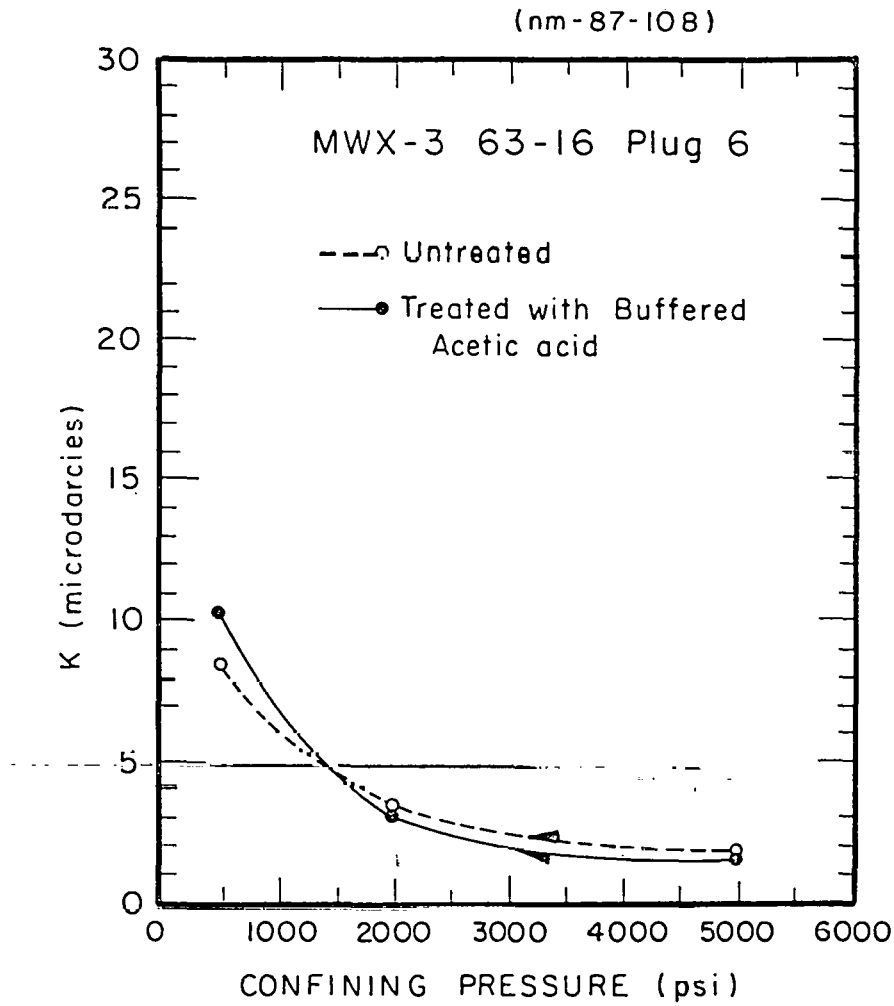

Figure 11c. Changes in permeability vs. confining pressure for various chemical treatments of a fluvial core (buffered acetic acid).

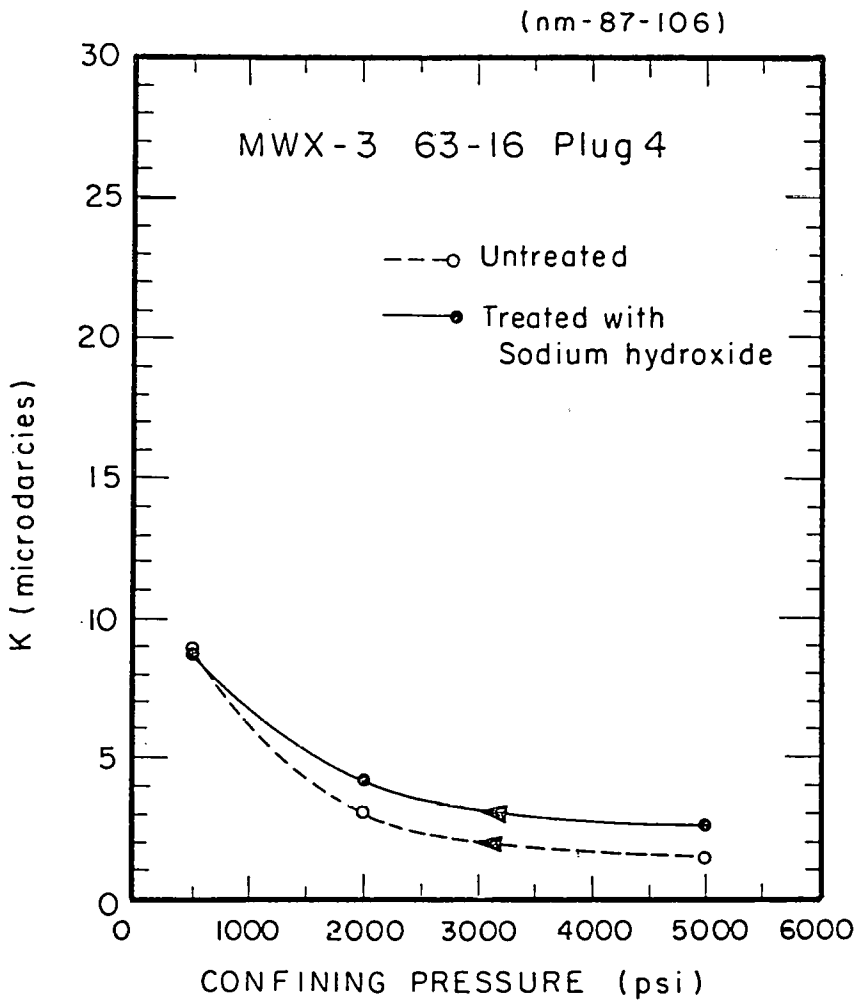

Figure 11d. Changes in permeability vs. confining pressure for various chemical treatments of a fluvial core (sodium hydroxide).

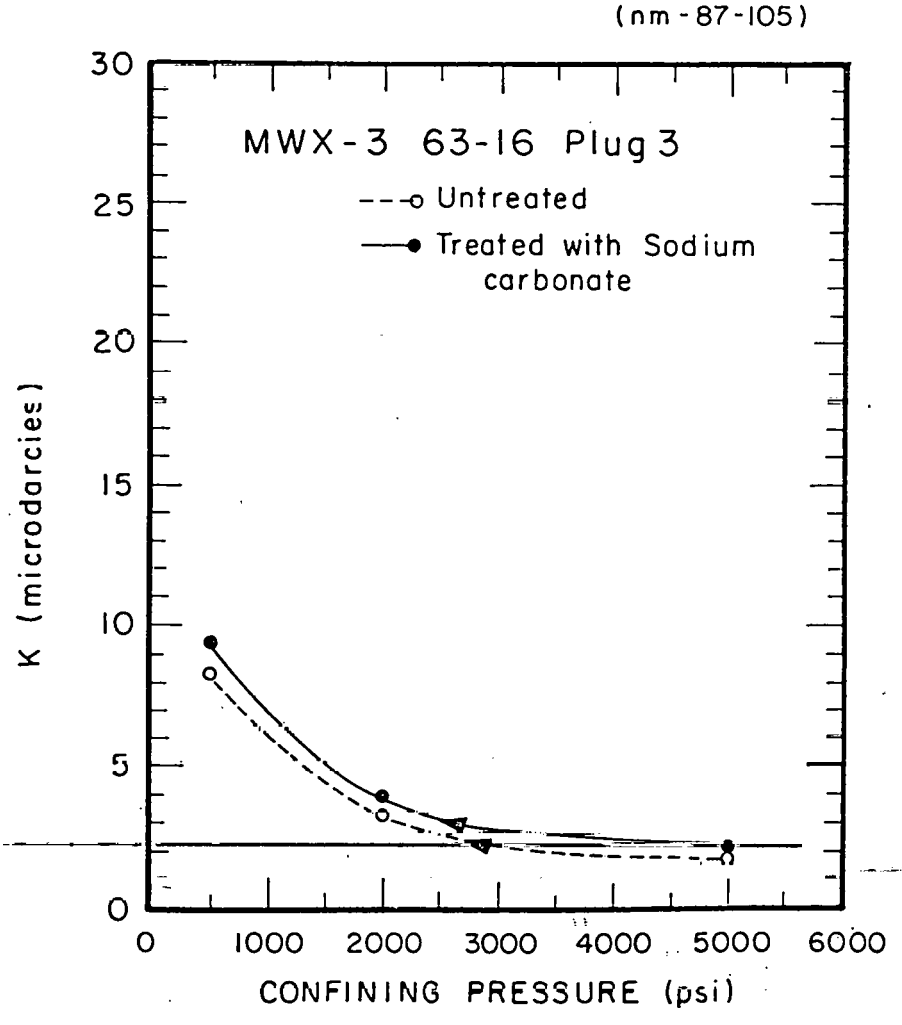

Figure 11e. Changes in permeability vs. confining pressure for various chemical treatments of a fluvial core (sodium carbonate) .

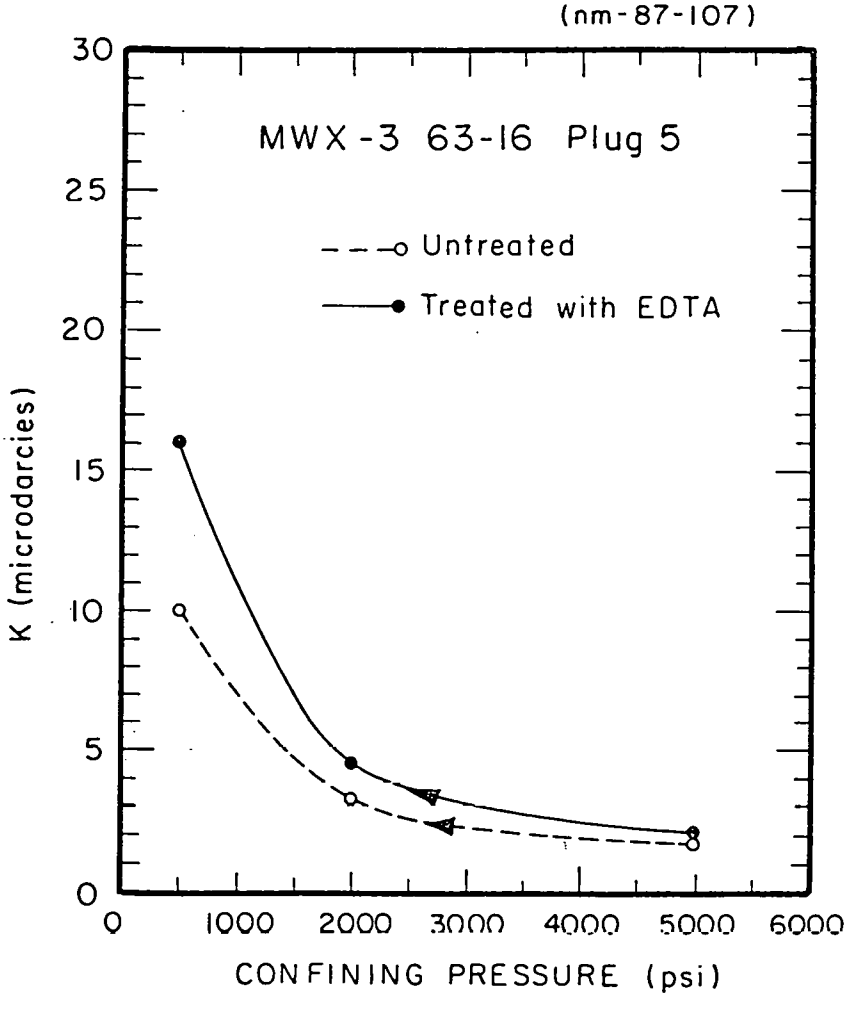

Figure 11f. Changes in permeability vs. confining pressure for various chemical treatments of a fluvial core (EDTA).

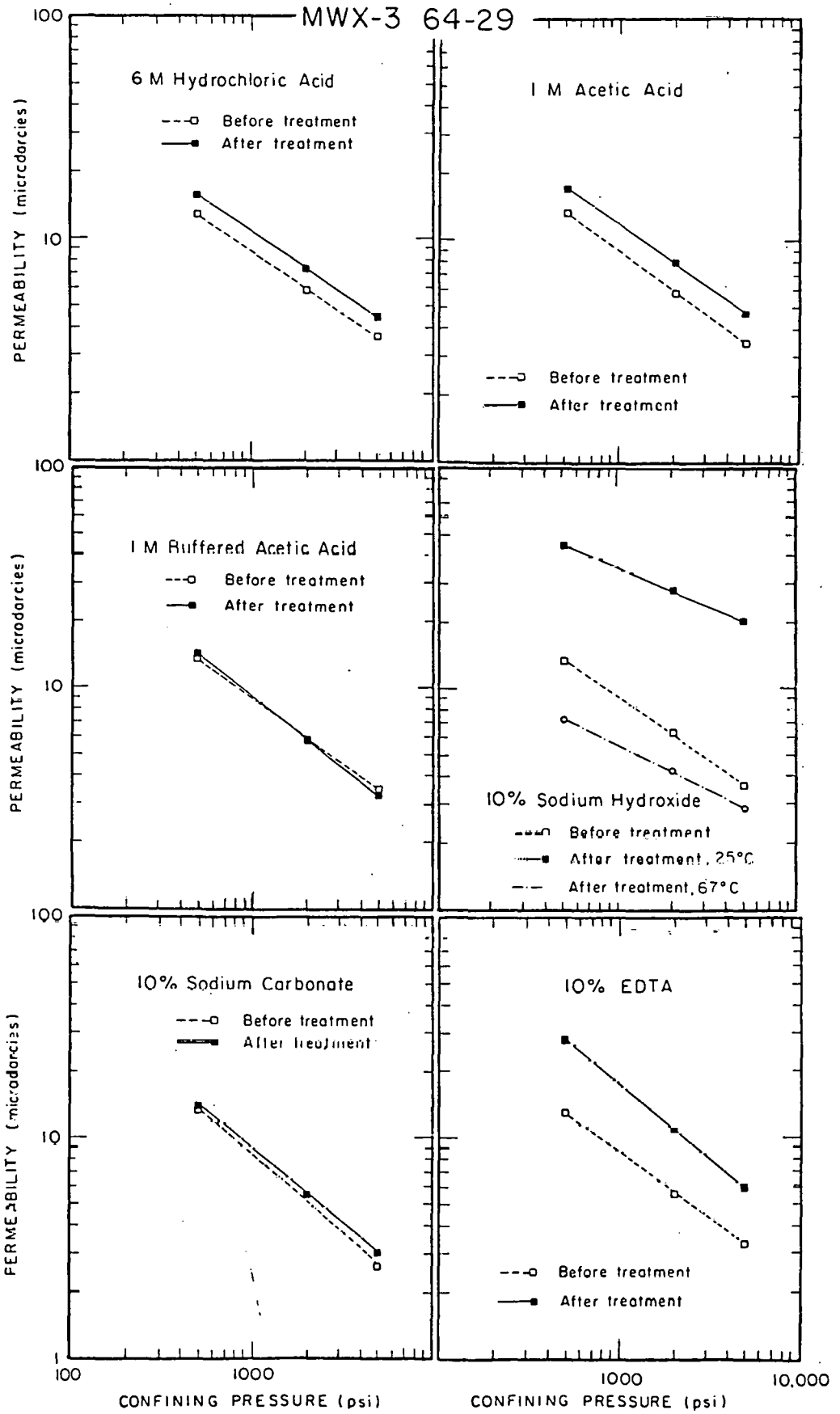

Figure 12. Log-log plots pf permeability vs. confining pressure for a coastal sample (changes in slope indicate relative changes in pressure sensitivity).

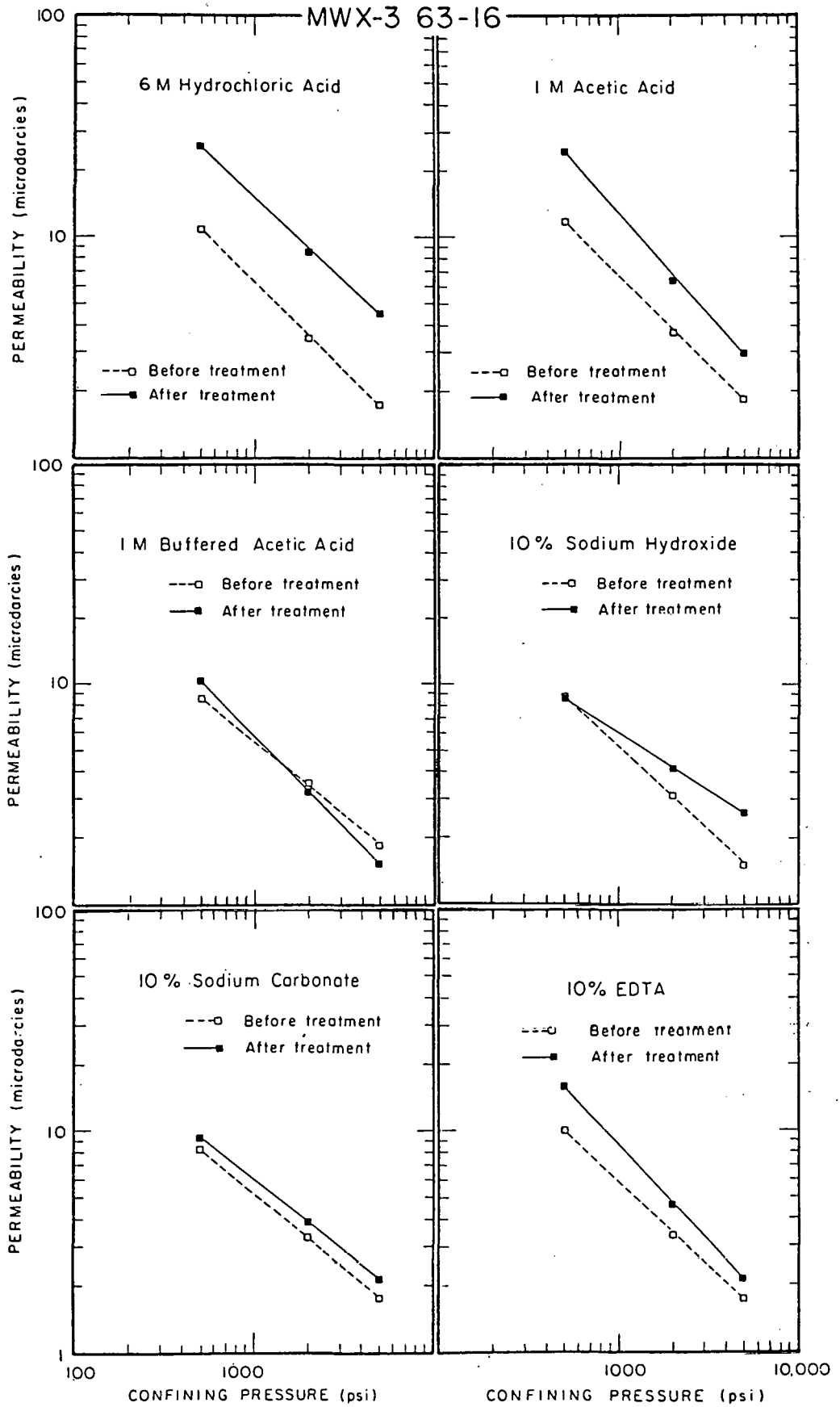

Figure 13. Log-log plots of permeability vs. confining pressure for a fluvial sample (changes in slope indicate relative changes in pressure sensitivity).

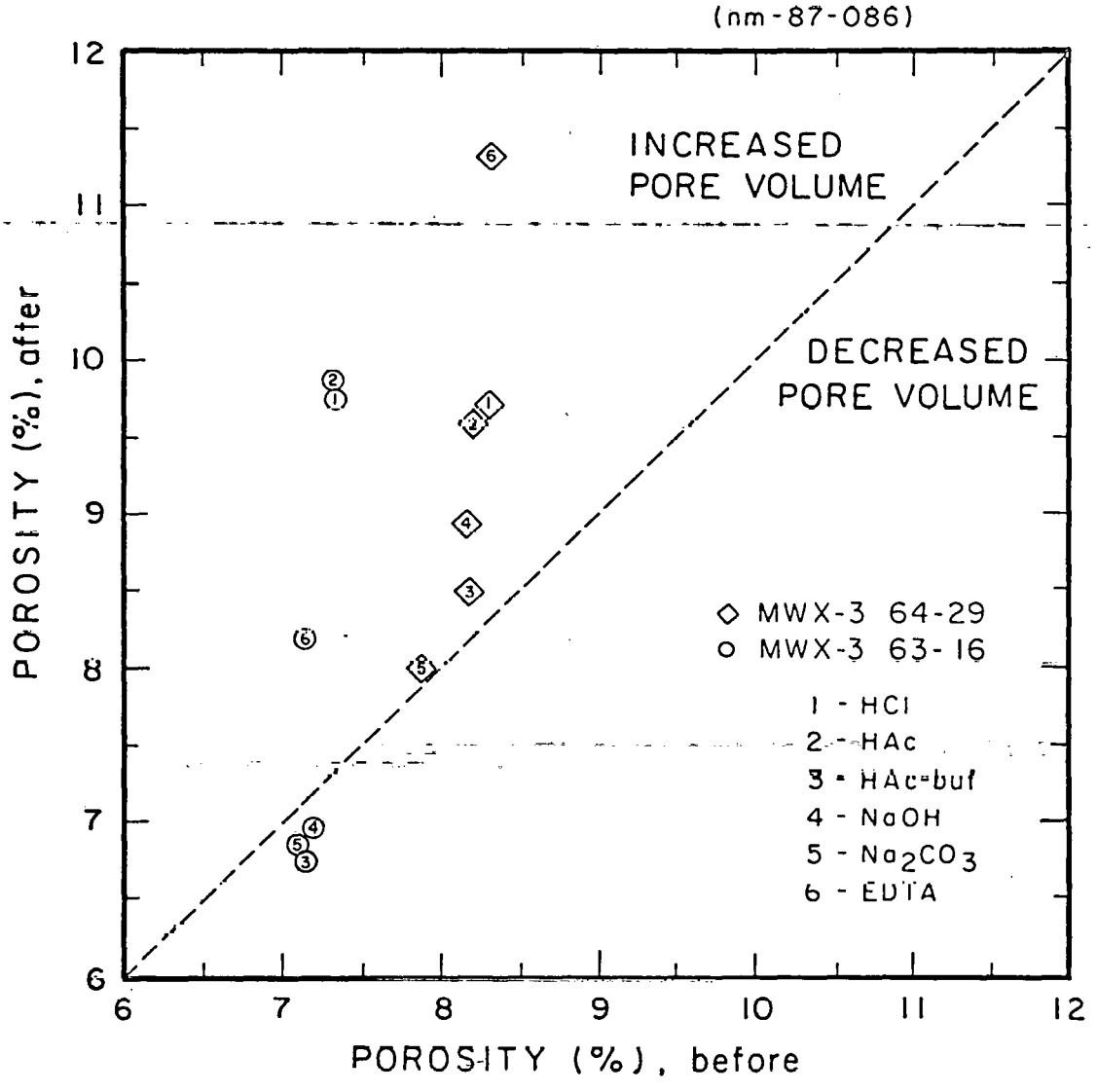

Figure 14. Porosity after chemical treatment vs. original porosity.

plots of permeability vs. confining pressure, decreased about 38% (Table 7 and Fig. 15). This was the largest decrease in pressure sensitivity and the largest increase in permeability of any of the tested chemicals. In the fluvial sample the results were somewhat different. Porosity and permeability at low confining pressure decreased very slightly but pressure sensitivity showed a 32% decrease. This decrease in pressure sensitivity is comparable to the effect of treating the coastal sample with NaOH (see Figs. 12 and 13).

Unlike sodium hydroxide, the acidic reagents increased porosity and permeability, but had little effect on pressure sensitivity, or increased it. The EDTA treatment increased all three parameters: porosity, permeability and pressure sensitivity, for both coastal and fluvial samples.

These results suggest at least two mechanisms, both of which dissolve material and increase pore space. The first of these, which is important for the strongly basic NaOH treatment, involves dissolution of silicates and alumino silicates in the high-aspect-ratio sheet pores, increasing conduction of fluid through the originally most constricted pores. Increasing the width of the sheet pores also decreases pressure sensitivity since the widened cracks are harder to close under pressure. In thin section, some dissolution of quartz overgrowths and widening of sheet pores could be seen for NaOH treatment of the coastal sample. Changes in the fluvial sample were not obvious from petrographic examination.

Further complexity may be contributed if some of the dissolved material reprecipitates as the NaOH solution moves through the core plug. The drop in pressure sensitivity for the fluvial sample, comparable to that observed for the coastal sample, argues that the same kind of initial sheet-pore widdening is occurring, but plugging caused by reprecipitation may counter the widening effect so that little or no net change is observed in either permeability or porosity.

Some additional NaOH floods were performed at higher temperature (67°C) with the objective of increasing the reaction rate and hence the effect of NaOH treatment. Fig. 12d shows the permeability vs. confining pressure relationship for a second plug MWX3 64-29. After treatment, permeabilities were lower than those measured for the original plug. The experiment was repeated for another coastal sample, MWX3 42-4. Results are shown in Fig. 16. Here the results for untreated and treated conditions are for the same core plug. Again the low pressure permeability is lower after treatment and there is large decrease in pressure sensitivity. This is consistent with the view that dissolution and widening of sheet pores account for decrease in pressure sensitivity with the absolute permeability determined by the degree of reprecipitation which is greater at 67°C than at ambient conditions.

The effect of acidic reagents requires a different explanation. Here porosity and permeability increase without a corresponding decrease in pressure sensitivity. In thin-section, dissolution of intergranular carbonates is observed. It appears that flow paths along sheet-pore networks are effectively shortened by removal of the carbonates but there is not much change in pressure sensitivity because this is controlled mainly by quartz overgrowths which form sheet pores at grain boundaries.

An additional sample of MWX3 64-29 was tested using oxalic acid because of recent suggestions about the importance of dicarboxylic acids in diagenetic processes.[14] Fig. 17 shows the results of treatment with 10% oxalic acid. Increases

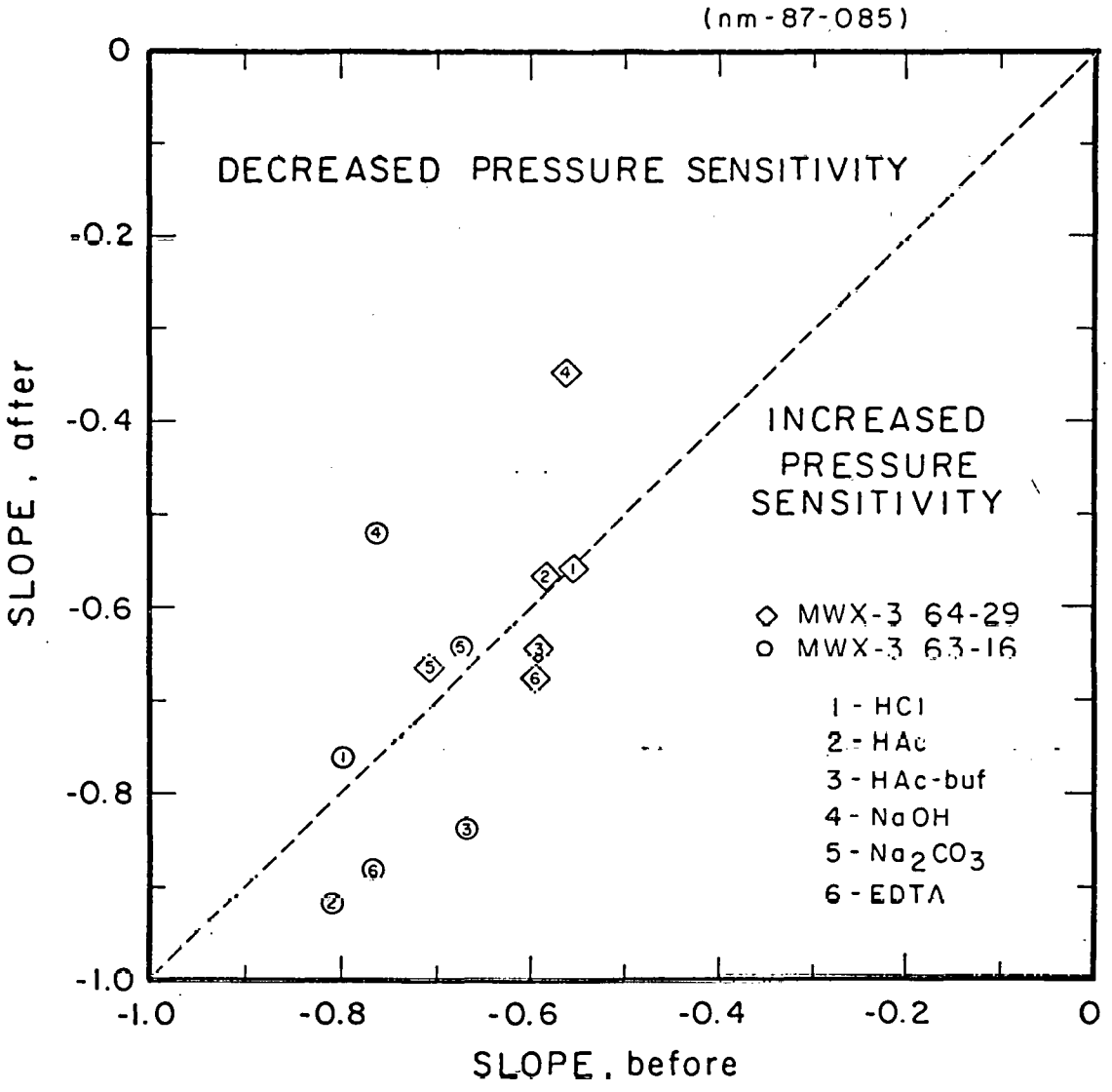

Figure 15. Slope of log K vs. log P after chemical treatment vs. original slope.

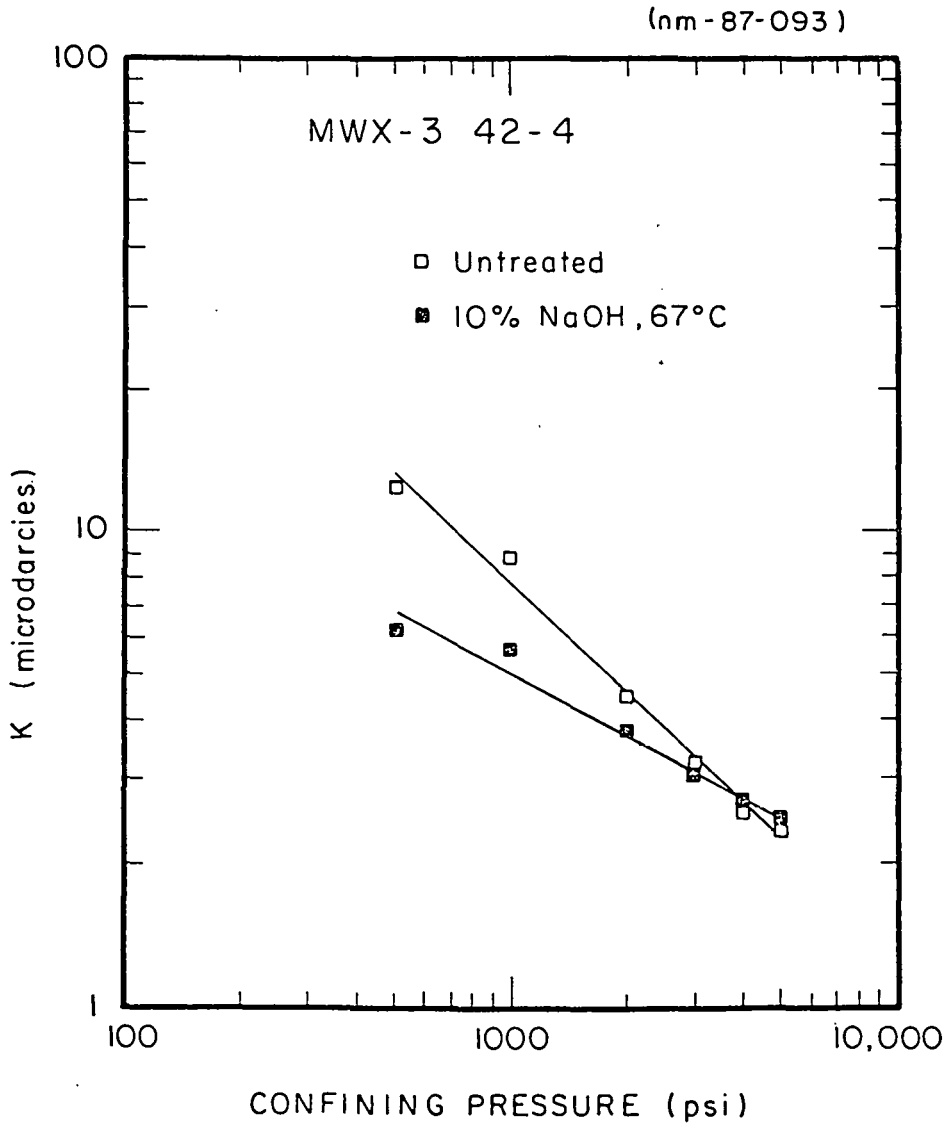

Figure 16. Effect of hot sodium hydroxide treatment on K vs. P relationship.

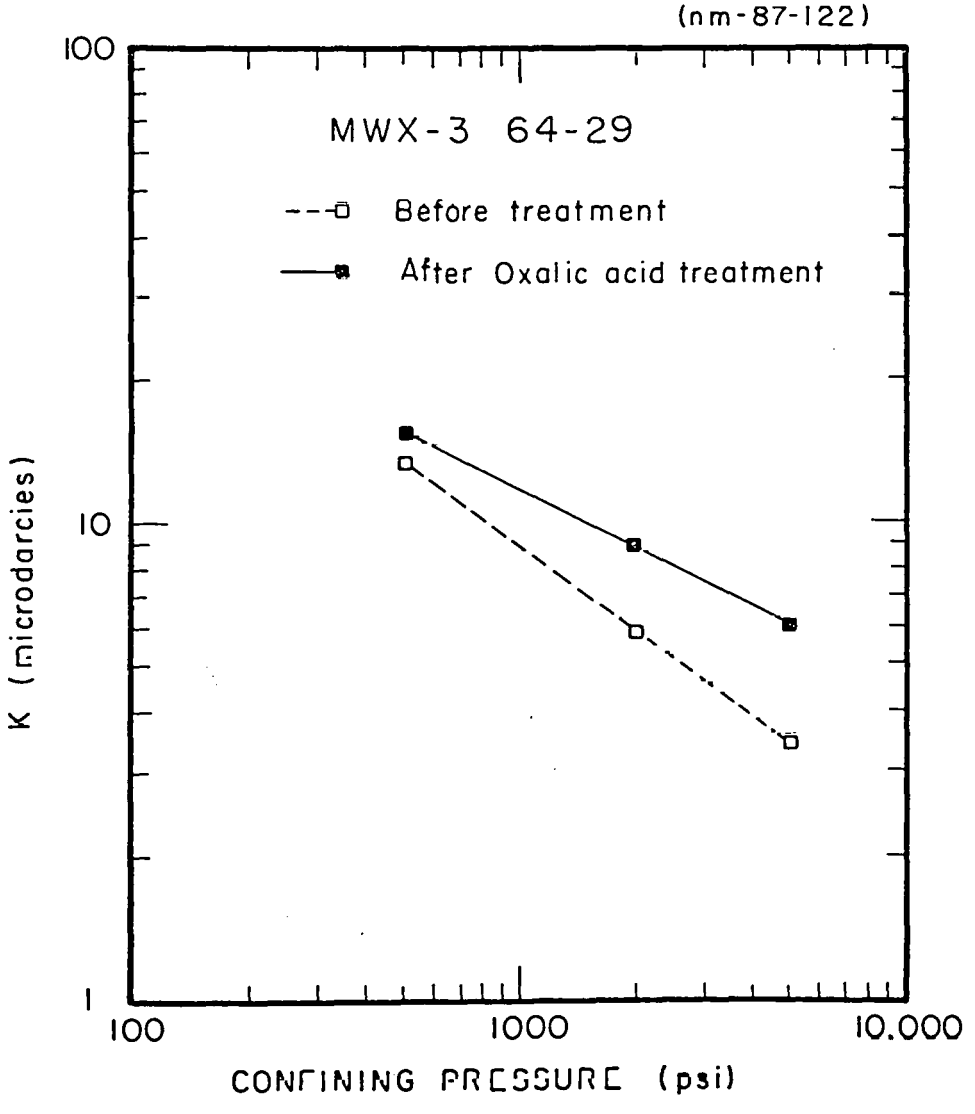

Figure 17. Effect of oxalic acid treatment on K vs. P relationship.

in permeability are similar to those seen for acetic acid, but there is also significant change in pressure sensitivity. Dicarboxylic acids can enhance solubility of silicates and alumino silicates[14] and thus oxalic acid may cause crack widening analagous to the effects of NaOH. Additional tests are needed to confirm the difference in actions of dicarboxylic and the monocarboxylic acid.

EDTA, a powerful chelating agent, increased porosity, permeability and pressure sensitivity for both the coastal and fluvial samples. The action of EDTA appeared to be most like the acidic reagents. Chelation of divalent cations may shift the position of equilibrium, promoting dissolution of calcium carbonate. As in the case of acetic and hydrochloric acids, this dissolution appears to add conductive pathways.

Surface areas measured before and after the full suite of chemical treatments are reported in Table 7 and Fig. 18. Each sample shows the greatest increase in surface area with the largest increases in absolute permeability (HCl treatment of MWX3 63-16 and NaOH treatment of MWX3 64-29). Beyond this one observation, no systematic trends in surface area with particular chemical treatments are seen. The surface areas of MWX3 64-29 were higher after treatment for 5 out of 6 tests whereas the MWX3 63-16 surface areas decreased for 4 cases out of 6.

SUMMARY OF CHEMICAL TREATMENT STUDY

It is possible to increase permeability of Multi-Well core by a wide variety of chemical treatments. The most consistent increases were observed with HCl, acetic acid and EDTA which increased permeability at all levels of confining pressure for both the coastal and fluvial samples. The fluvial sample was changed more by the acidic reagents and the coastal was more affected by EDTA.

Sodium hydroxide had a major effect on pressure sensitivity, making samples significantly less sensitive in all tests. This result suggests that NaOH widens sheet pores by dissolution of quartz overgrowths or pore lining clay minerals. The absolute permeability following treatment with NaOH depended on the balance between dissolution and reprecipitation. In one case, MWX3 64-29 at 25°C, a dramatic rise in permeability was observed. In other tests run at both 25° and 67°C, permeabilities rose only slightly or decreased.

Neither sodium carbonate nor buffered acetic acid had a major effect on the permeability of the Multi-Well samples under the conditions of these tests. Changes in surface area with chemical treatment do not show any distinct trends with respect to changes in permeability and pressure sensitivity.

The effect of oxalic acid treatment of a coastal sample was to increase permeability but decrease pressure sensitivity. This suggests that comparable tests should be run in a fluvial sample followed by an experiment at elevated temperature to see whether plugging is observed, as with NaOH.

TASK 4 EFFECT OF WATER ON GAS PRODUCTION

Work performed under Task 4 for Phase III concerns the effect of drying on the properties of low permeability gas sands. The proposed work was to compare permeabilities from preserved reservoir core samples (not allowed to dry after recovery) to conventional cores (i.e. cores which were not protected from drying).

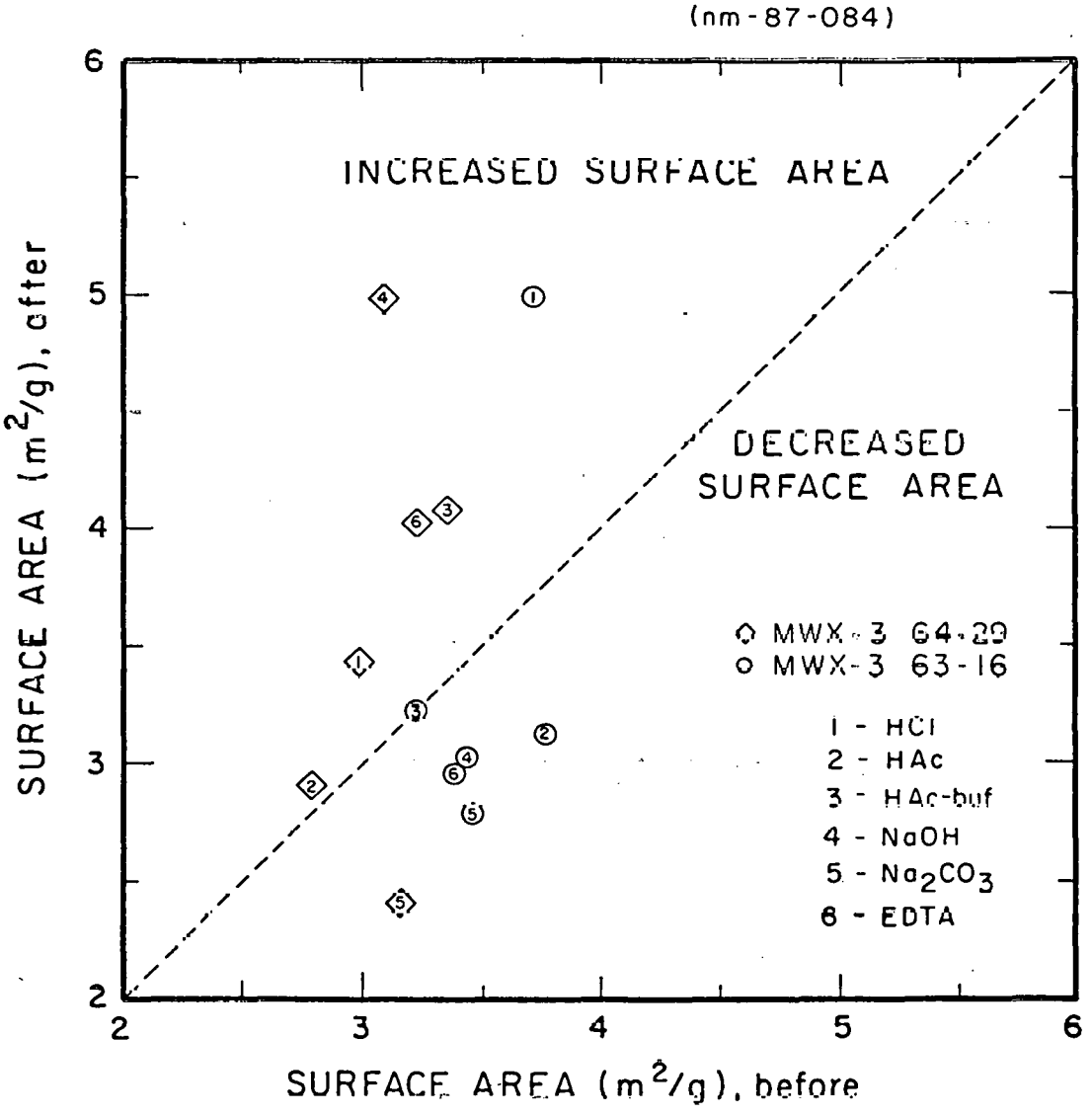

Figure 18. Surface areas from nitrogen adsorption before and after chemical treatment.

Preliminary results are also presented on comparisons of the effect of confining pressure on permeability and electrical conductivity.

INTRODUCTION

For most sedimentary rocks, brine permeabilities are significantly lower than Klinkenberg gas permeabilities.[10] For low permeability gas sands the difference is often a factor of 5 to 20.[10] In addition to differences in gas and brine permeabilities it has also been found that drying can cause changes in pore structure. Permeabilities of undried preserved cores can be much lower than those given by the usual core analysis procedure of storing cores in a dry state and then resaturating them with brine for permeability measurements. Circumstances under which drying could have marked effect on pore structure and permeability were demonstrated by Heavyside et al.[15] and Pallatt, Wilson and McHardy.[16] Detailed investigation was made of cores from the Magnus field. These showed significant increase in permeability with drying. Production tests indicated water permeabilities many times lower than those measured by normal core testing. It was suspected that capillary forces which develop during drying caused changes in pore structure. Electron micrographs of samples which had been subjected to critical point drying (drying without phase change) showed the presence of filamentous illite. The clay was no longer present in this form after drying.[16]

Tight gas sands, as demonstrated in particular by their adsorption properties, contain a high percentage of microporosity. Because changes in the structure of microporosity caused by drying may seriously affect measurements on cores from tight gas sands, comparisons have been made of the flow properties of fresh cores (wrapped and sealed for prevention of drying directly after recovery from the field) and conventional (dried) cores.

PRESERVED CORES

Sealed core samples obtained during the course of the MWX field experiment were used to study the effects of drying (see Table 8). Stored samples had been wrapped with Saran plastic and aluminum foil and then dipped in hot molten plastic which sets up around the core in a coating of about 1/4-1/2" in thickness. After breaking the seal, the samples were stored in a high humidity environment so that plugs could be cut at will from a core which had never been allowed to dry, at least intentionally.

PERMEABILITY MEASUREMENTS

Experimental

Flow tests were performed on plugs half-inch in diameter by approximately one inch in length using methods described previously.[5] Preserved core plugs were saturated with either distilled water or brine and liquid permeabilities were measured for first unloading from 5000 psi down to 500 psi. Core plugs used in relative permeability measurement were then allowed to dry by evaporation to the desired saturation. Relative permeabilities to nitrogen gas were determined at 60%, 45%, 30% and 15% saturations. Dried cores were heated at 110°C for several hours. Gas permeability was measured for oven-dried plugs and the core was then resaturated and

Table 8

Summary of Tests Performed on Multi-Well Preserved Core Samples

Sample ID	Depth (ft)	Initial Moisture Content	Permeability Measurements			Desorption Adsorption	Gas Permeability (K_∞)
			Water	Brine	Relative		
MWX3 42-4	6546.5-6547.1		X	X	X	X	X
MWX1 33-10	5962.6-5969.0			X	X	X	X
MWX1 33-12	5968.5-5969.0	X					
MWX3 58-11	4916.7-4917.3	X		X			
MWX3 58-19	4900.1-4901.0	X					
MWX3 59-1	4923.1-4923.6	X					

measurements of liquid and relative permeabilities were repeated. Core plugs were then dried to constant weight at 110°C and gas permeabilities were remeasured.

ABSOLUTE BRINE PERMEABILITIES OF PRESERVED AND DRIED CORES

Preserved cores, as received, were generally less than 100% saturated. Distilled water and brine were used to raise the preserved core saturation to 100% before performing permeability measurements. Several considerations went into the choice of fluid. Salinities in the Multi-Well cores are uncertain because it is difficult to obtain brine samples, and samples might not be representative due to changes in salinity caused by invasion of cores by drilling fluid. Results suggest that salinities, in the Multi-Well gas sands are relatively low, being about 10,000 ppm.[17]

After a core is dried, salt will be retained in the core so that the original concentration should be restored by resaturation with distilled water. However, during redissolution of the salt, extreme local concentration gradients could arise, which could cause clay damage. These extremes can be avoided by resaturating with a brine. A 3.55% NaCl solution was tested as being representative of the formation. In other tests, brine permeabilities were measured using 8% KNO_3, a composition used by Jennings et al.[18] for improved clay stabilization and reduced corrosion. NaN_3 (0.02%) was added to the brine solution to control the growth of micro-organisms. Comparison of results obtained using different brines and distilled water provided an indication of the relative seriousness of the compromises that must be made in adoption of core testing procedures.

RESULTS

Absolute Permeabilities

Measurements of the effect of drying on absolute permeabilities to brine and gas as a function of a confining pressure (first unloading) were reported previously for core sample MWX3 42-4.[8] Three additional sets of data have now been obtained (Figs. 19-21). In all cases the permeabilities of the preserved cores were lower than those of the dried cores at all levels of overburden pressure.[19] Drying approximately doubled the measured permeabilities. However, for core MWX1 33-10 at confining pressures above 2,000 psi permeabilities for the preserved core were extremely low, being less than 0.01 μd.

Relative Permeability to Gas

Permeabilities to gas with reduction in water saturation were also compared for preserved and dried cores (Figs. 22, 23). At a given level of overburden and brine saturation, gas permeabilities of the preserved cores is always less than those of the dried cores. As water saturation is reduced, differences in the two sets of data become less. These differences are virtually eliminated when the water saturation is reduced to 30%, suggesting that this is sufficient desaturation to cause structural changes because of capillary forces which develop during drying.

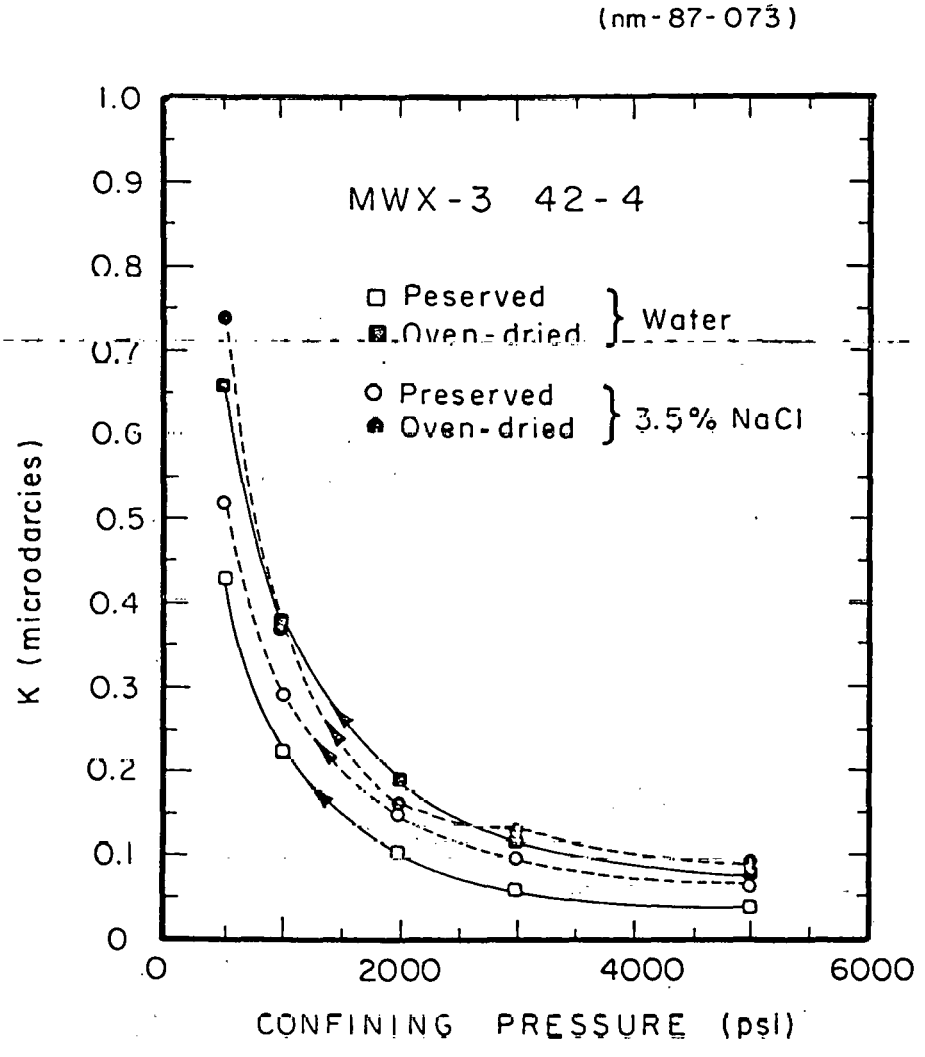

Figure 19. Change in P vs. K relationship for preserved and dried cores (MWX3 42-4)

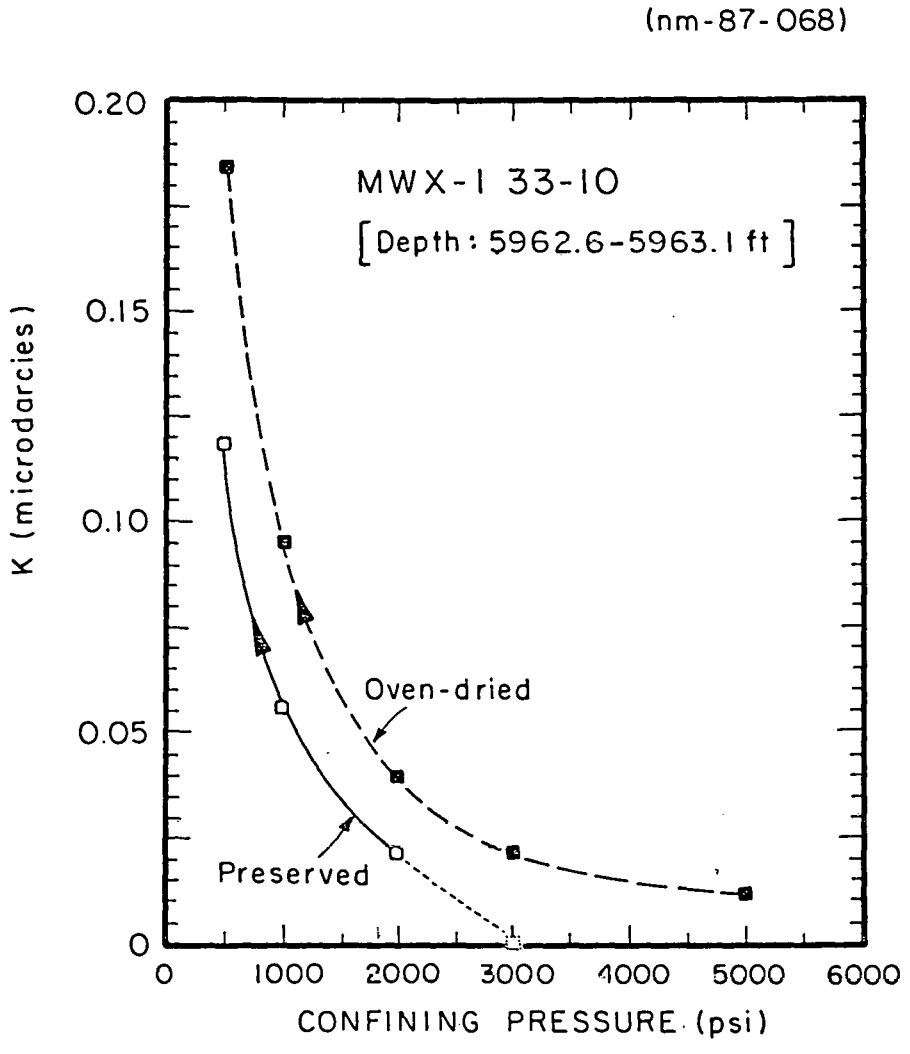

Figure 20. Increase in permeability caused by drying (MWX1 33-10).

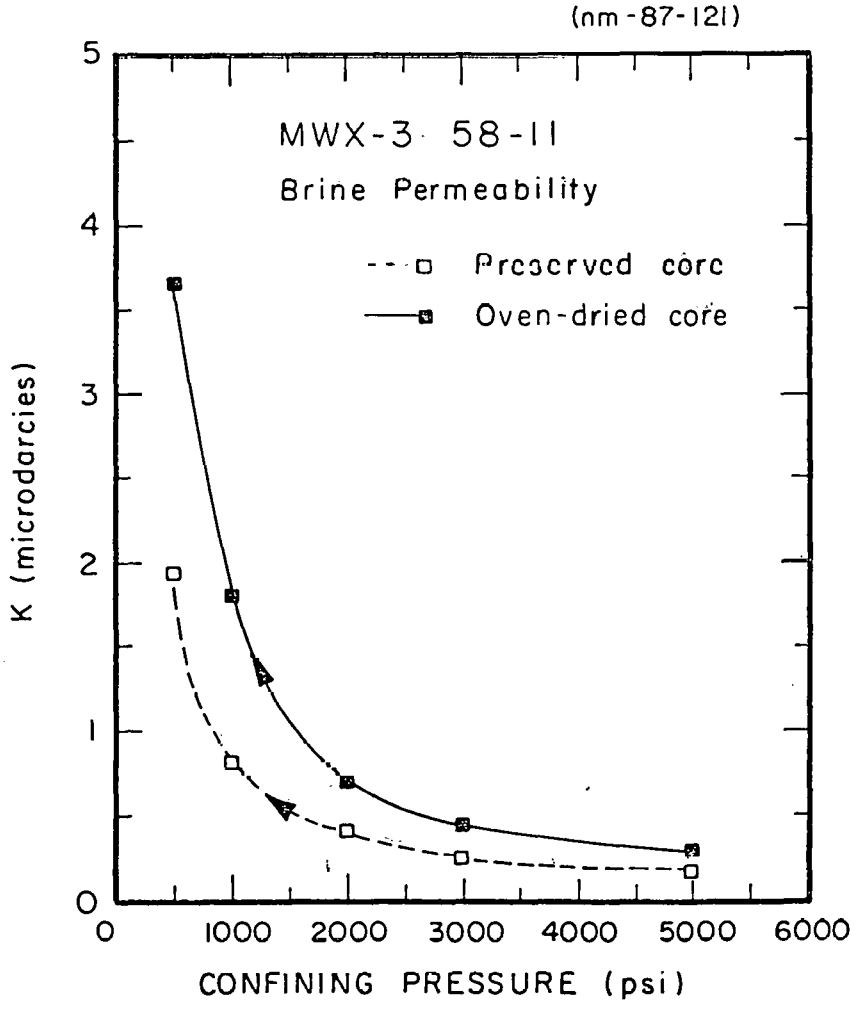

Figure 21. Increase in permeability caused by drying (MWX3 58-11).

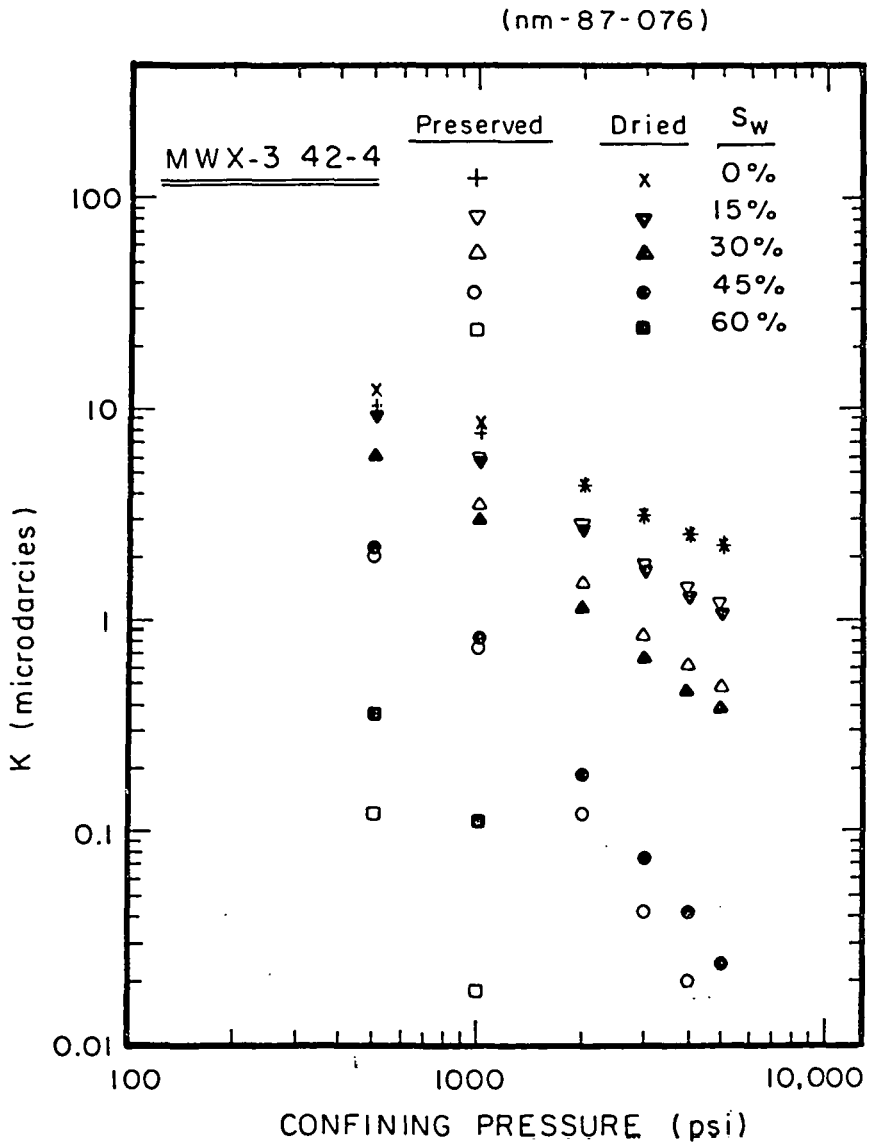

Figure 22. Relative permeability to gas for preserved and previously dried core (MWX3 42-4).

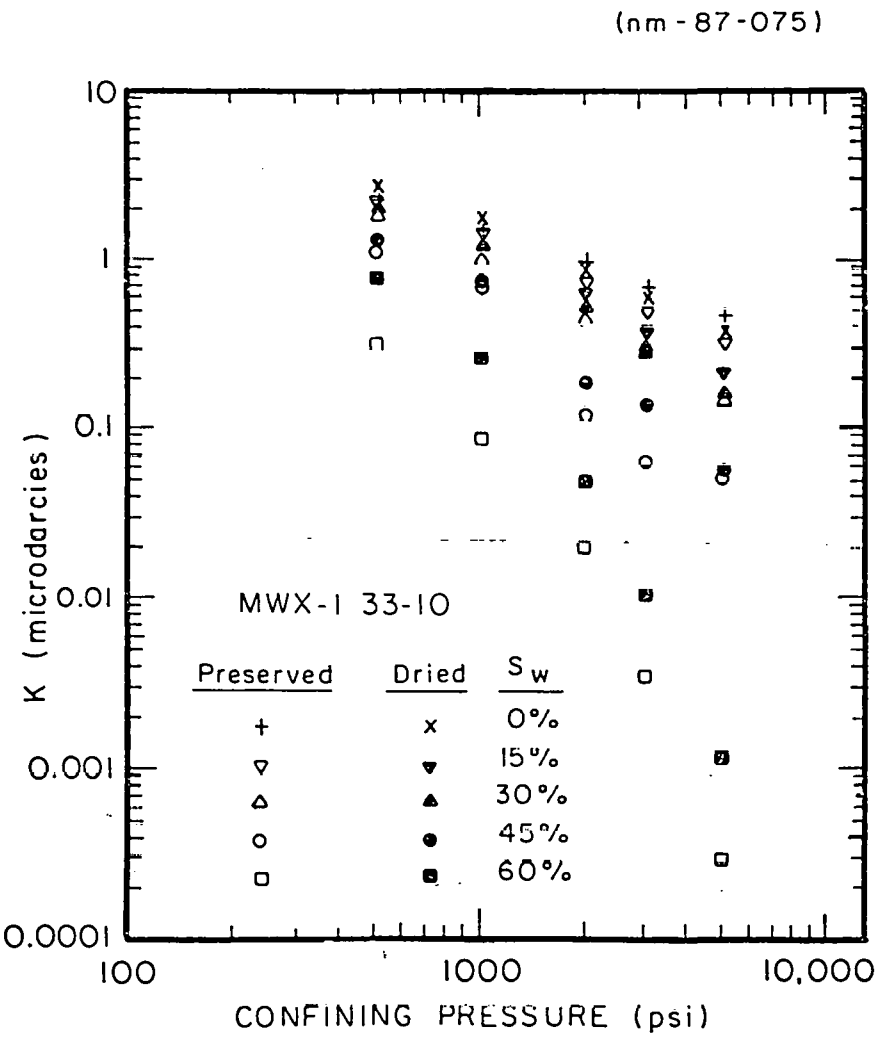

Figure 23. Relative permeability to gas for preserved and previously dried core (MWX1 33-10).

DESORPTION-ADSORPTION ISOTHERMS

Experimental

Desorption-adsorption isotherms were determined at ambient temperature. A series of 8 humidity chambers were established with relative humidities of 20% to 98%, using appropriate concentrations of sulfuric acid.[20] Core plugs of 1/2" diameter by 1" in length were cut from the preserved core samples close to where plugs were taken for permeability measurements. Plugs were brought up to 100% water saturation using distilled water and then placed in the highest humidity chamber. Cores were weighed periodically until constant weight was obtained. The samples were then transferred to the next highest humidity chamber and so on. Equilibration times were longest (about three weeks) for the highest humidity. The dry weight for the preserved core, obtained after equilibration of the sample at 20% humidity, was used as a base weight for calculation of water saturations. Core plugs were oven-dried at 110°C to constant weight and desorption-adsorption measurements were repeated.

Results

Desorption isotherms were measured for both preserved and dried plugs from whole core samples MWX3 42-4 and MWX1 33-10. For both plugs, desorption from the preserved condition gave generally higher water saturations at a given relative humidity than the dried samples. Desorption isotherms for MWX1 33-10 are shown in Fig. 24. This behavior implies that pore volume associated with very small pores (in the range of 10-100 nm) decreases when the sample is dried. Adsorption isotherms are in much closer correspondence, indicating that drying to 20% relative humidity at room temperature has a comparable effect on pore structure to oven drying at 110°C (see Fig. 25). Similar but less pronounced desorption-adsorption behavior was given by MWX3 42-4 (see Fig. 26). The larger effect observed for MWX1 33-10 is consistent with the larger difference in permeabilities observed for preserved and oven-dried cores (see Fig. 20).

MOISTURE CONTENT OF PRESERVED CORES

Experimental

Multi-Well core samples used in these experiments had been cut from the formation about 4 years previously and had been protected from drying by a combination of Saran Wrap, aluminum foil and plastic coating (seal peel). Because of concerns that the preservation procedure was not adequate to prevent water loss, four preserved cores were sacrificed for direct measurements of water content. (Test plugs are normally cut from whole core samples using water as the cutting fluid with care being taken to minimize mechanical damage.) After removing the seal peel and unwrapping the cores, they were broken by severe mechanical shock. Moisture contents of pieces of whole core were determined by weighing the core before and after drying.

Results

Results are shown in Table 9. It is seen that in one instance the water saturation was only 20%. From adsorption isotherms for comparable rocks this is about the same moisture content to be expected at ambient conditions. The sample at

(nm-87-078)

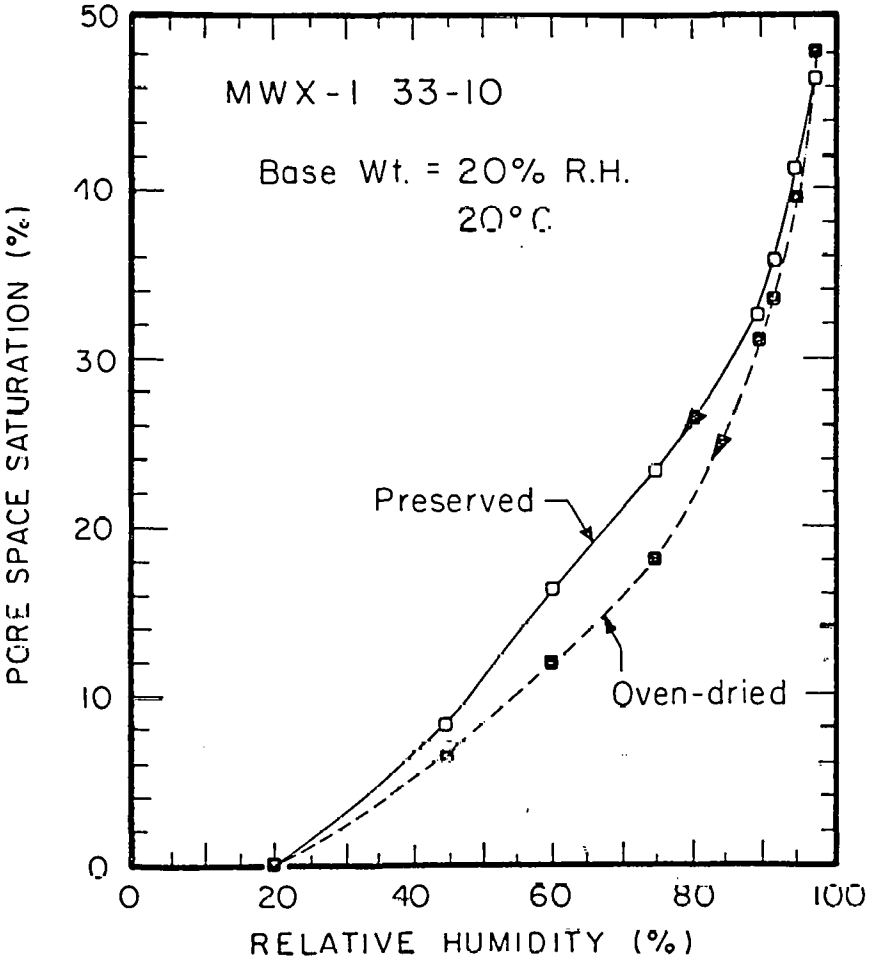

Figure 24. Desorption isotherms for preserved and oven-dried cores (MWX1 33-10).

(nm-87-069)

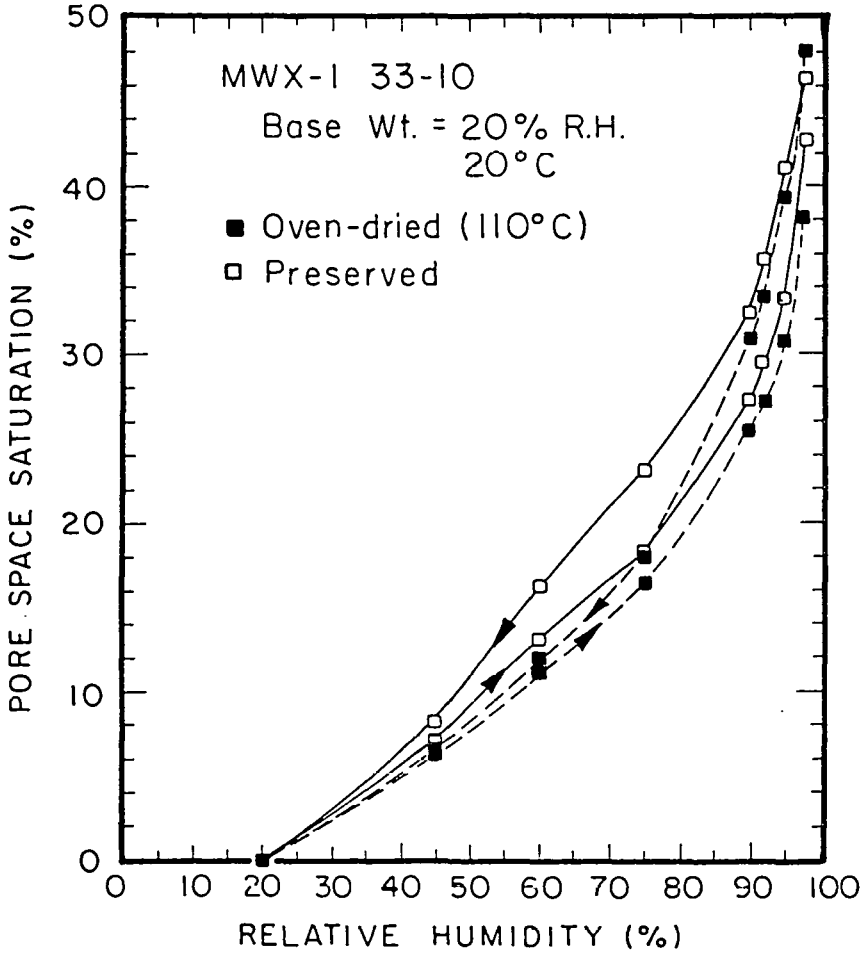

Figure 25. Adsorption hysteresis for dried and preserved cores (MWX1 33-10).

(nm-87-071)

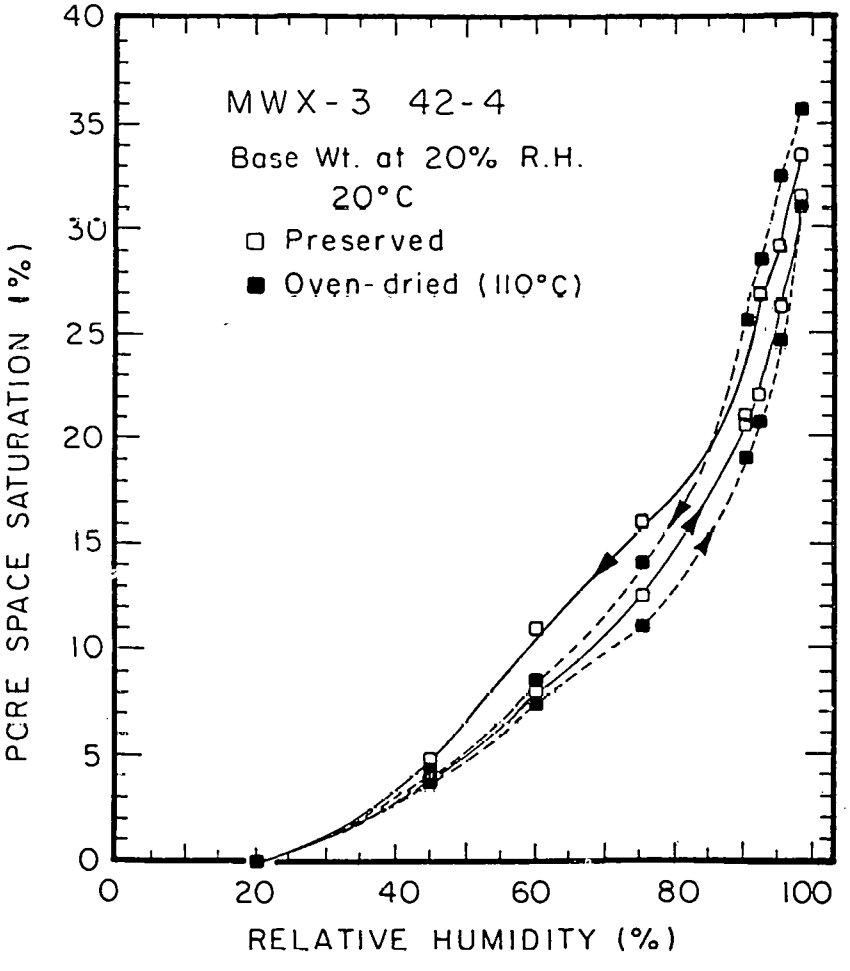

Figure 26. Adsorption hysteresis for preserved and oven-dried core (MWX3 42-4).

Table 9

Initial Moisture Content

Well I.D.	Water Saturation (%)
MWX-1 33-12	22.1
MWX-3 58-19	40.2
MWX-3 58-11	81.5
MWX-3 59-1	70.9

40% water saturation is also considered to be unacceptably low. The two other cores showed satisfactory levels of water saturation even after storage for about four years. Tests performed on MWX3 58-11 showed effects of drying on permeability to brine that were similar to previously obtained results.

The measurements of water content of preserved cores show that the preservation procedures used for MWX cores sometimes work but are not generally reliable. Because of the possibility that preserved cores may have dried to some extent during storage, the effects of drying will be no less than those measured. The problem of core preservation is not limited to low permeability gas sands, and the need to test preserved cores is becoming well recognized. Improved methods of core preservation were recently reported by Auman[21] (see Fig. 27). These should be applied to low permeability gas sands. Further tests of preserved cores and the effects of drying will be made if properly preserved or fresh cores from tight gas sands become available.

ELECTRICAL RESISTIVITY OF TIGHT SANDS

Electrical resistivity measurements of tight sand core samples, in addition to their value to formation evaluation, provide a further approach to investigating pore structure. Preliminary measurements of formation factor vs. confining pressure have yielded interesting results. Log-log plots of formation factor vs. gas permeability for a given core yielded linear plots (see Figs. 28-31). Examples using data[22] for samples from three wells from the Travis Peak formation that show the same form of behavior are presented in Figs. 32-34. In further work on MWX samples, measurements of brine permeability vs. confining pressure will be included so that plots of permeability vs. formation factor can be prepared in which all results are for brine saturated cores.

SUMMARY

In Phase III core analysis work on 35 whole matrix samples has been completed. Measurements included porosity, surface areas, adsorption isotherms, x-ray diffraction, mineral analysis from thin sections, pore casts and measurements of Klinkenberg permeabilities (K_∞) at confining pressures ranging from 500 to 5000 psi. Results showed porosities ranging from 3 to 12%, surface areas from 0.97 to 4.35 m^2/g, and permeabilities ranging from 0.026 to 44.3 μd at 5000 psi confining pressure. Pore size and change in pore size with confining pressure were determined from the slopes of Klinkenberg plots. The tested cores showed wide variation in sensitivity of permeability to confining pressure with the ratio of $K_{\infty,500}$ to $K_{\infty,5000}$ for first unloading ranging from 1.5 to 45. Pressure sensitivity was found to correlate with depositional history. At any given level of permeability, pressure sensitivity increased with decrease in depth according to origin in the progradational sequence: marine/shoreline, lower coastal, paludal, fluvial.

Investigation of diagenesis and types and effects of secondary pores showed distinct differences between zones, but the role of the observed pore structures in determining pressure sensitivity is not clear. Trends in grain size, cementation, and the properties of quartz overgrowths are believed to be important factors in determining permeability and pressure sensitivity.

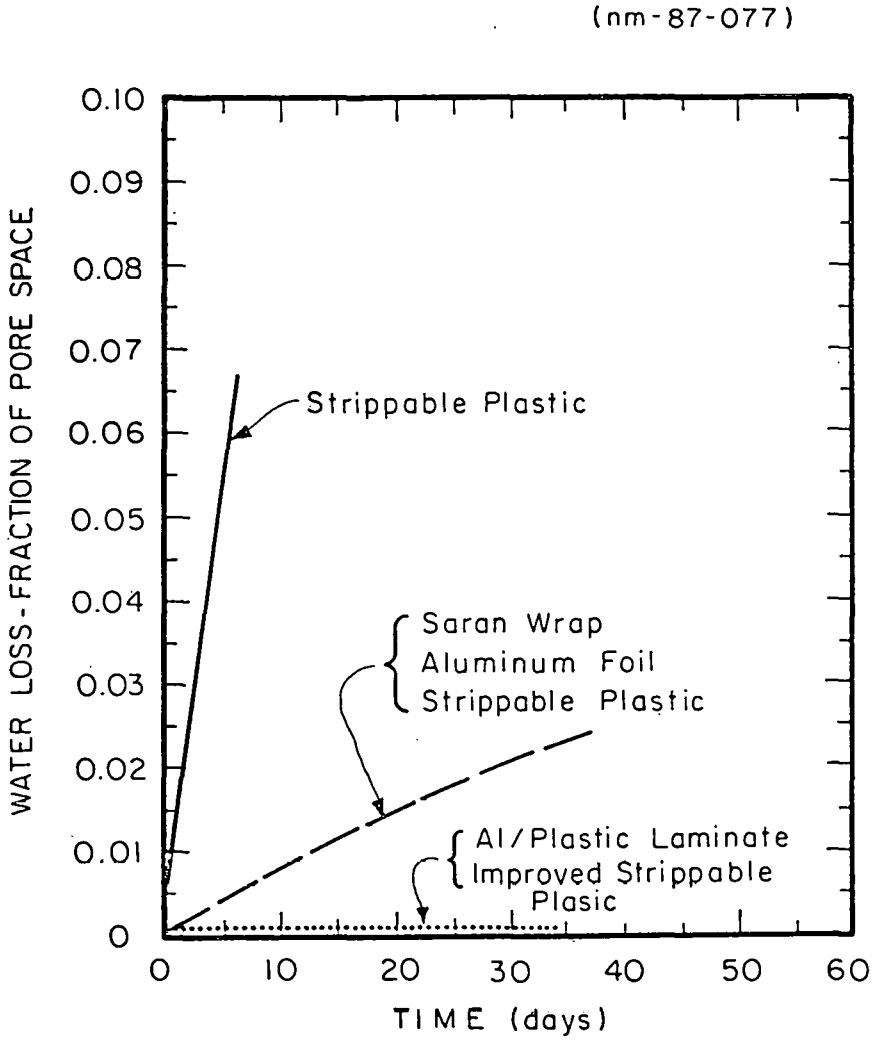

Figure 27. Water loss for various core preservation methods.[21]

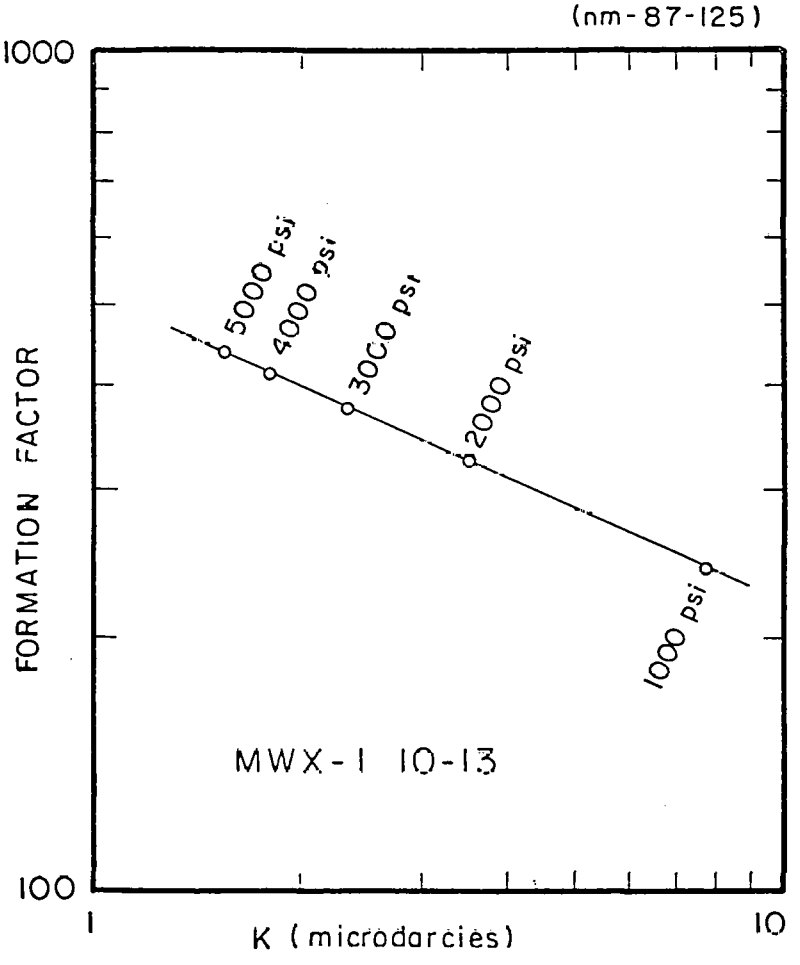

Figure 28. Formation factor vs. permeability (Klinkenberg corrected) for MWX1 10-13.

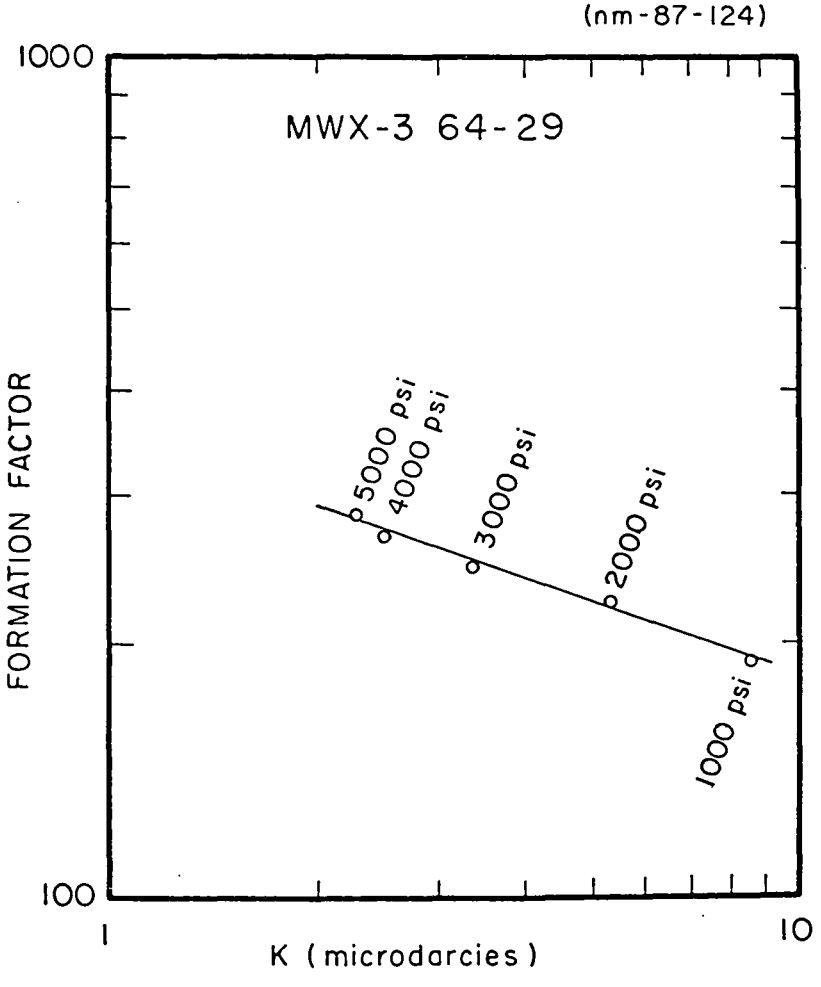

Figure 29. Formation factor vs. permeability (Klinkenberg corrected) for MWX3 64-29.

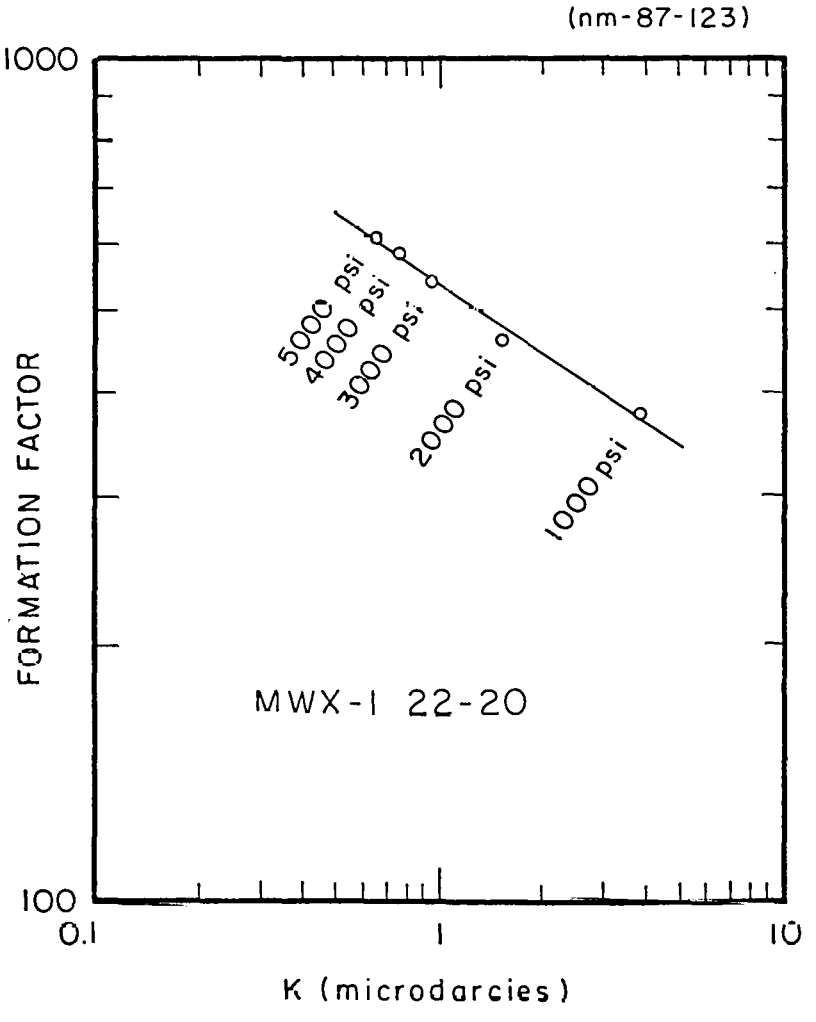

Figure 30. Formation factor vs. permeability (Klinkenberg corrected) for MWX1 22-20.

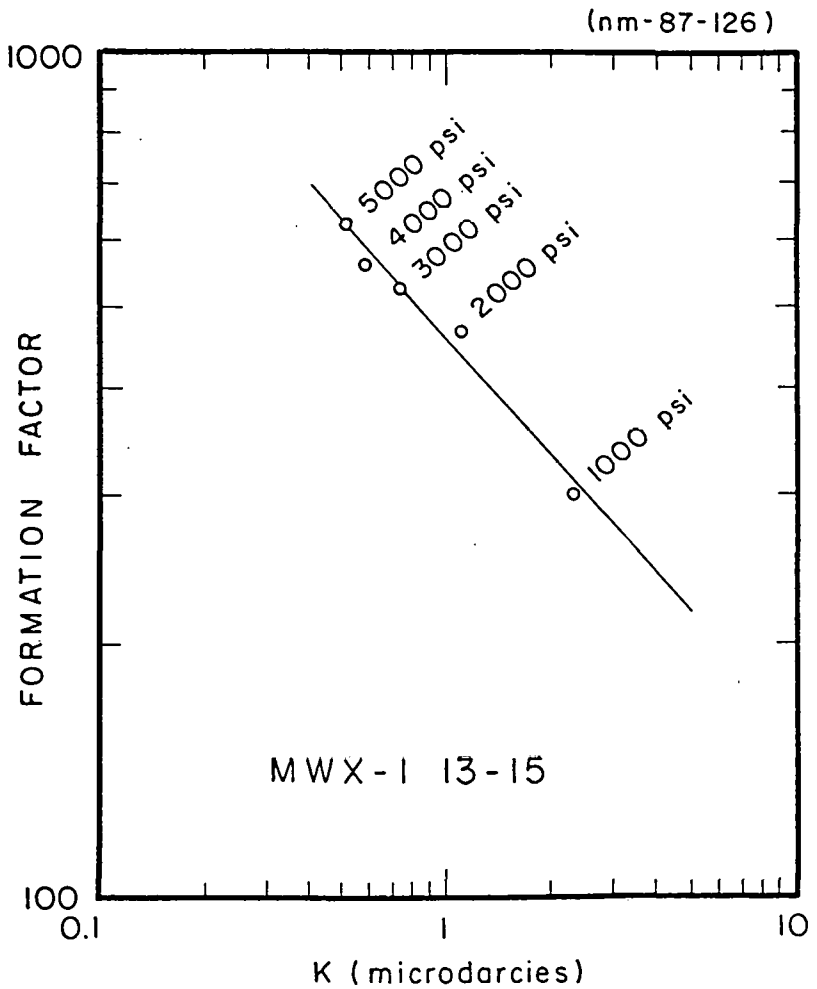

Figure 31. Formation factor vs. permeability (Klinkenberg corrected) for MWX1 13-15.

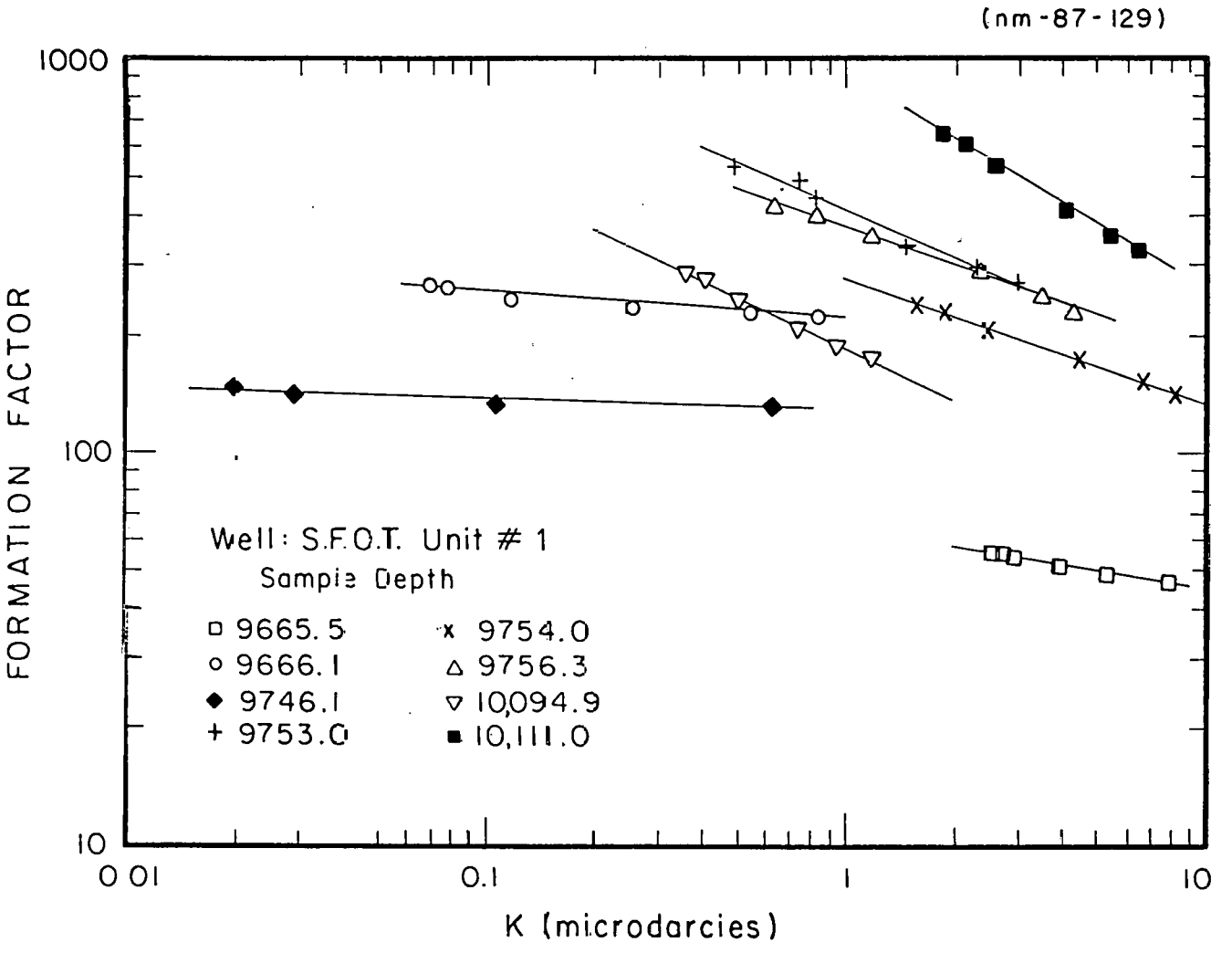

Figure 32. Formation factor vs. permeability (Klinkenberg corrected) for samples from Well: S.F.O.T. Unit #1.[22]

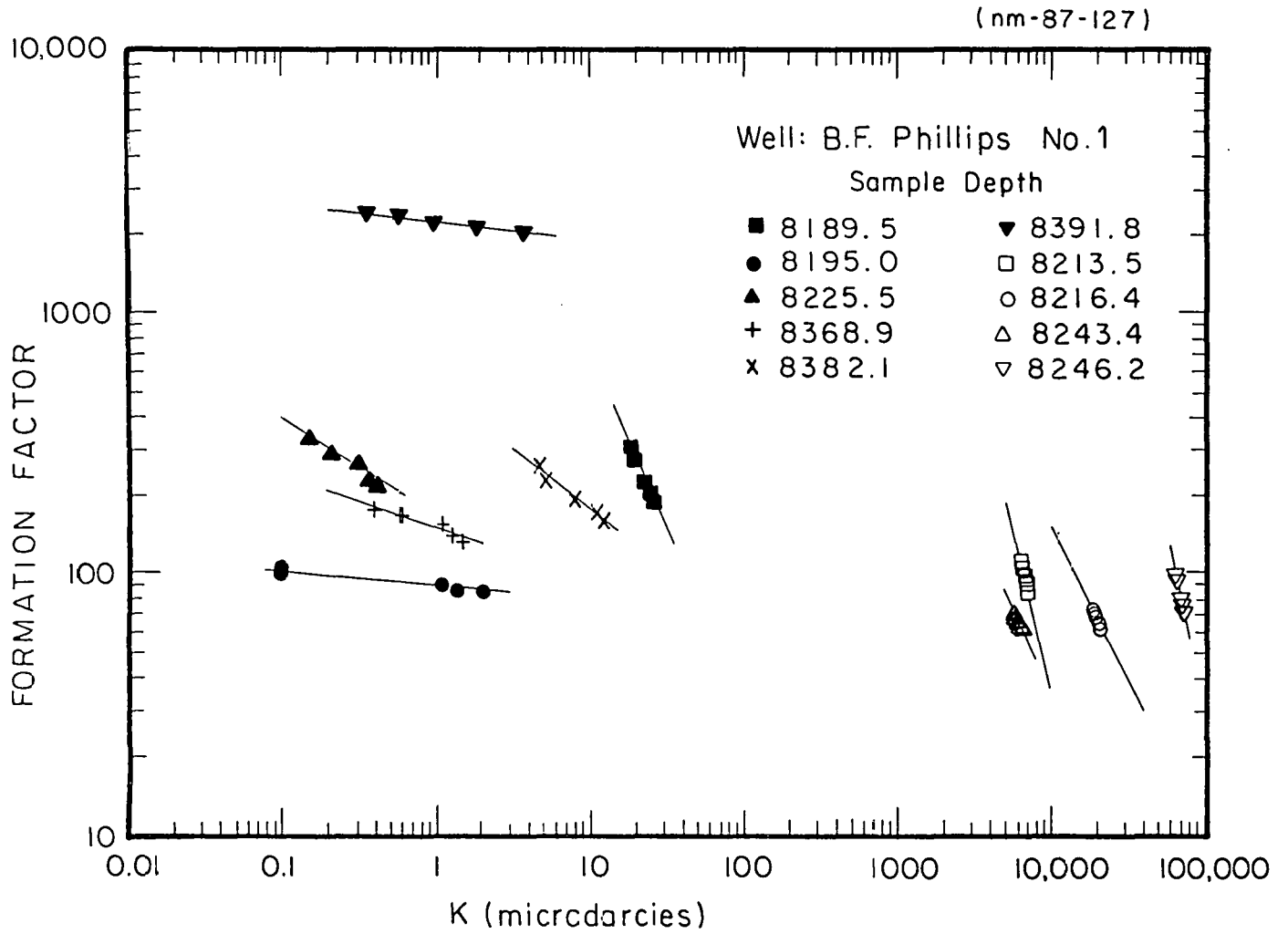

Figure 33. Formation factor vs. permeability (Klinkenberg corrected) for samples from Well: B.F. Phillips Unit #1.[22]

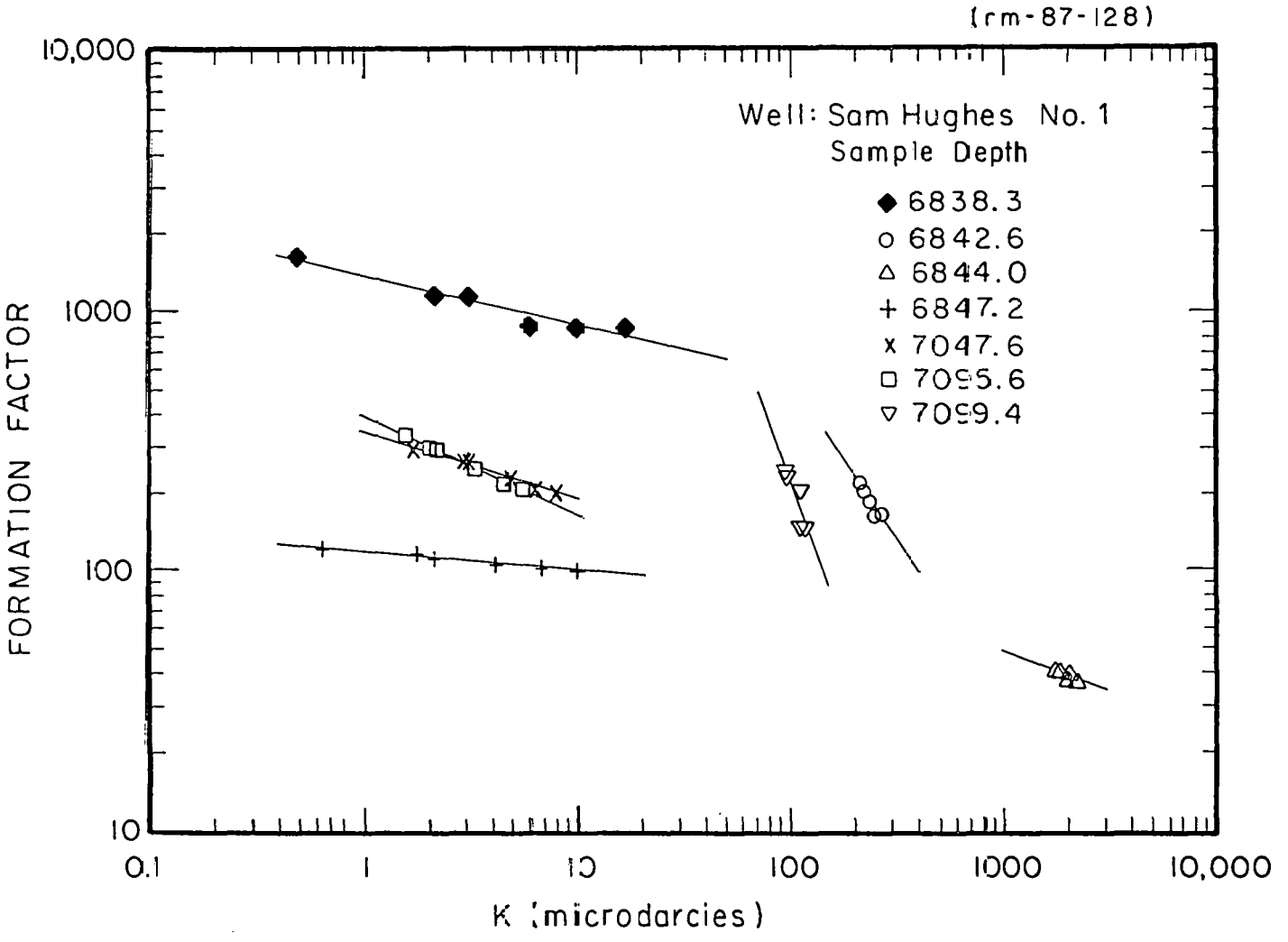

Figure 34. Formation factor vs. permeability (Klinkenberg corrected) for samples from Well: Sam Hughes Unit #1.[22]

Changes in pore structure with confining pressure are being investigated by preparation of thin sections of cores after impregnation with resin which was set up at various levels of confining pressure. A surface staining technique has been found to be extremely useful in revealing the fine pore structure of low permeability gas sands. This work may lead to generalizations on the effect of confining pressure on pore structure that are based on direct observation.

Advanced core analysis has also been carried out on naturally fractured cores because it is suspected that fractures sometimes provide paths of high permeability which will permit gas to flow more readily from the matrix rock to the wellbore. Multi-Well cores which have mineralized fractures are usually obvious because the fractures are vertical and filled with calcite. Detailed studies have now been made on eleven cores containing mineralized fractures. Permeabilities of cores containing fractures in the direction of flow are sometimes more and sometimes less than those of neighboring rock matrix but they are all of about the same order of magnitude. While calcite fractures are not generally very permeable, removal of calcite from the mineralized fracture by flow of acetic acid through the core has been observed to increase permeability about four orders of magnitude.

Matrix core samples were treated with seven selected chemicals. These were selected to obtain indication as to which minerals occupy critical positions within the pore space with respect to permeability and its pressure sensitivity. Permeability of a fluvial core responded most to acid treatments whereas a coastal core responded more to sodium hydroxide. However, interpretation of sodium hydroxide treatments is made difficult by precipitation effects. Future work will concentrate on use of chemicals which give the largest increases in permeability. UV reflectance microscopy will be used to study changes in pore structure resulting from the chemical treatments.

Comparison of brine permeabilities for fresh and dried low permeability sandstones show that drying always results in an increase in permeability. Measurements of moisture contents of preserved cores from MWX shows that preservation techniques are not always reliable. Further tests of properly preserved or fresh cores from tight gas sands will be made if such samples become available.

Preliminary studies of the electrical properties of low permeability gas sands have yielded interesting results. Changes in formation factor and permeability with confining pressure for a given core were measured in separate experiments. Log-log plots of formation factor vs. permeability were all found to be linear. Tests of a large amount of data measured by other laboratories gave similar relationships. Further work on this topic will include comparisons using permeabilities measured for brine rather than air. Under these conditions the fluid and electrical conductivities can be compared with brine as the fluid in both cases.

OBJECTIVES FOR PHASE IV

TASK 1 ADVANCED CORE ANALYSIS

Advanced core analysis data has been obtained for 35 MWX matrix core samples. Because of the relationship found between depositional environment and pressure sensitivity, advanced core analysis measurements will be performed on four additional marine sandstones. This will provide a further test of the correlation and also provide a broader range of data for cores from this zone.

(a) Further correlations will be tested between measured flow properties, clay content, adsorption behavior and surface areas.

(b) Recently developed surface staining UV fluorescence techniques will be applied to investigate microporosity and changes in pore structure caused by application of overburden pressure, for samples that represent a range of pressure sensitivities.

TASK 2 GAS FLOW IN MINERALIZED FRACTURES

Chemical treatment of mineralized fractures offers a means of enhancing fracture connectivity. Tests will be made on flow of acetic acid in mineralized fractures under the following conditions.

(a) Change in permeability with flow of acetic acid will be tested for cores cut so that with mineralized fractures lie along the length of the core.

(b) Changes in permeability will be measured before and after treatment with acetic acid for cores refractured along the plane of weakness given by the mineralized tectonic fracture.

TASK 3 CHANGES IN MATRIX PROPERTIES AFTER CHEMICAL TREATMENT

The results obtained to date were intended to provide a broad guide as to the effect of chemical treatment of low permeability gas sands. Future studies will focus on those chemicals which had significant effect on permeability and pressure sensitivity. The results obtained using NaOH point to the likely importance of quartz overgrowths or pore lining clay minerals in controlling pressure sensitivity. Further experiments will be aimed at delineating effects of dissolution and reprecipitation. Further studies of acid treatment will be made to confirm that enhanced permeability occurs for a wider variety of core samples. Special attention will be given to changes in pore structure. The previously described technique of surface staining of thin sections for UV reflectance microscopy will be applied to examination of the effects of chemical treatment on pore structure.

TASK 4 PROPERTIES OF TIGHT SANDS RELATED TO WATER CONTENT

Electrical Resistivities

Changes in formation factors of low permeability gas sands with change in overburden pressure will be compared with changes in flow properties under comparable stress conditions. Relationships between change in gas permeabilities and formation factors with confining pressure will be supplemented by obtaining brine permeabilities. Brine permeability measurements are needed because these correspond to the brine saturated condition at which formation factors are measured.

Capillary Pressure Measurements

Comparisons will be made between capillary pressures measured by high speed centrifuge and those obtained for duplicate samples using mercury injection for at least six core samples.

REFERENCES

1. Lorenz, J.C.: "Reservoir Sedimentology in Mesaverde Rocks at the Multi-Well Experiment Site," Sandia Report SAND83-1078 (1983) 1-36.

2. Lorenz, J.C.: "Reservoir Sedimentology of Mesaverde Rocks at the MWX Site," U.S. Geological Survey Open File Report 84-757 (1984) 21-32.

3. Pitman, J.K. and Spencer, C.W.: "Petrology of Selected Sandstones in the MWX Wells (Northwest Colorado) and Its Relationship to Borehole Geophysical-Log-Analysis and Reservoir Quality," U.S. Geological Survey Open File Report 84-757 (1984) 33-66.

4. Kilmer, N.H., Morrow, N.R., and Pitman, J.K.: "Pressure Sensitivity of Low Permeability Sandstones," J. Pet. Sci. & Eng. (August 1987) 1, 65-81.

5. Brower, K.R. and Morrow, N.R.: "Fluid Flow in Cracks as Related to Low Permeability Gas Sands," Soc. Pet. Eng. J. (April 1985) 191-201.

6. Ruzyla, K. and Jezek: "Staining Method for Recognition of Pore Space in Thin and Polished Sections," J. Sed. Pet. (1987), submitted manuscript.

7. Ward, J.S. and Morrow, N.R.: "Capillary Pressures and Gas Relative Permeabilities of Low Permeability Sandstone," paper SPE/DOE 13882 presented at the 1985 SPE/DOE Symposium on Low Permeability Reservoirs, Denver, May 19-22.

8. Morrow, N.R., Ward, J.S., Brower, K.R., and Cather, S.M.: "Rock Matrix and Fracture Analysis of Flow in Western Tight Gas Sands," PRRC 86-11, New Mexico Petroleum Recovery Research Center, quarterly technical progress report prepared for the U.S. Department of Energy and the New Mexico Research and Development Institute for the period July-September 1987.

9. Gies, R.M.: "An Improved Method for Viewing Micropore Systems in Rocks with the Polarizing Microscope," paper SPE 13136 presented at the 1984 SPE Annual Meeting, Houston, Sept. 16-19.

10. Jones, F.O. and Owens, W.W.: "A Laboratory Study of Low-Permeability Gas Sands," J. Pet. Tech. (Sept. 1980) 1631.

11. Lorenz, J.C., Branagan, P., Warpinski, N.R. and Sattler, A.R.: "Fracture Characteristics and Reservoir Behavior of Stress-Sensitive Fracture Systems in Flat-Lying Lenticular Formations," Proc., 1986 SPE Unconventional Gas Technology Symposium, Louisville, May 18-21, 423-436.

12. Lorenz, J.C. and Sattler, A.R.: "Fracture Permeability in Plugs," Memorandum of Record, (March 24, 1986).

13. J. Sonderegger, K.R. Brower, and V. LeFebre: "A Preliminary Investigation of Strontianite Dissolution Kinetics," Am. J. Sci. (1976) 276, 997-1022.

14. Surdam, R.C., Boese, S.W., and Crossey, L.J.: "The Chemistry of Secondary Porosity, Part 2: Aspects of Porosity Modification," AAGP Memoir, (1985) 37, 127-149.

15. Heavyside, J., Langley, G.O., and Pallatt, N.: "Permeability Characteristics of Magnus Reservoir Rock," 1983 European Formation Evaluation Symposium, London, March.

16. Pallatt, N., Wilson, J., and McHardy, B.: "The Relationship Between Permeability and the Morphology of Diagenetic Illite in Reservoir Rocks," J. Pet. Tech. (Dec. 1982) 2871.

17. Sattler, A.R., personal communication.

18. Jennings, J.B., Carroll, H.B. and Raible, C.J.: "The Relationship of Permeability to Confining Pressure in Low Permeability Rock," paper SPE 9870 presented at the 1981 SPE/DOE Symposium on Low Permeability Gas Reservoirs, Denver, May 27-29.

19. Morrow, N.R.: "Effects of Drying on Absolute and Relative Permeabilities of Low Permeability Gas Sands," paper presented at the 1987 Clay Minerals Society Meeting, Socorro, NM, October 19-21.

20. CRC Handbook of Chemistry and Physics, 59th Edition, R.C. Weast (Ed.), CRC Press (1978).

21. Auman, J.B.: "A Laboratory Evaluation of Core Preservation Materials," paper SPE 15381 presented at the 1986 SPE Annual Technical Conference and Exhibition, New Orleans, LA, Oct. 5-8.

22. "Tight Gas Sand Core Analysis," Petrophysical Services Inc. for ResTech Inc., Houston (Jan. 1986) Final Report, Mountain View, CA.

APPENDIX

Clays Present (Ratios)
Water Adsorption-Desorption Isotherms
BET Surface Area of Core

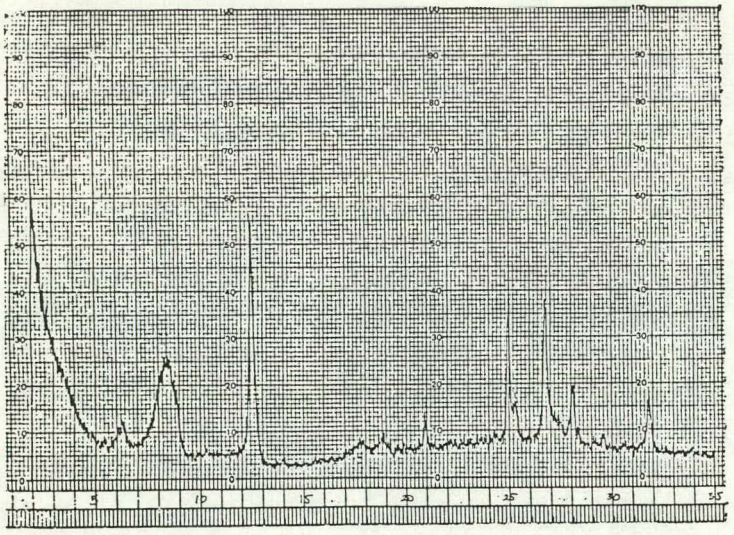

AIR DRIED

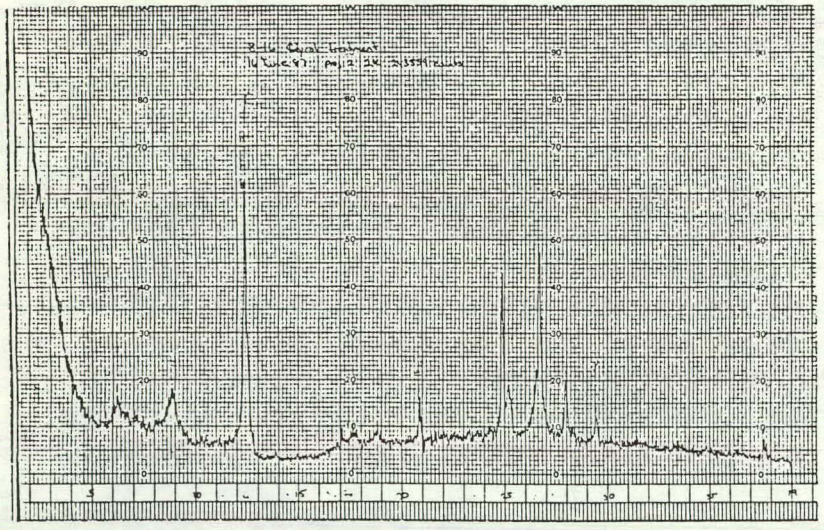

ETHYLENE GLYCOL TREATED

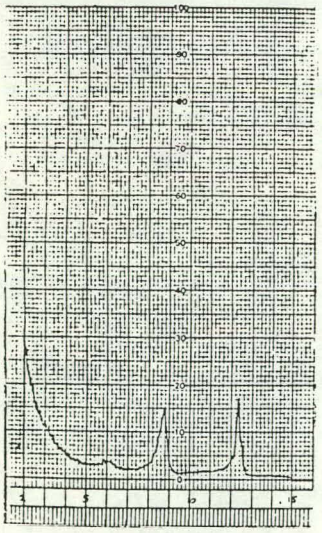

HEAT TREATED

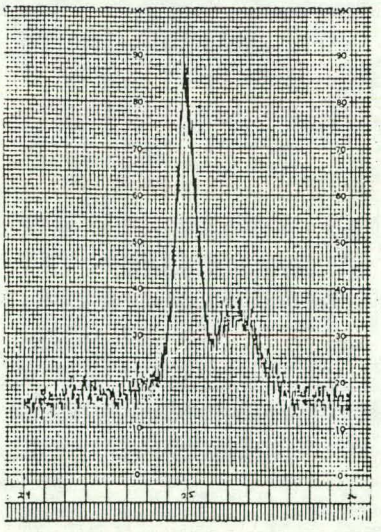

ETHYLENE GLYCOL TREATED

Clays Present (Ratios):

Illite	2
Mixed-Layer Clay	2
Kaolinite	2
Chlorite	3

Water Adsorption-Desorption Isotherm

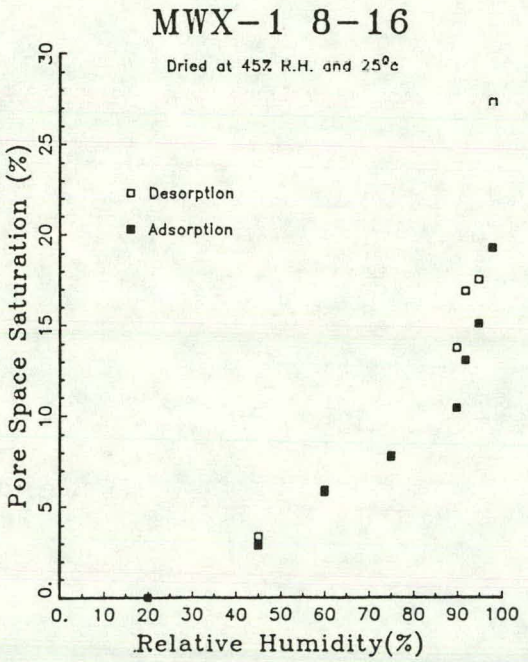

BET Surface Area of Core = 2.54 m^2/g

Figure A1. Properties related to microporosity - MWX1 8-16.
[Depth: 4548.4-4548.9 ft.; Zone: fluvial]

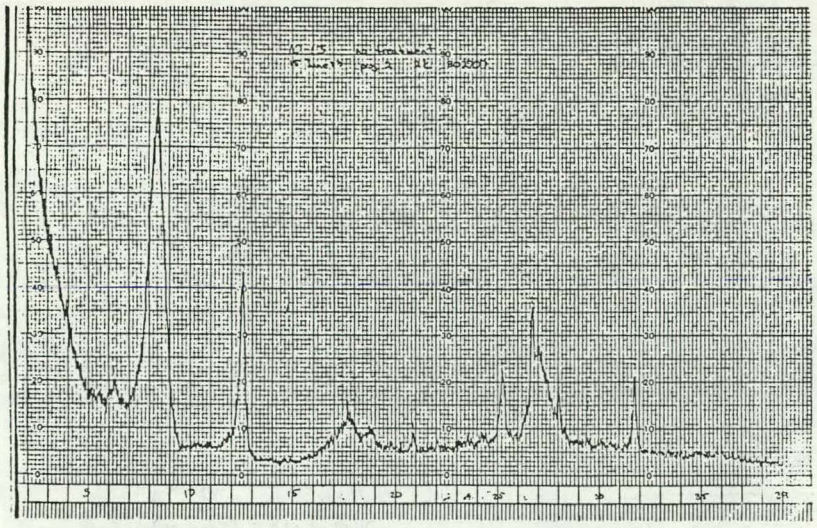

AIR DRIED

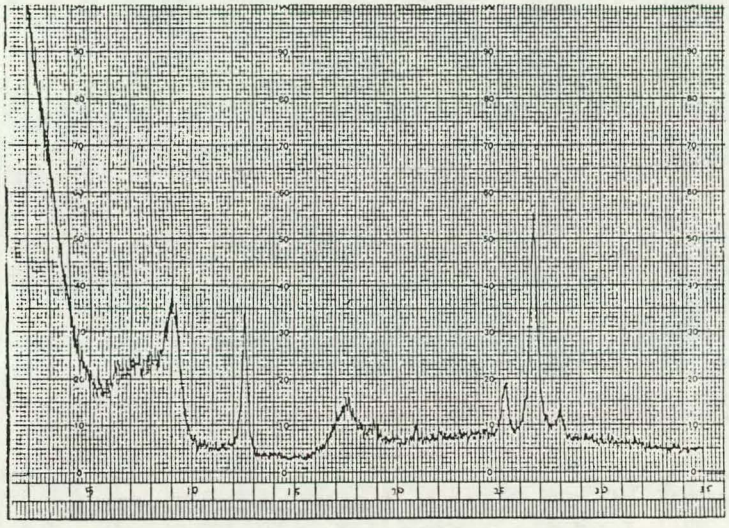

ETHYLENE GLYCOL TREATED

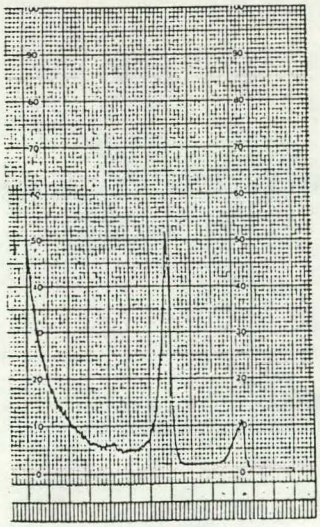

HEAT TREATED

Clays Present (Ratios):

Illite	5
Mixed-Layer Clay	3
Chlorite	2

Water Adsorption-Desorption Isotherm

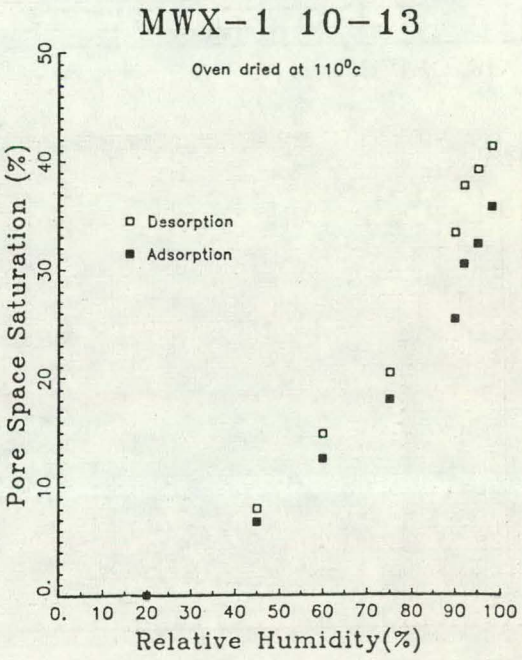

BET Surface Area of Core = 1.30 m^2/g

Figure A2. Properties related to microporosity - MWX1 10-13.
[Depth: 4699.7-4700.5 ft.; Zone: fluvial]

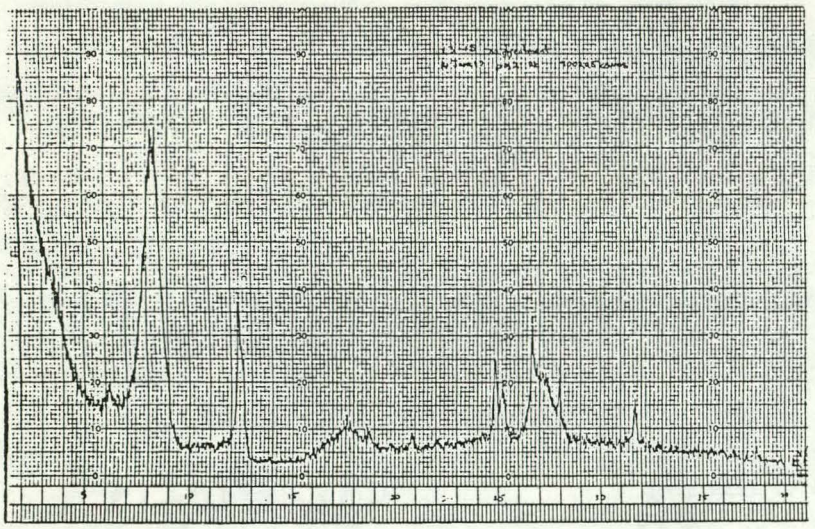

AIR DRIED

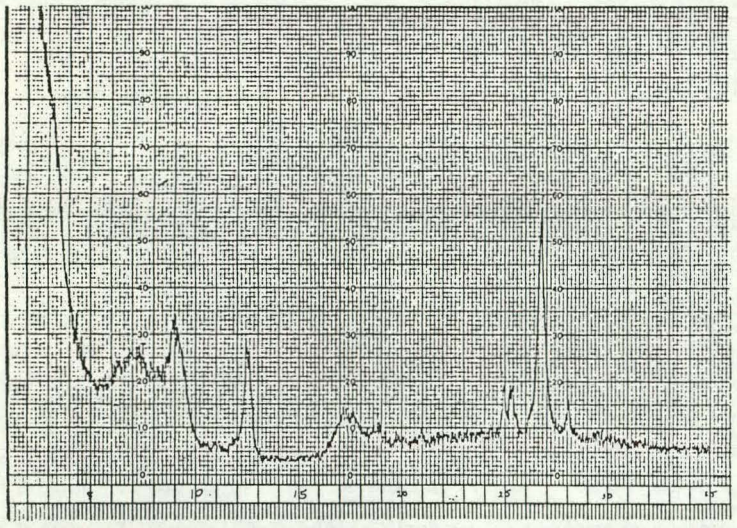

ETHYLENE GLYCOL TREATED

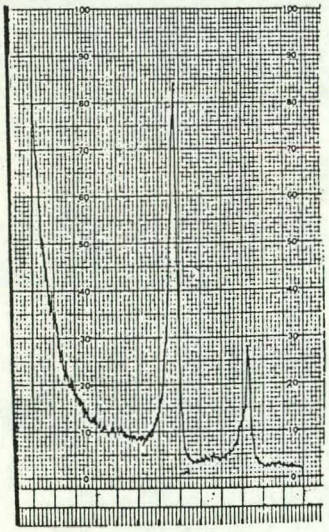

HEAT TREATED

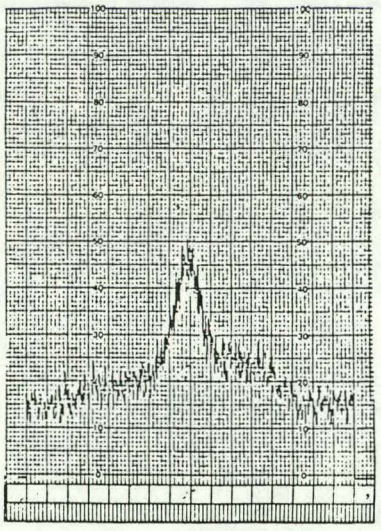

ETHYLENE GLYCOL TREATED

Clays Present (Ratios):

Illite	2
Mixed-Layer Clay	5
Kaolinite	1
Chlorite	1

Water Adsorption-Desorption Isotherm

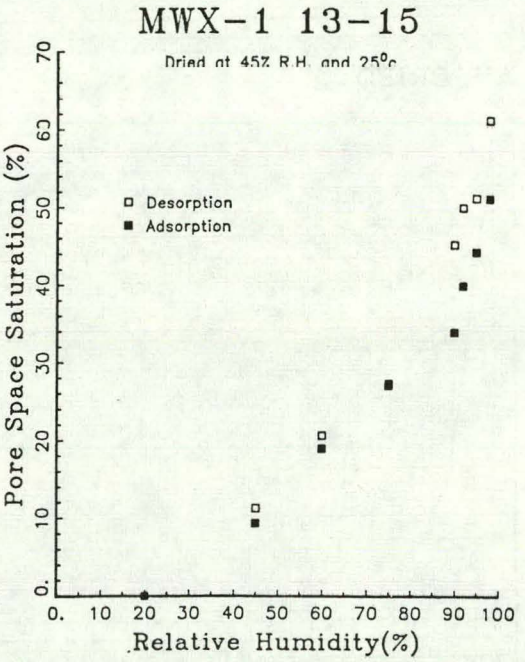

BET Surface Area of Core = 1.98 m^2/g

Figure A3. Properties related to microporosity - MWX1 13-15.
[Depth: 4851.0-4851.5 ft.; Zone: fluvial]

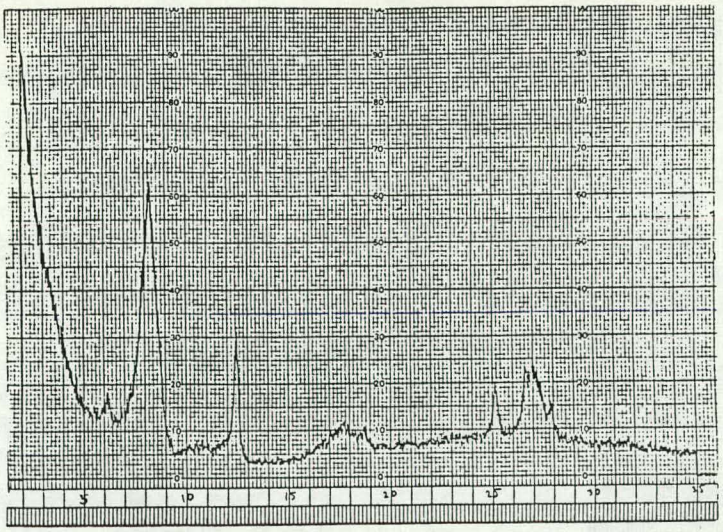

AIR DRIED

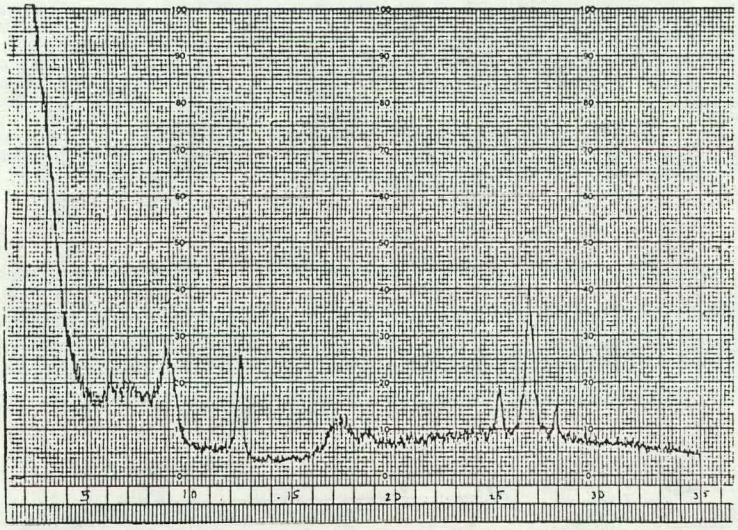

ETHYLENE GLYCOL TREATED

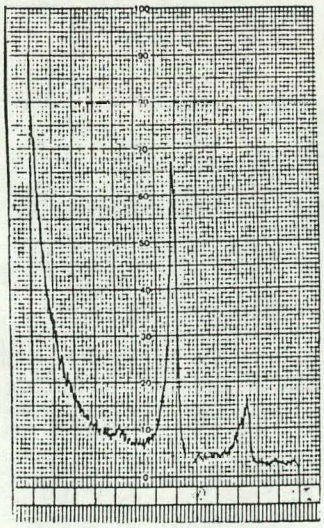

HEAT TREATED

Clays Present (Ratios):

Illite	3
Mixed-Layer Clay	6
Chlorite	2

Water Adsorption-Desorption Isotherm

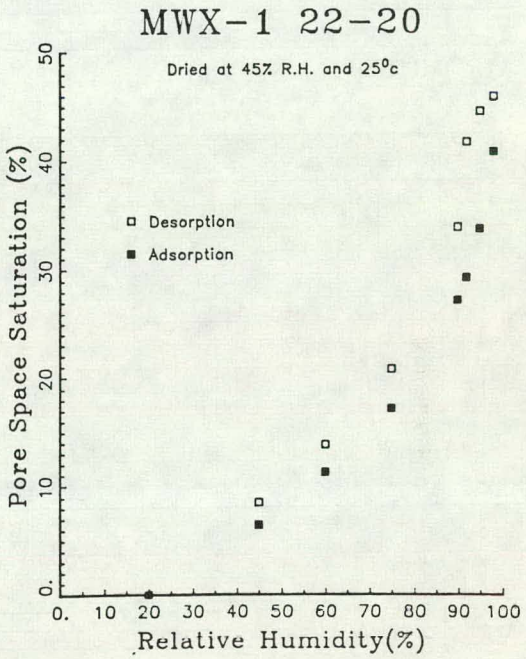

BET Surface Area of Core = 1.36 m^2/g

Figure A4. Properties related to microporosity - MWX1 22-20.
[Depth: 5357.2-5357.7 ft.; Zone: fluvial]

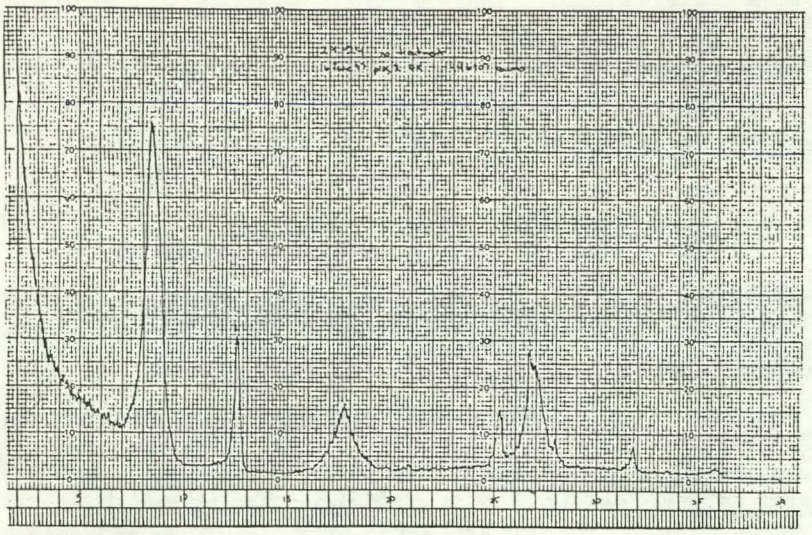

AIR DRIED

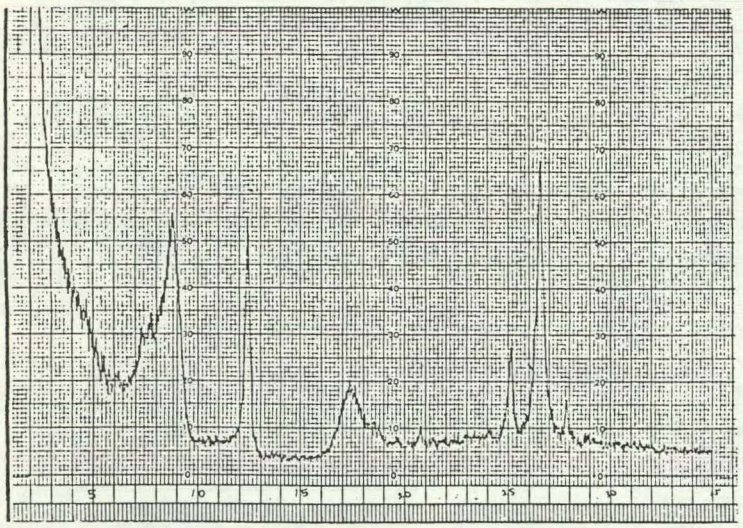

ETHYLENE GLYCOL TREATED

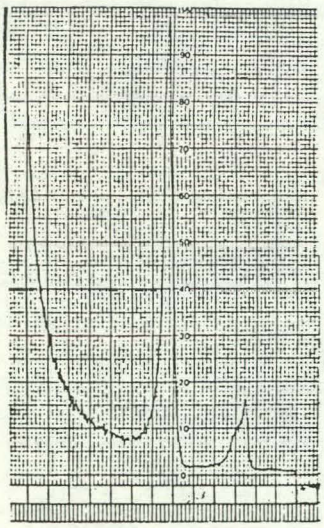

HEAT TREATED

Clays Present (Ratios):

Illite	3
Mixed-Layer Clay	7
Chlorite	Trace

Water Adsorption-Desorption Isotherm

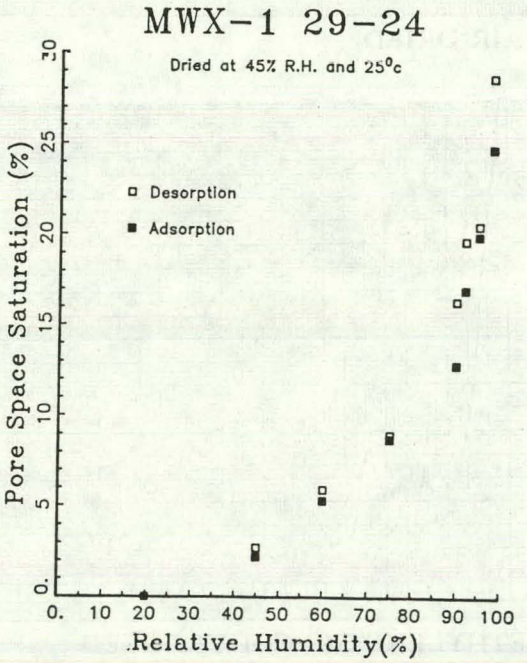

BET Surface Area of Core = 1.74 m^2/g

Figure A5. Properties related to microporosity - MWX1 29-24.
[Depth: 5725.7-5726.6 ft.; Zone: fluvial]

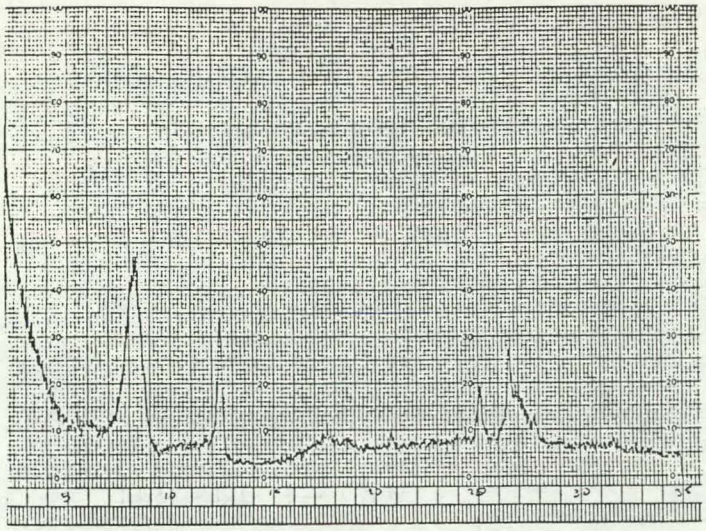

AIR DRIED

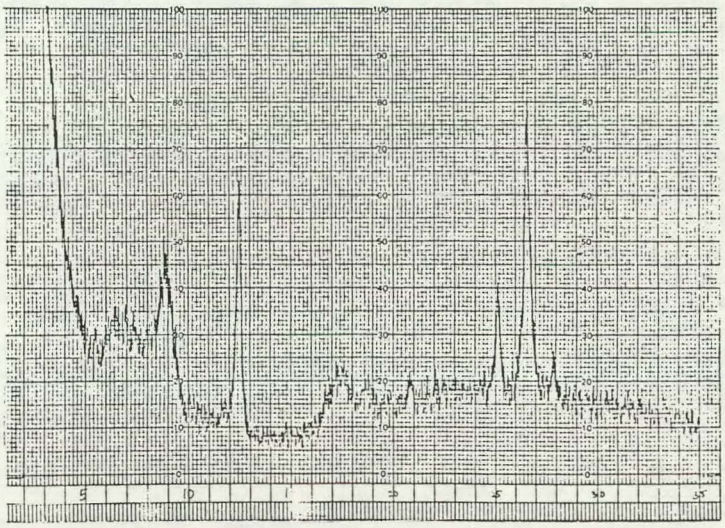

ETHYLENE GLYCOL TREATED

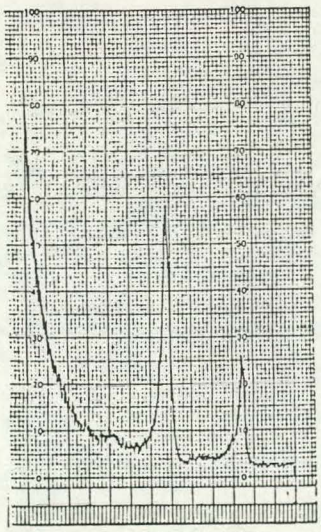

HEAT TREATED

Clays Present (Ratios):

Illite	3
Mixed-Layer Clay	6
Kaolinite	1

Water Adsorption-Desorption Isotherm

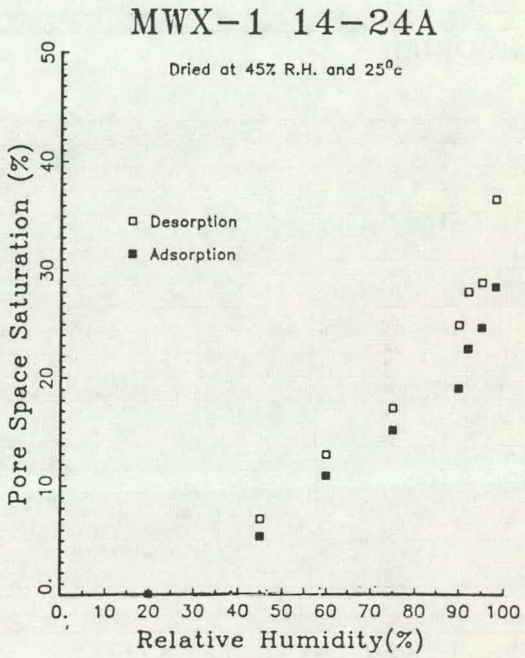

BET Surface Area of Core = 0.97 m^2/g

Figure A6. Properties related to microporosity - MWX1 14-24A.
[Depth: 4917.9-4918.2 ft.; Zone: fluvial]

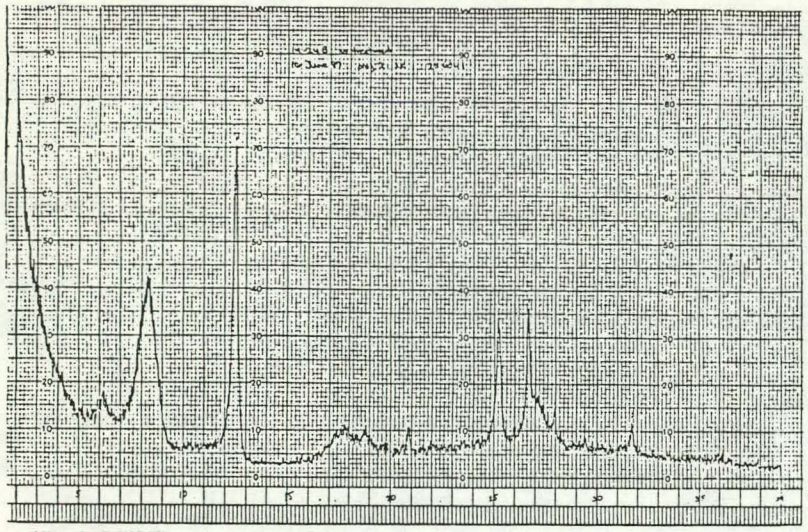

AIR DRIED

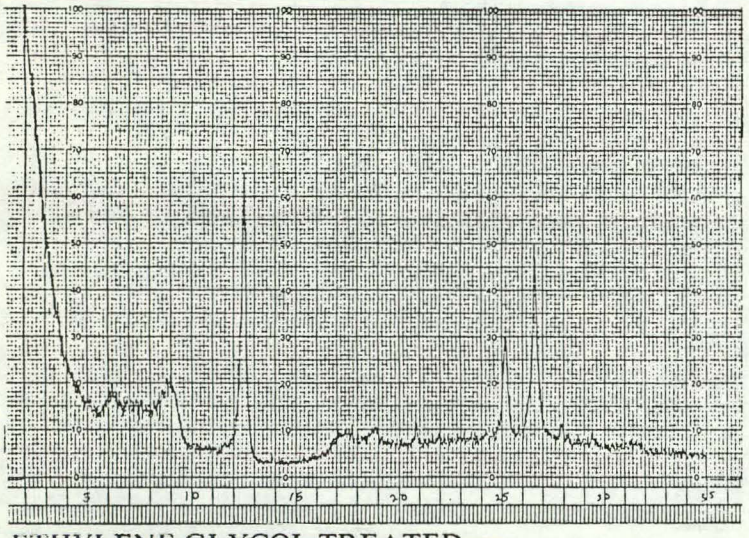

ETHYLENE GLYCOL TREATED

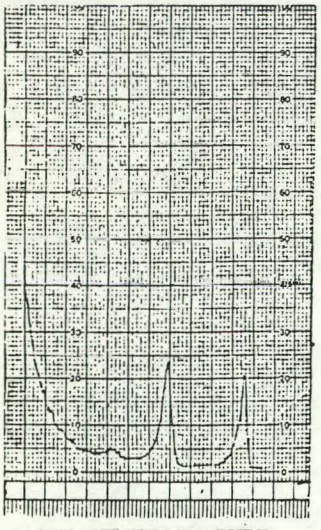

HEAT TREATED

Clays Present (Ratios):

Illite	3
Mixed-Layer Clay	6
Chlorite	2

Water Adsorption-Desorption Isotherm

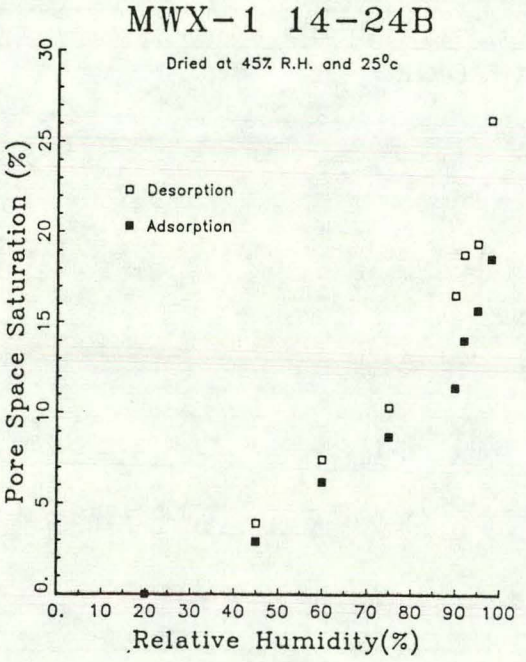

BET Surface Area of Core = 0.98 m^2/g

Figure A7. Properties related to microporosity - MWX1 14-24B.
[Depth: 4918.2-4918.9 ft.; Zone: fluvial]

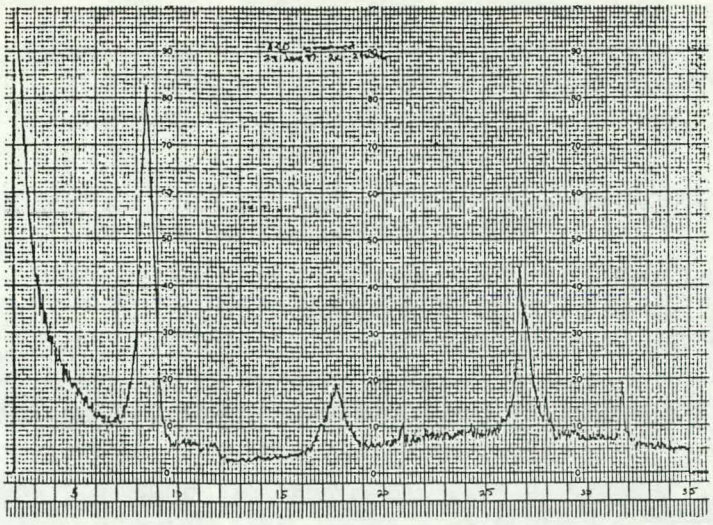

AIR DRIED

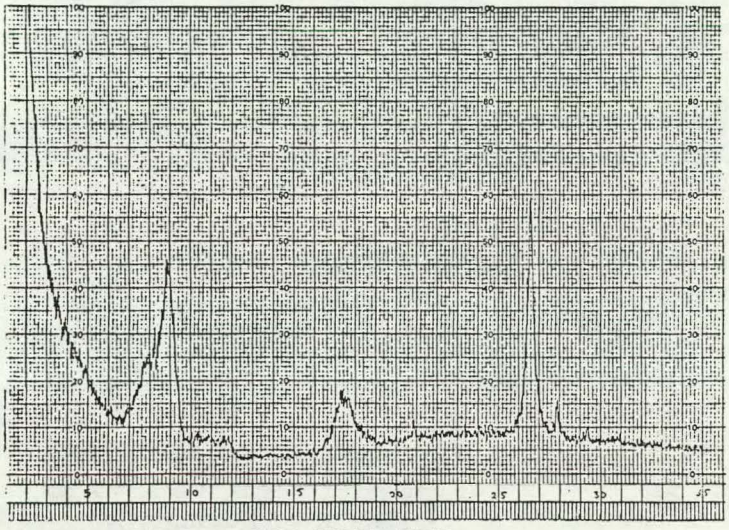

ETHYLENE GLYCOL TREATED

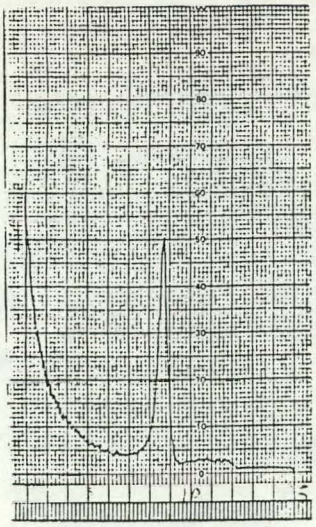

HEAT TREATED

Clays Present (Ratios):

Illite	4
Mixed-Layer Clay	6

Water Adsorption-Desorption Isotherm

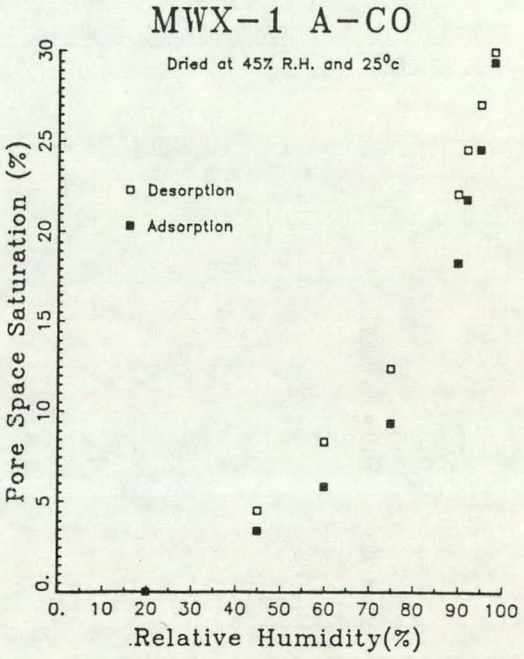

BET Surface Area of Core = 1.12 m^2/g

Figure A8. Properties related to microporosity - MWX1 A-CO.
[Depth: 6402.1-6402.7 ft.; Zone: coastal]

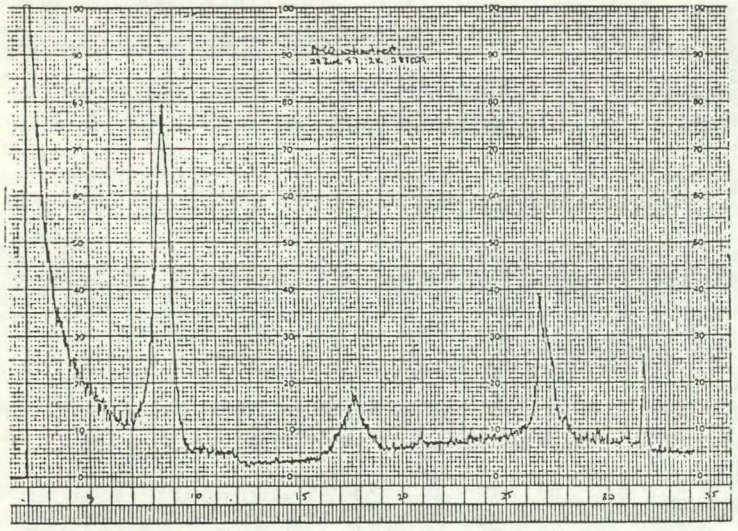

AIR DRIED

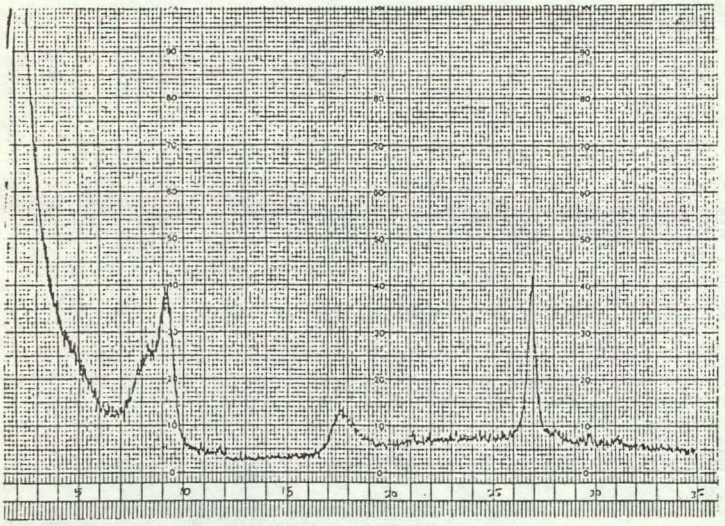

ETHYLENE GLYCOL TREATED

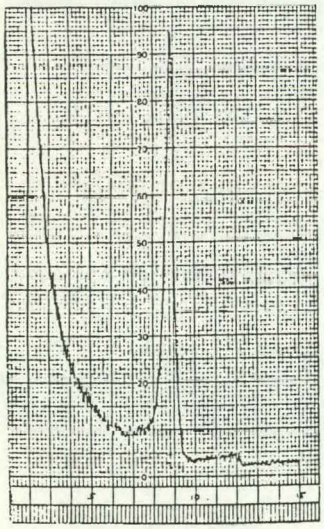

HEAT TREATED

Clays Present (Ratios):

Illite	4
Mixed-Layer Clay	6

Water Adsorption-Desorption Isotherm

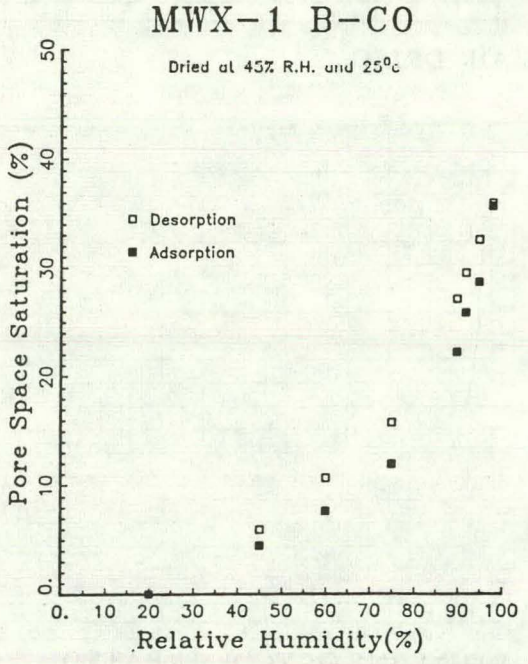

BET Surface Area of Core = 1.27 m^2/g

Figure A9. Properties related to microporosity - MWX1 B-CO.
[Depth: 6435.3-6436.1 ft.; Zone: coastal]

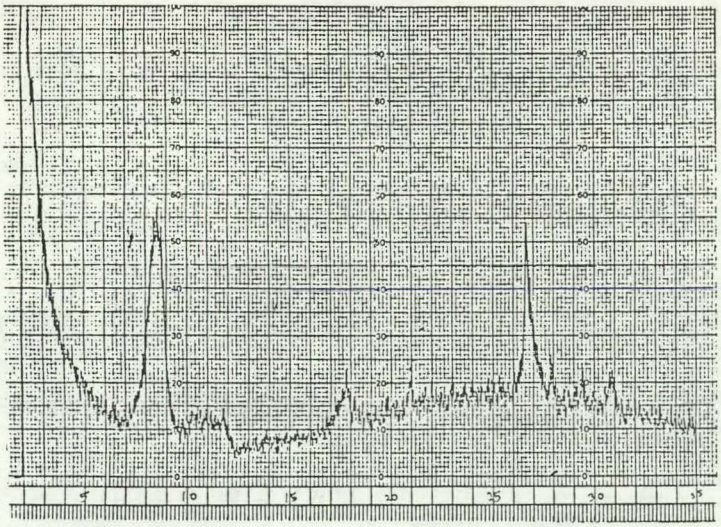

AIR DRIED

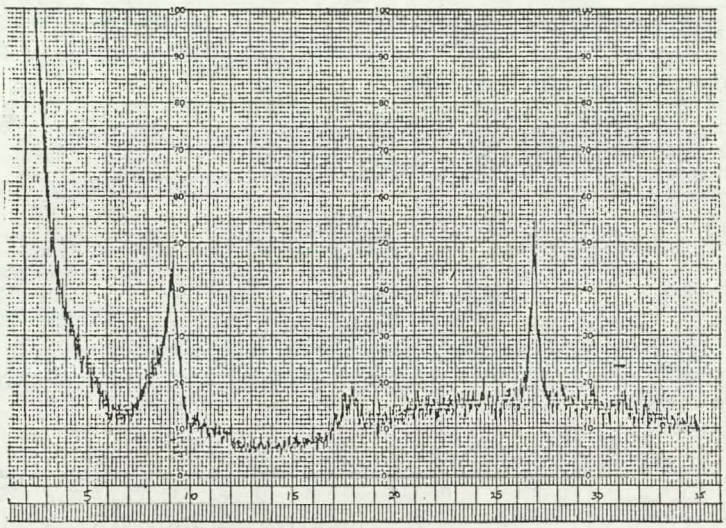

ETHYLENE GLYCOL TREATED

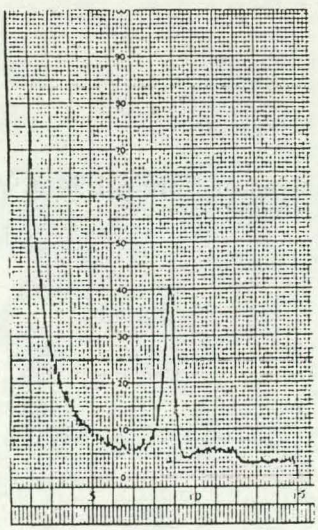

HEAT TREATED

Clays Present (Ratios):

Illite	5
Mixed-Layer Clay	5

Water Adsorption-Desorption Isotherm

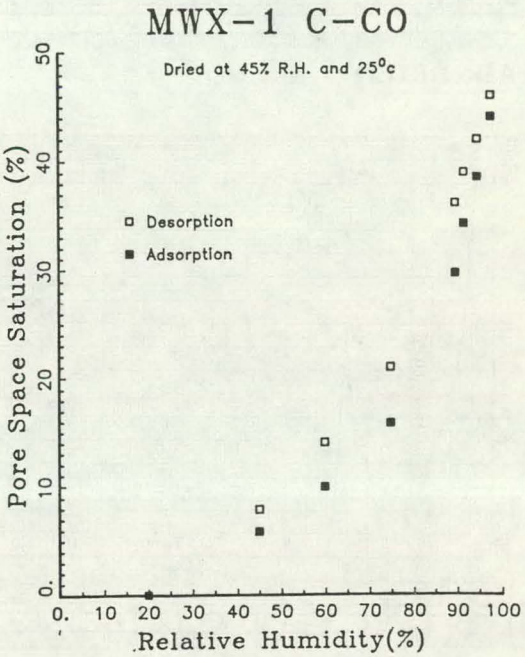

BET Surface Area of Core = 2.00 m^2/g

Figure A10. Properties related to microporosity - MWX1 C-CO.
[Depth: 6502.7-6503.2 ft.; Zone: coastal]

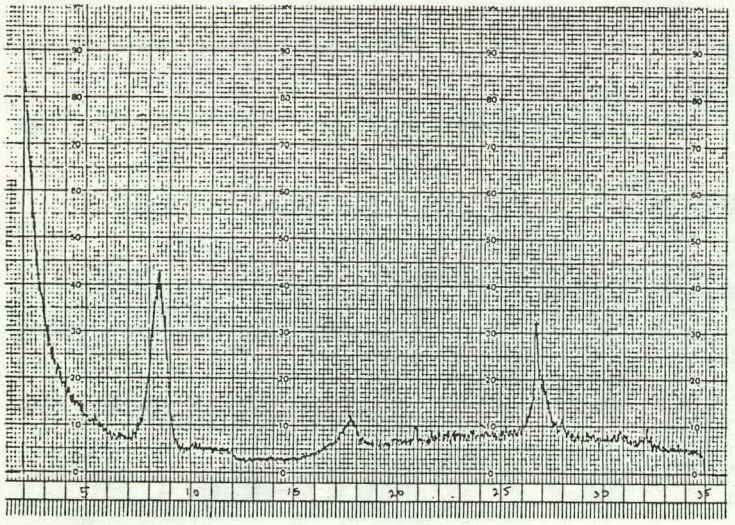

AIR DRIED

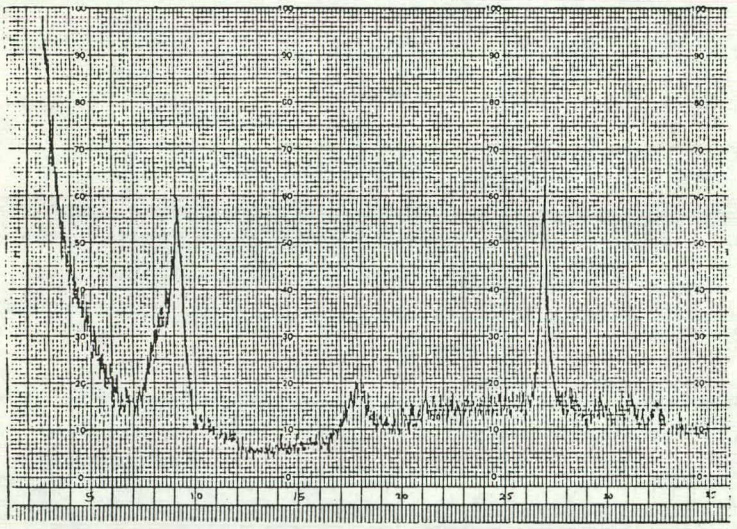

ETHYLENE GLYCOL TREATED

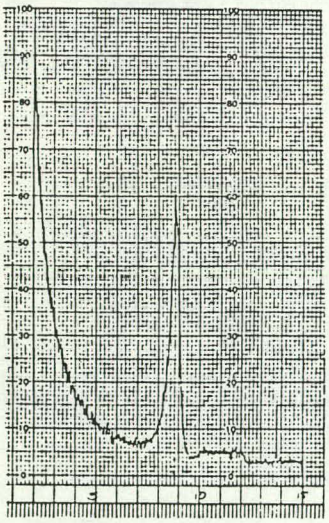

HEAT TREATED

Clays Present (Ratios):

Illite	4
Mixed-Layer Clay	6

Water Adsorption-Desorption Isotherm

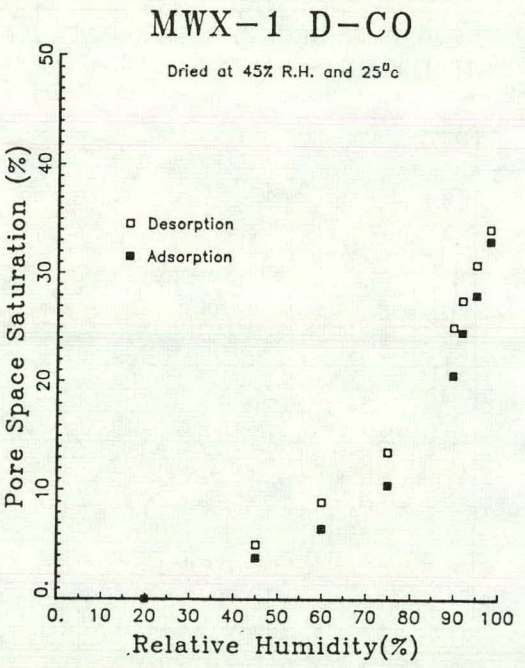

BET Surface Area of Core = 1.94 m^2/g

Figure A11. Properties related to microporosity - MWX1 D-CO.
[Depth: 6536.5-6537.1 ft.; Zone: coastal]

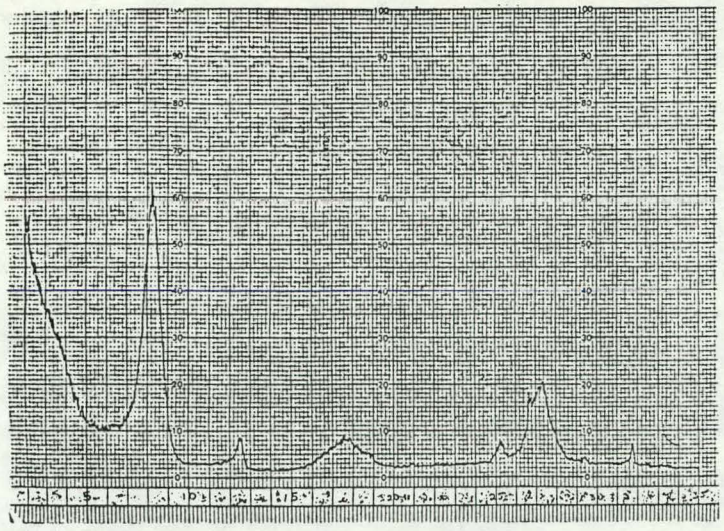

AIR DRIED

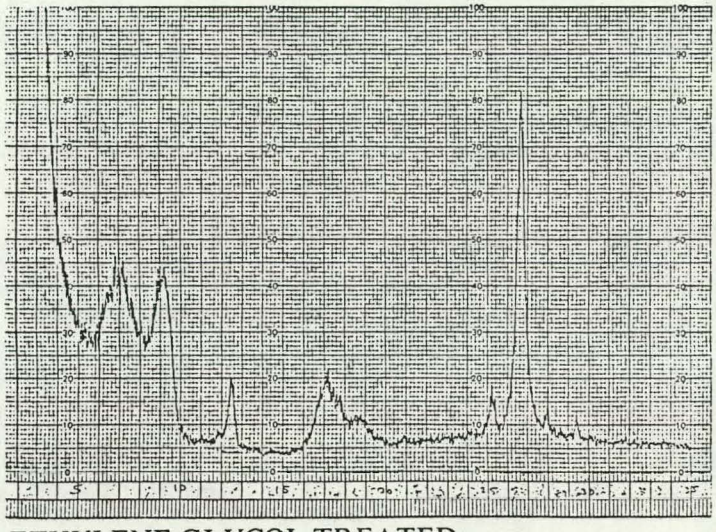

ETHYLENE GLYCOL TREATED

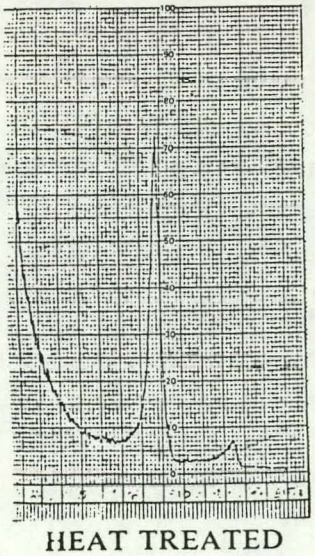

HEAT TREATED

Clays Present (Ratios):

Illite	2
Mixed-Layer Clay	6
Chlorite	1

Water Adsorption-Desorption Isotherm

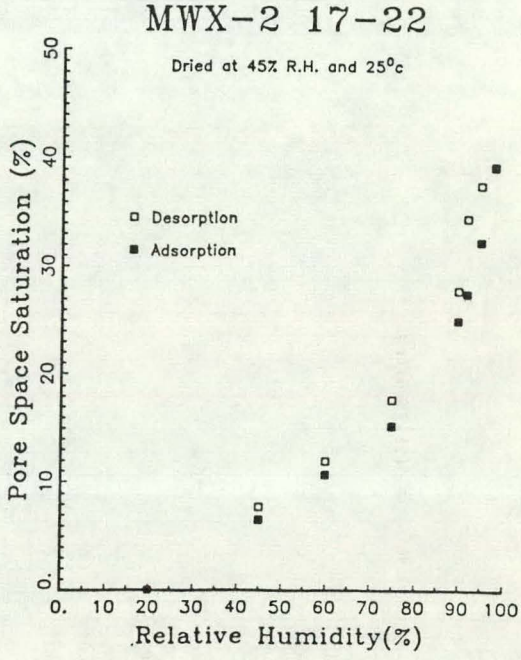

BET Surface Area of Core = 1.44 m^2/g

Figure A12. Properties related to microporosity - MWX2 17-22.
[Depth: 4937.0-4937.8 ft.; Zone: fluvial]

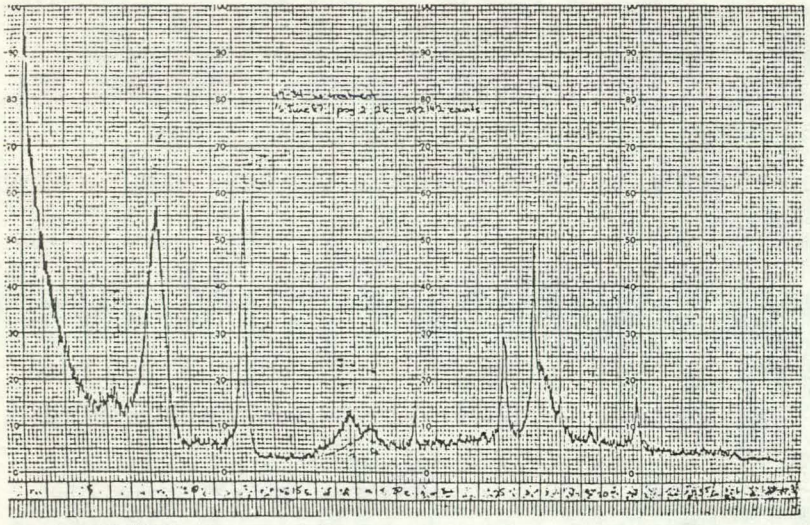

AIR DRIED

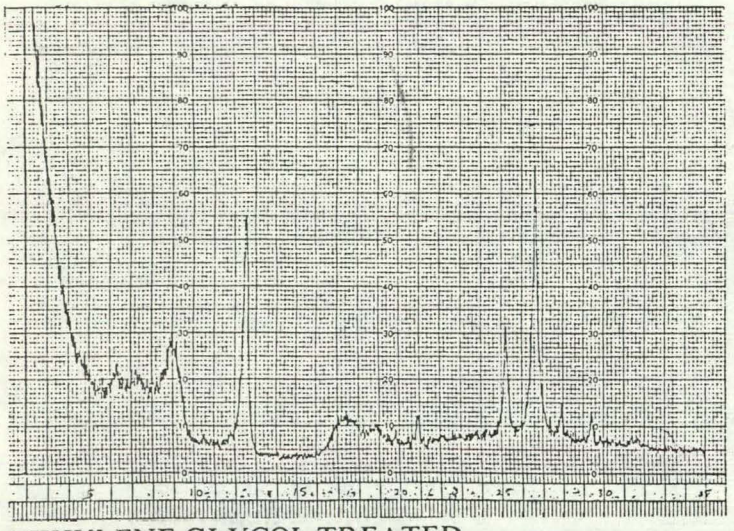

ETHYLENE GLYCOL TREATED

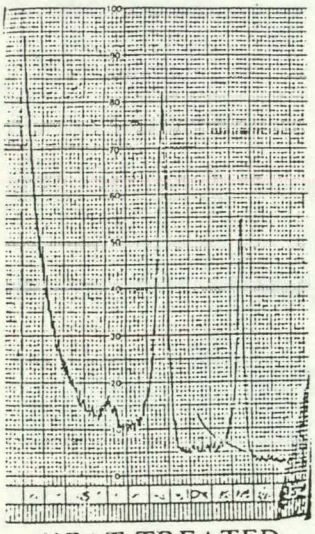

HEAT TREATED

Clays Present (Ratios):

Illite	3
Mixed-Layer Clay	6
Chlorite	2

Water Adsorption-Desorption Isotherm

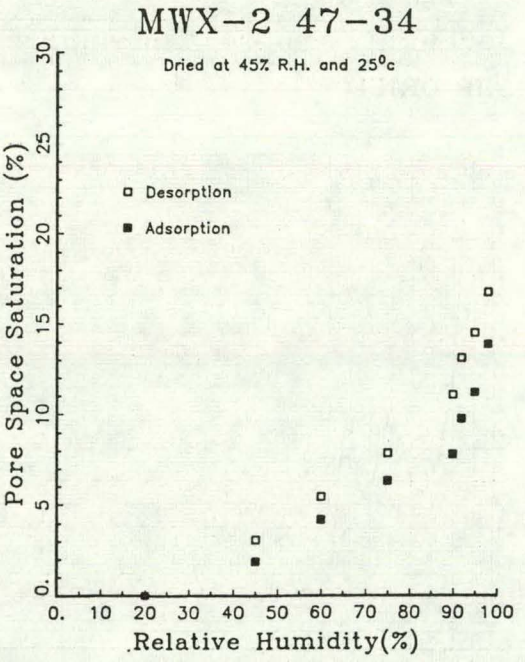

BET Surface Area of Core = 1.07 m^2/g

Figure A13. Properties related to microporosity - MWX2 47-34.
[Depth: 4915.5-4916.6 ft.; Zone: fluvial]

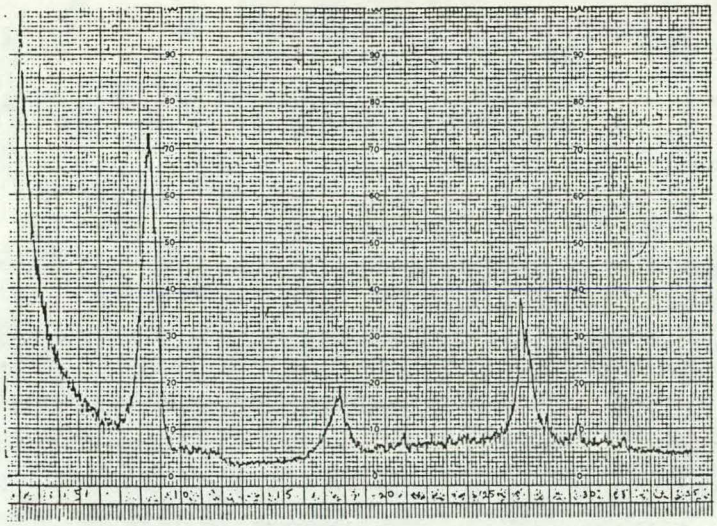

AIR DRIED

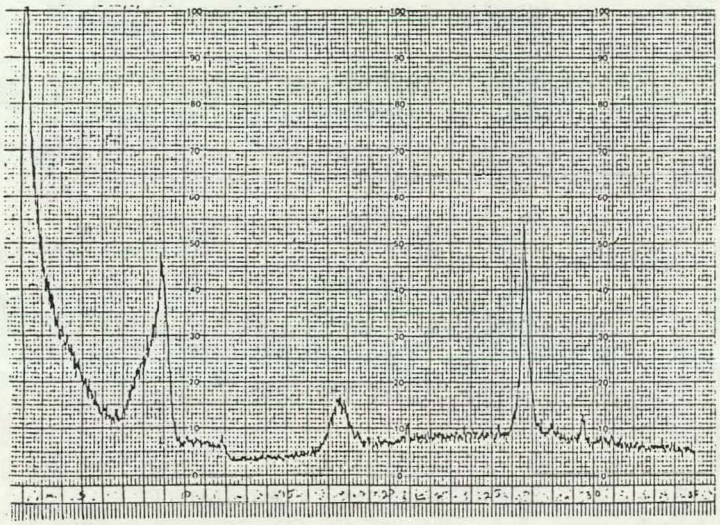

ETHYLENE GLYCOL TREATED

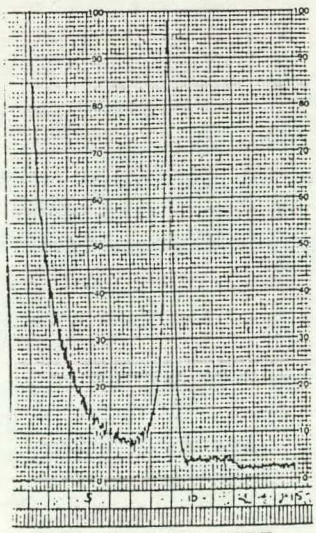

HEAT TREATED

Clays Present (Ratios):

Illite	5
Mixed-Layer Clay	5

Water Adsorption-Desorption Isotherm

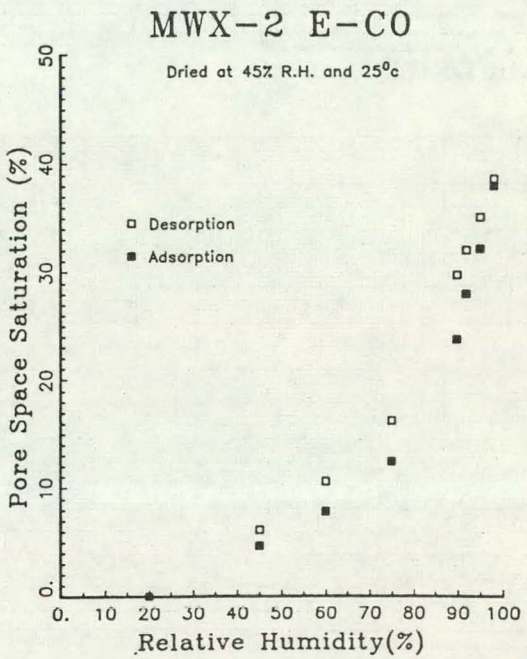

BET Surface Area of Core = 2.13 m^2/g

Figure A14. Properties related to microporosity - MWX2 E-C0.
[Depth: 6432.6-6433.2 ft.; Zone: coastal]

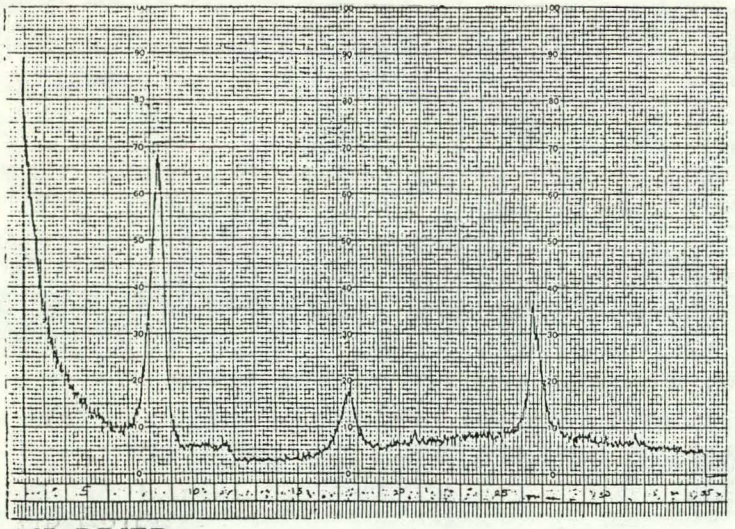

AIR DRIED

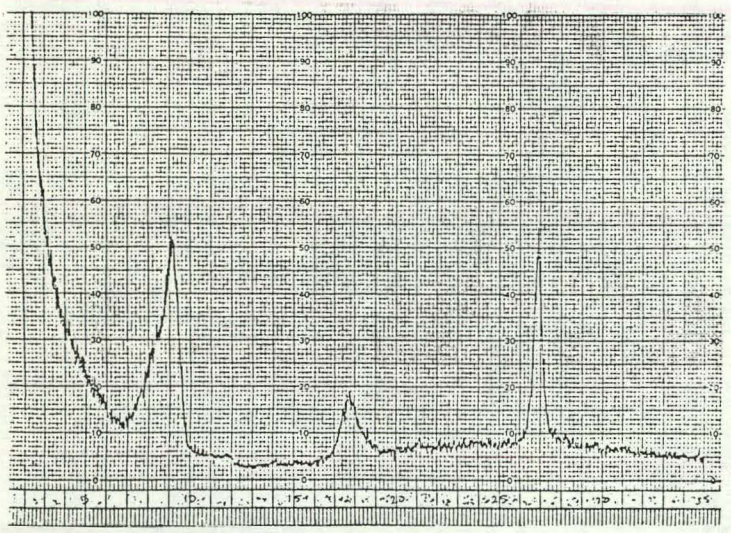

ETHYLENE GLYCOL TREATED

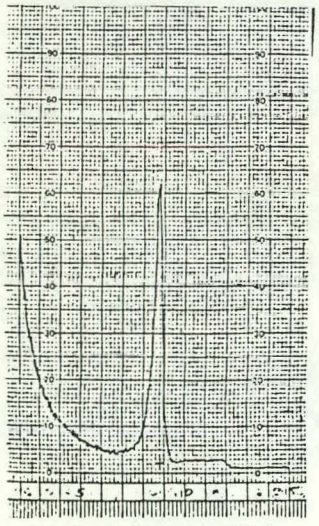

HEAT TREATED

Clays Present (Ratios):

Illite	4
Mixed-Layer Clay	6

Water Adsorption-Desorption Isotherm

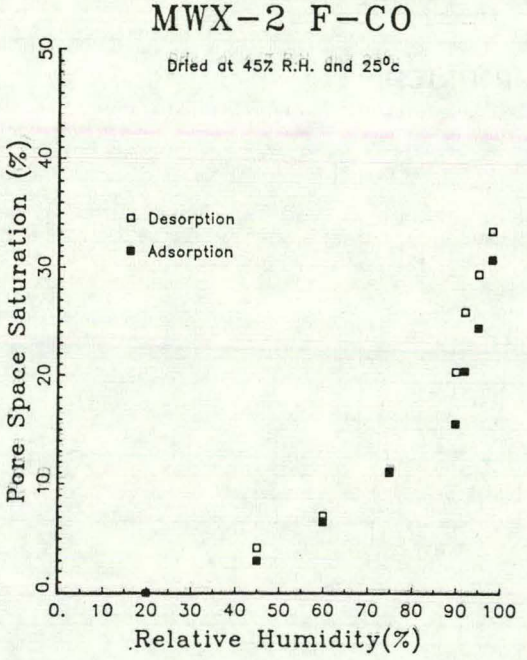

BET Surface Area of Core = 1.50 m^2/g

Figure A15. Properties related to microporosity - MWX2 F-CO.
[Depth: 6452.0-6453.0 ft.; Zone: coastal]

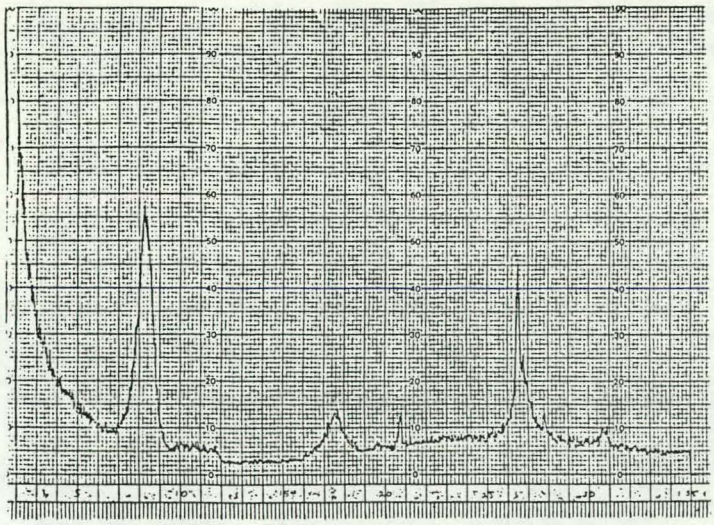

AIR DRIED

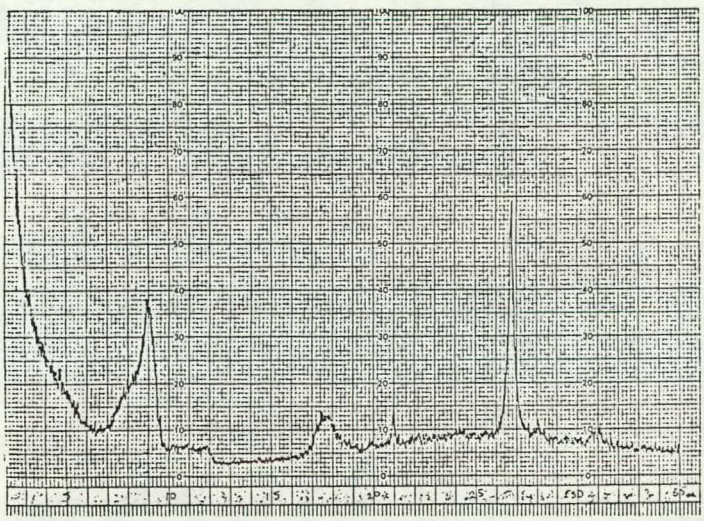

ETHYLENE GLYCOL TREATED

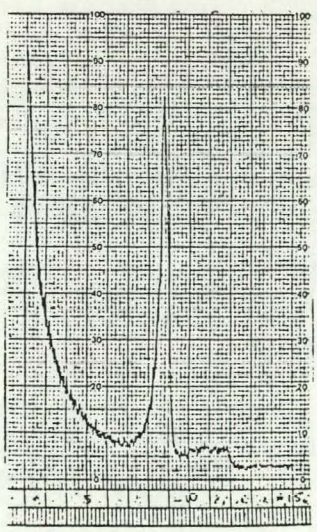

HEAT TREATED

Clays Present (Ratios):

Illite	4
Mixed-Layer Clay	6

Water Adsorption-Desorption Isotherm

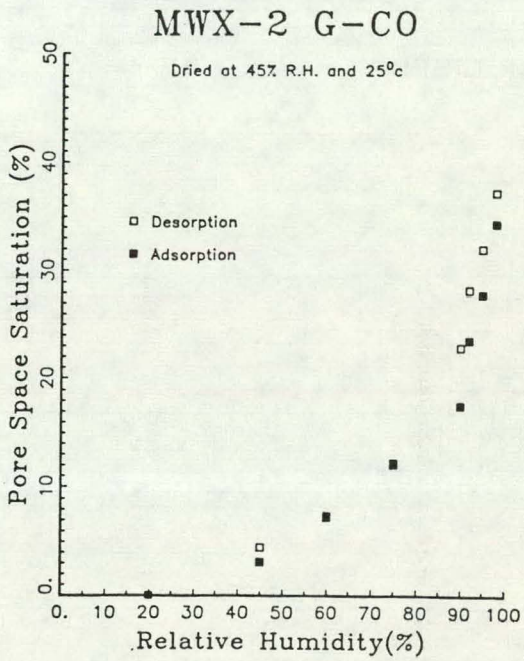

BET Surface Area of Core = 1.79 m^2/g

Figure A16. Properties related to microporosity - MWX2 G-CO.
[Depth: 6471.8-6472.3 ft.; Zone: coastal]

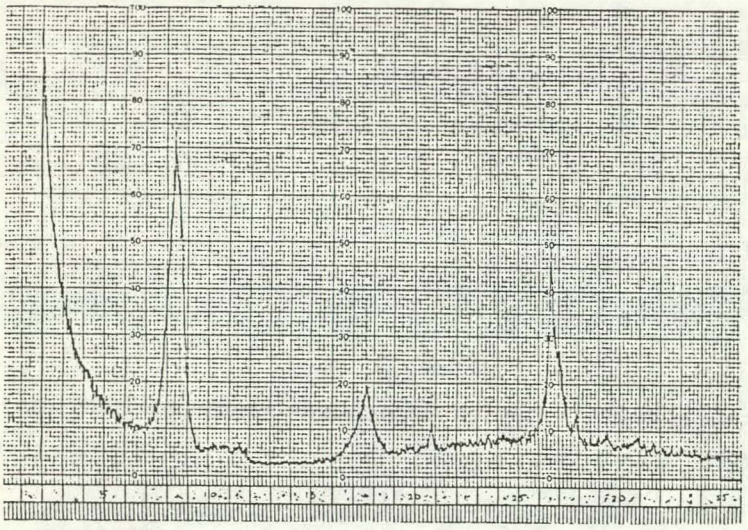

AIR DRIED

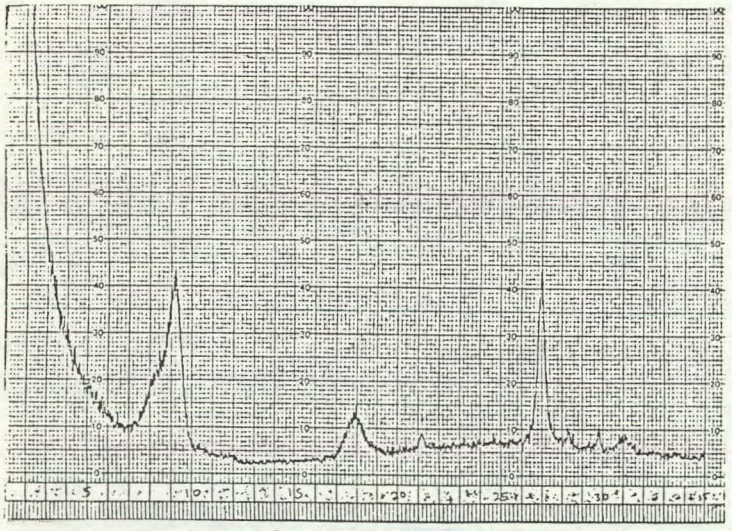

ETHYLENE GLYCOL TREATED

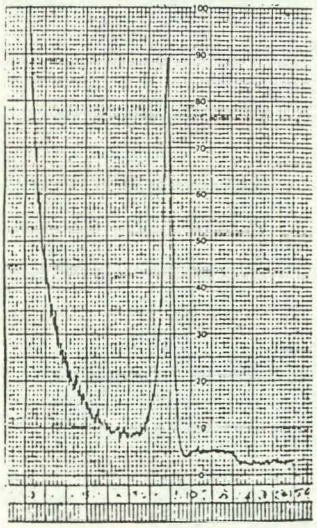

HEAT TREATED

Clays Present (Ratios):

Illite	4
Mixed-Layer Clay	6

Water Adsorption-Desorption Isotherm

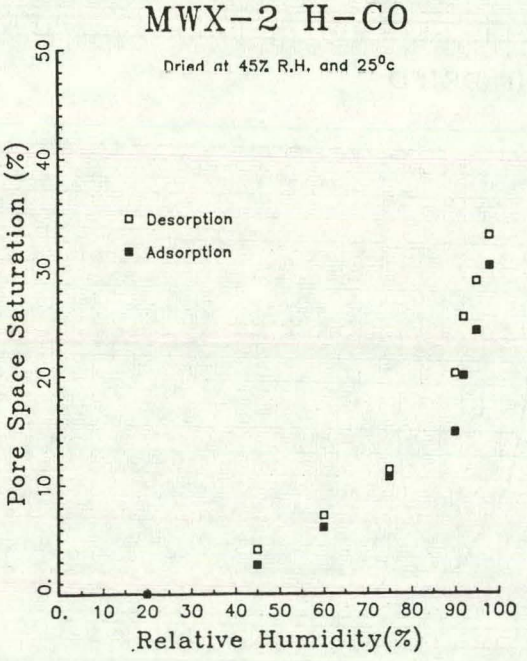

BET Surface Area of Core = 1.41 m^2/g

Figure A17. Properties related to microporosity - MWX2 H-CO.
[Depth: 6507.4-6508.0 ft.; Zone: coastal]

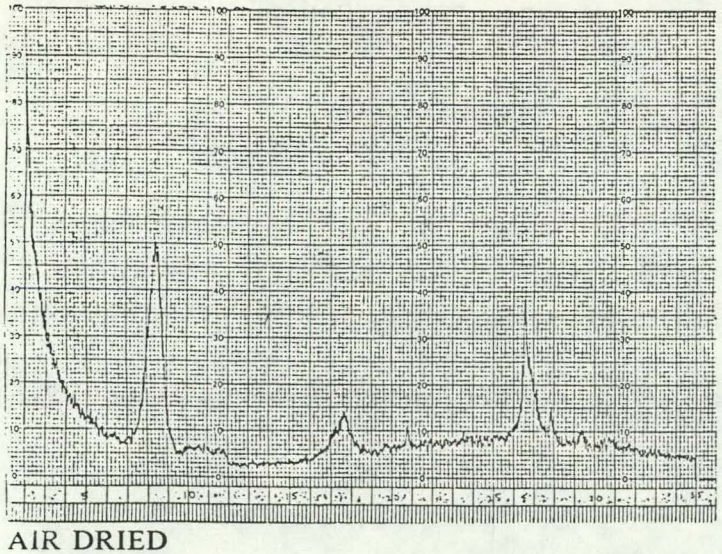

AIR DRIED

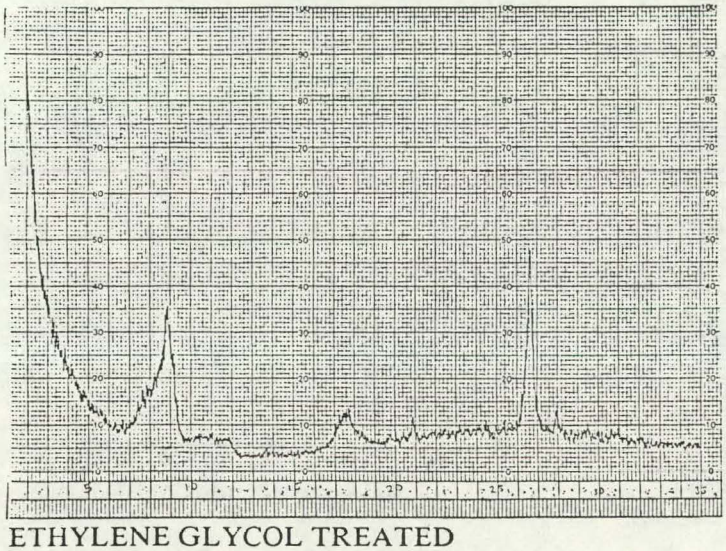

ETHYLENE GLYCOL TREATED

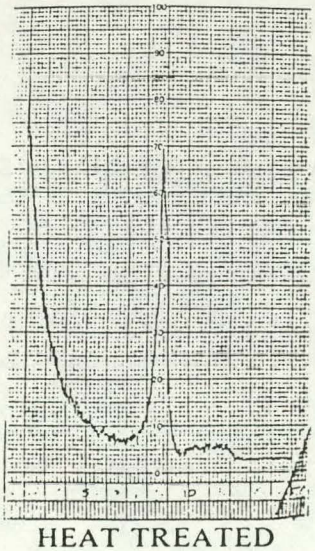

HEAT TREATED

Clays Present (Ratios):

Illite	5
Mixed-Layer Clay	5

Water Adsorption-Desorption Isotherm

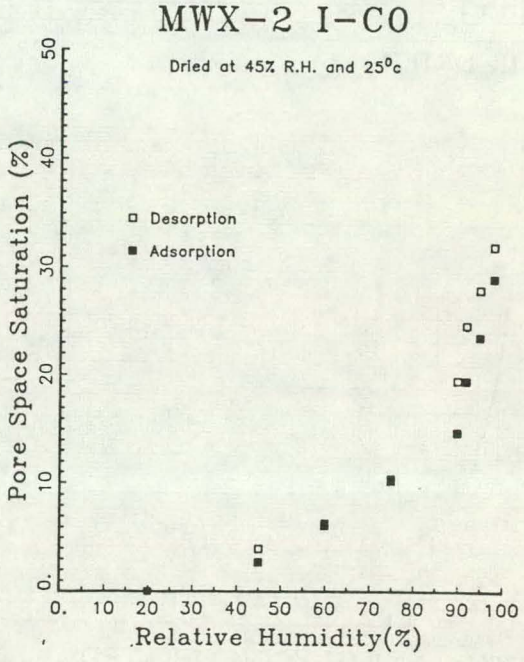

BET Surface Area of Core = 1.50 m^2/g

Figure A18. Properties related to microporosity - MWX2 I-CO.
[Depth: 6537.0-6537.9 ft.; Zone: coastal]

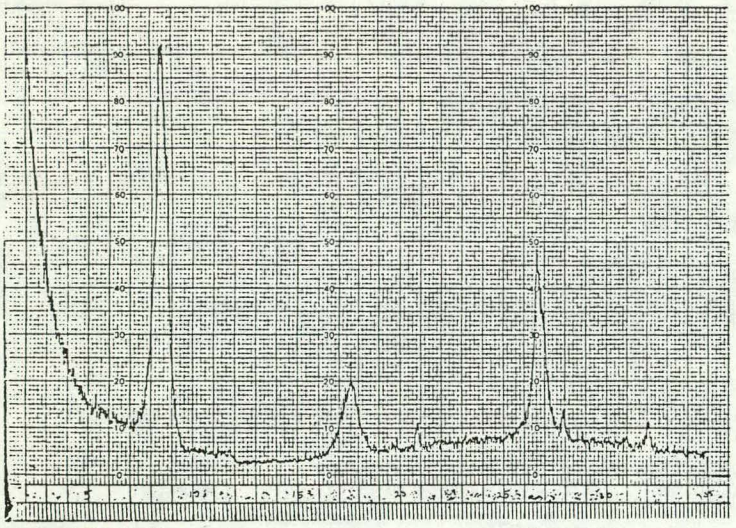

AIR DRIED

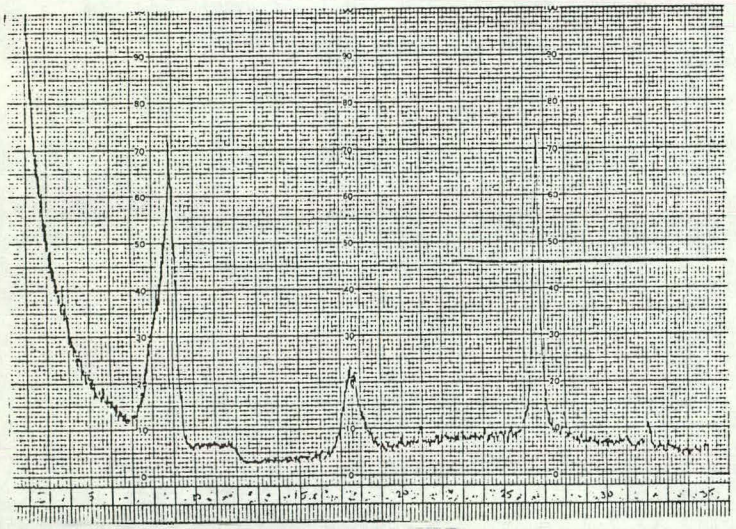

ETHYLENE GLYCOL TREATED

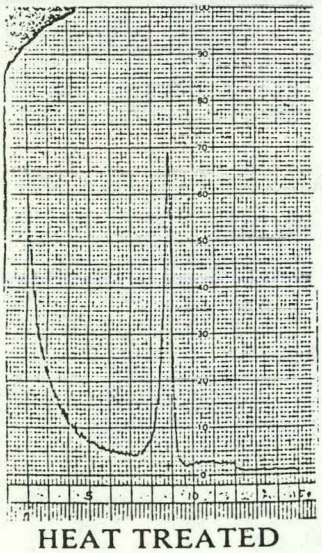

HEAT TREATED

Clays Present (Ratios):

Illite	5
Mixed-Layer Clay	5

Water Adsorption-Desorption Isotherm

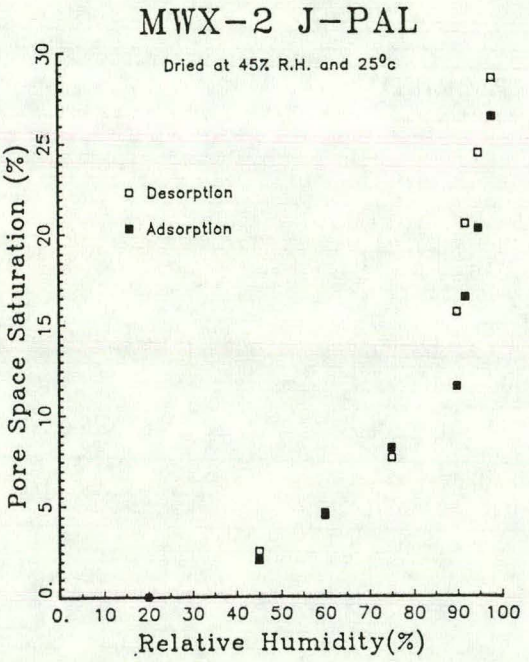

BET Surface Area of Core = 2.15 m^2/g

Figure A19. Properties related to microporosity - MWX2 J-PAL.
[Depth: 7119.4-7120.3 ft.; Zone: paludal]

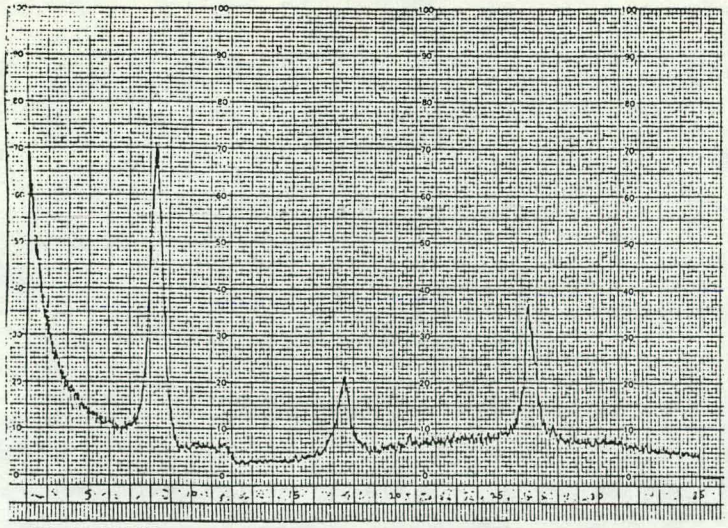

AIR DRIED

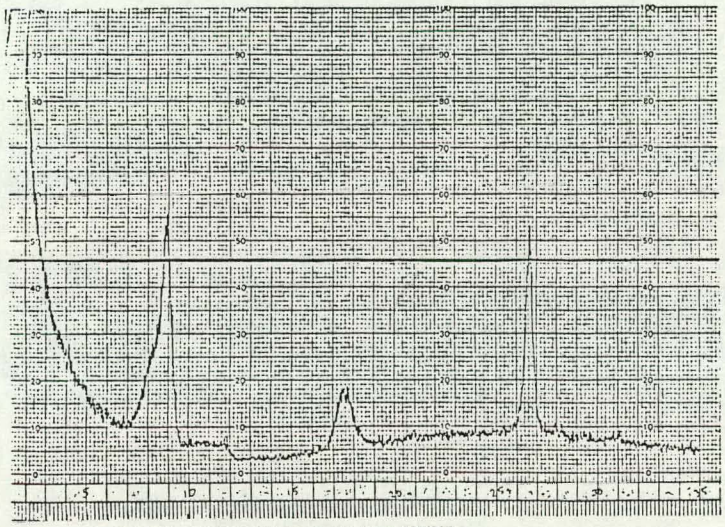

ETHYLENE GLYCOL TREATED

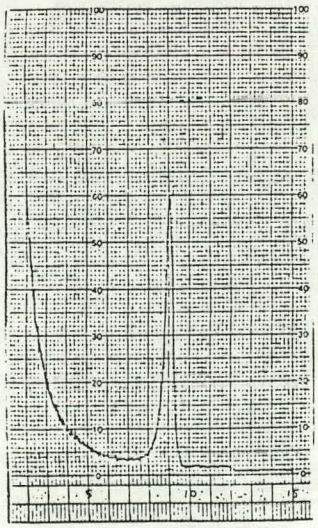

HEAT TREATED

Clays Present (Ratios):

Illite	4
Mixed-Layer Clay	6

Water Adsorption-Desorption Isotherm

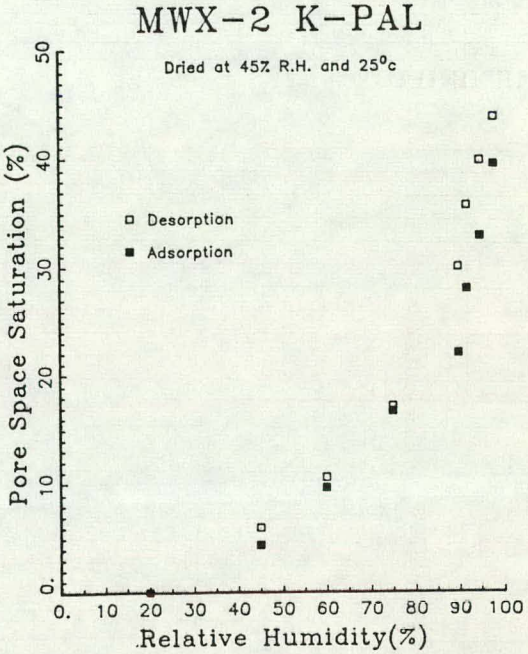

BET Surface Area of Core = 1.94 m^2/g

Figure A20. Properties related to microporosity - MWX2 K-PAL.
[Depth: 7139.2-7139.9 ft.; Zone: paludal]

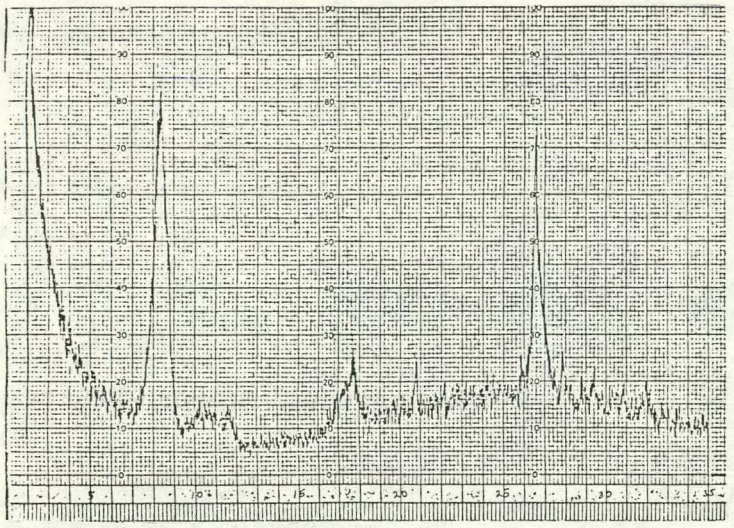

AIR DRIED

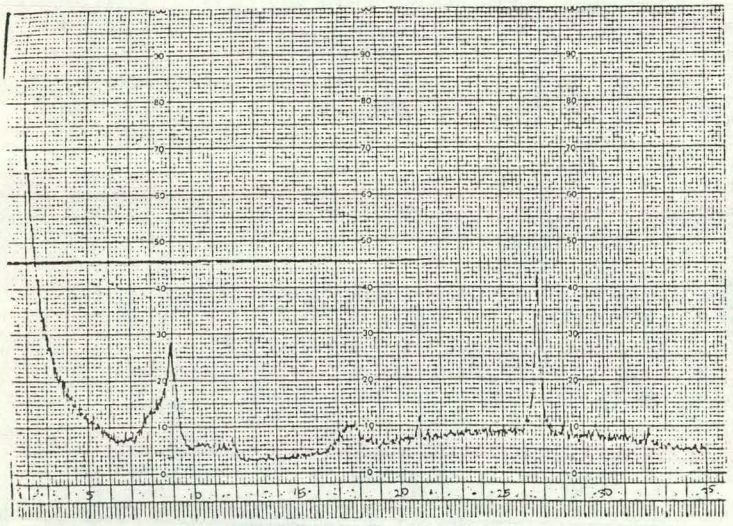

ETHYLENE GLYCOL TREATED

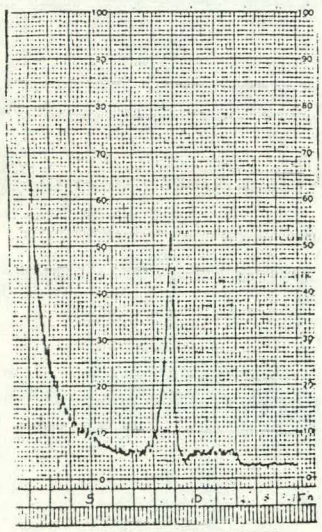

HEAT TREATED

Clays Present (Ratios):

Illite	5
Mixed-Layer Clay	5

Water Adsorption-Desorption Isotherm

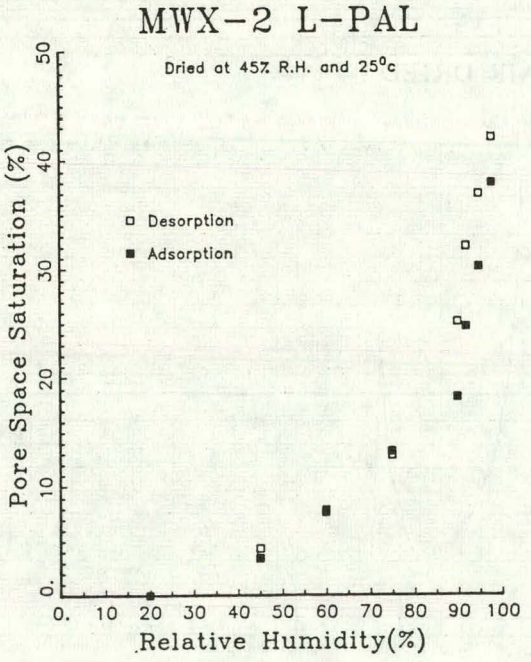

BET Surface Area of Core = 1.44 m^2/g

Figure A21. Properties related to microporosity - MWX2 L-PAL.
[Depth: 7278.9-7279.7 ft.; Zone: paludal]

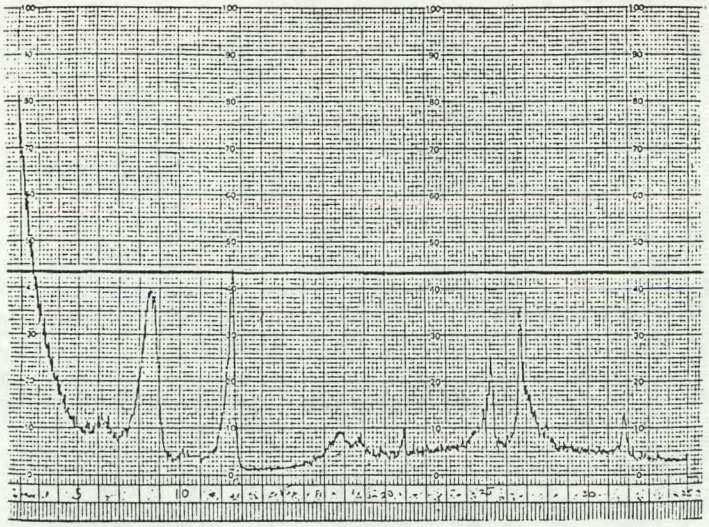

AIR DRIED

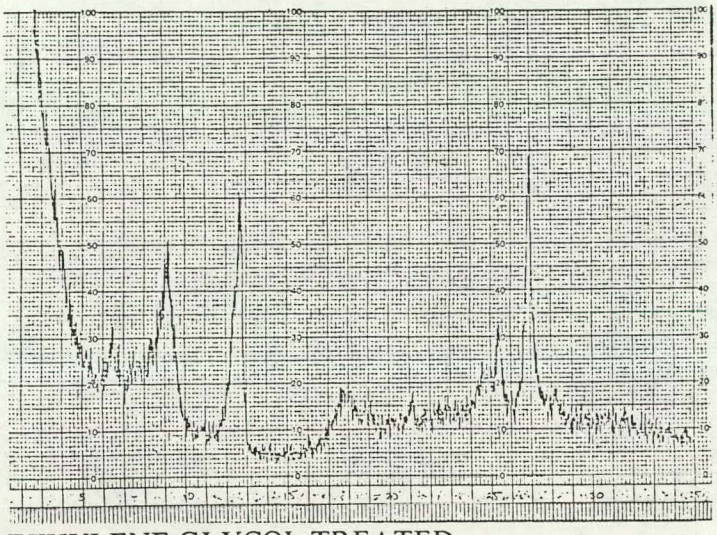

ETHYLENE GLYCOL TREATED

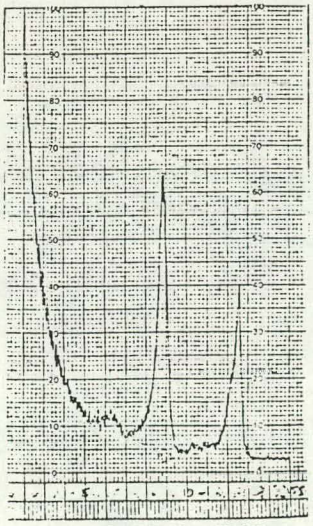

HEAT TREATED

Clays Present (Ratios):

Illite	2
Mixed-Layer Clay	4
Kaolinite	0.3
Chlorite	2

Water Adsorption-Desorption Isotherm

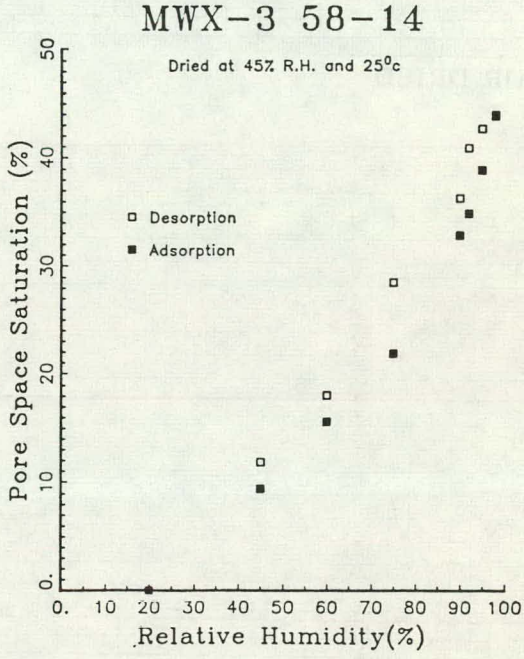

BET Surface Area of Core = 2.97 m^2/g

Figure A22. Properties related to microporosity - MWX3 58-14.
[Depth: 4918.1-4918.7 ft.; Zone: fluvial]

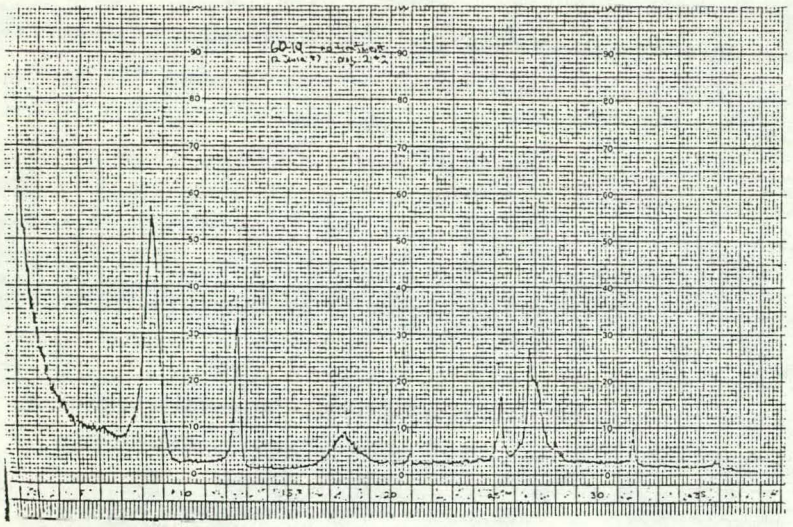

AIR DRIED

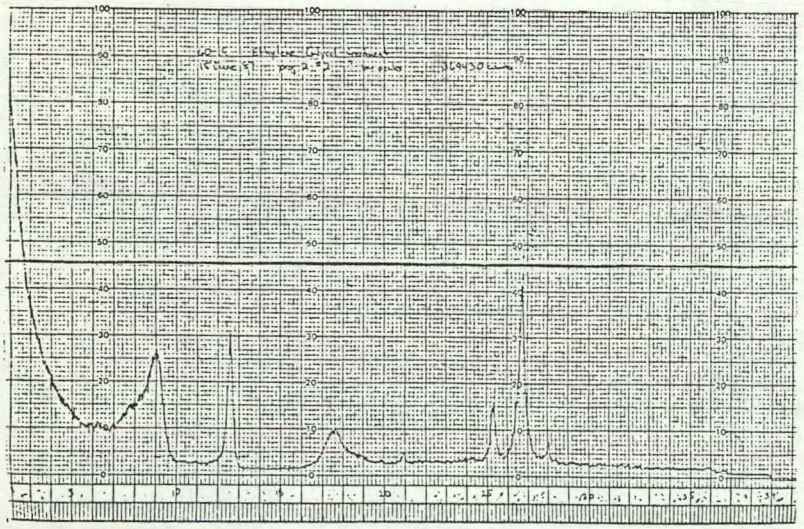

ETHYLENE GLYCOL TREATED

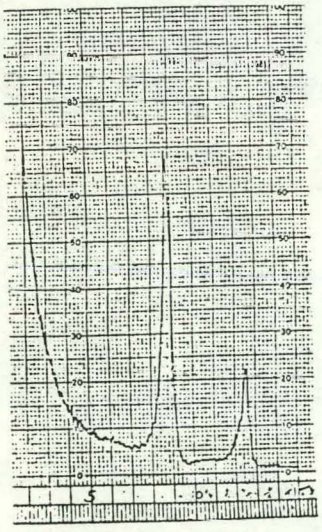

HEAT TREATED

Clays Present (Ratios):

Illite	3
Mixed-Layer Clay	6
Chlorite	0.5

Water Adsorption-Desorption Isotherm

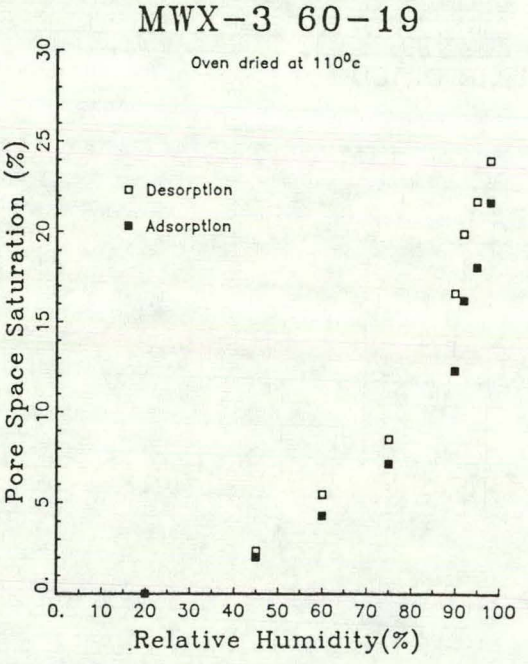

BET Surface Area of Core = 2.80 m^2/g

Figure A23. Properties related to microporosity - MWX3 60-19.
[Depth: 5726.3-5726.8 ft.; Zone: fluvial]

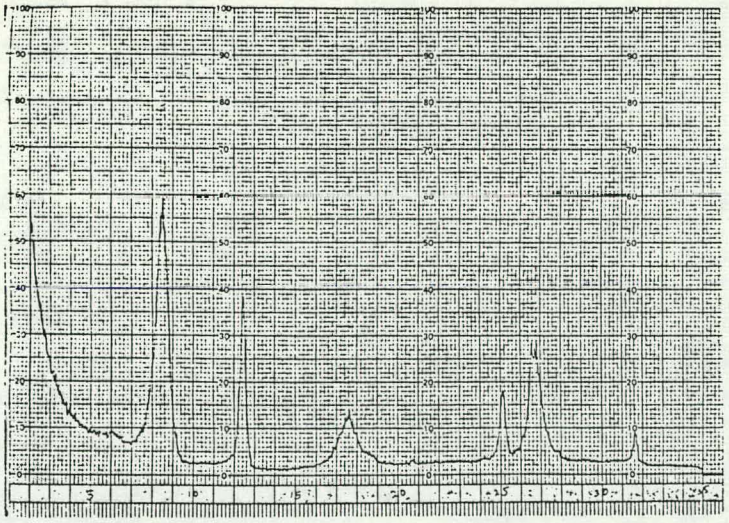

AIR DRIED

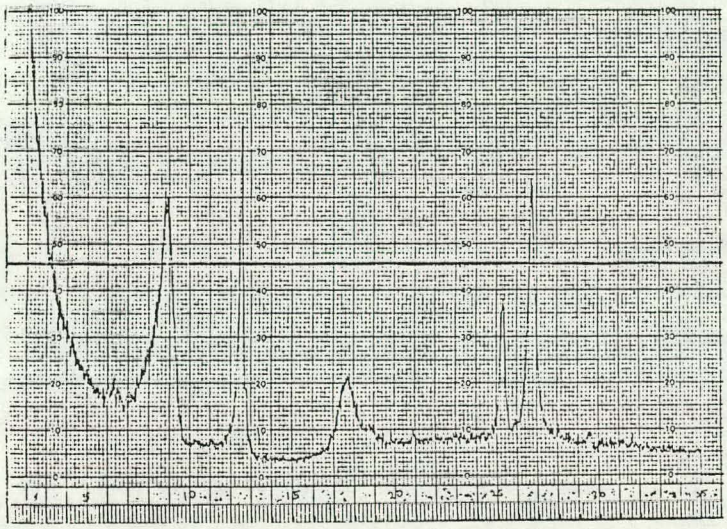

ETHYLENE GLYCOL TREATED

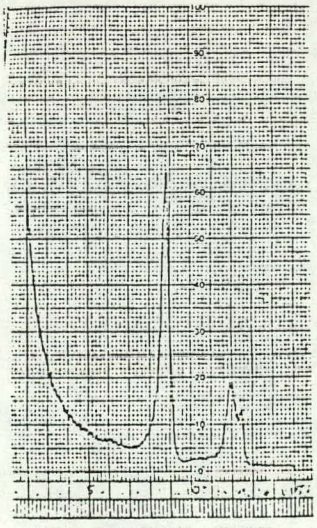

HEAT TREATED

Clays Present (Ratios):

Illite	4
Mixed-Layer Clay	5
Chlorite	1

Water Adsorption-Desorption Isotherm

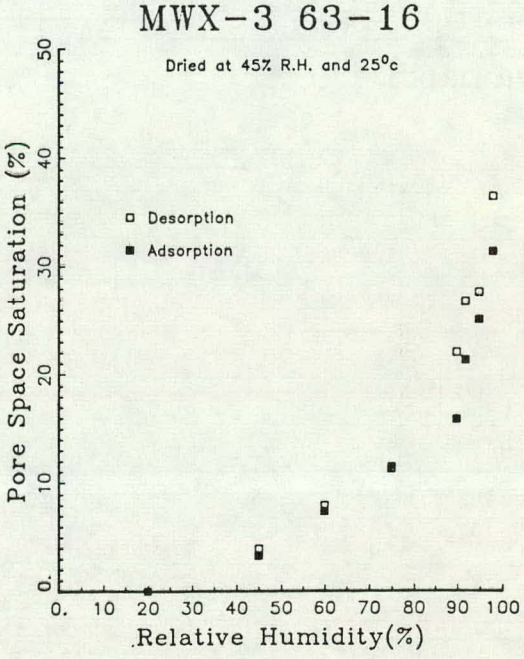

BET Surface Area of Core = 3.11 m^2/g

Figure A24. Properties related to microporosity - MWX3 63-16.
[Depth: 5832.1-5832.6 ft.; Zone: fluvial]

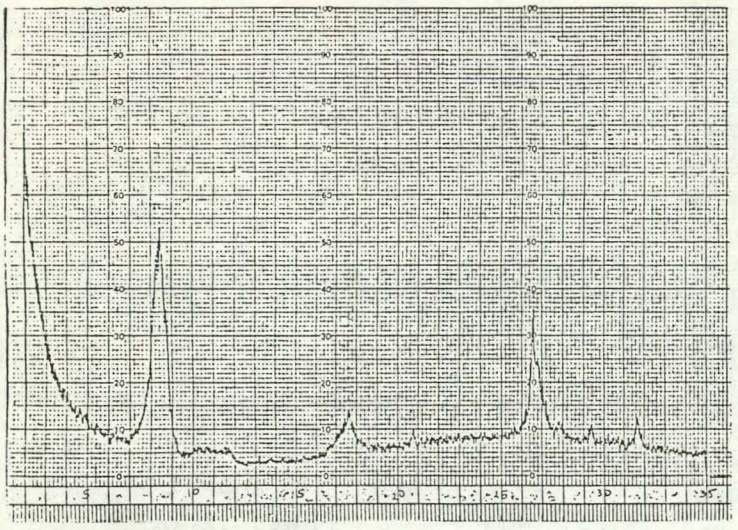

AIR DRIED

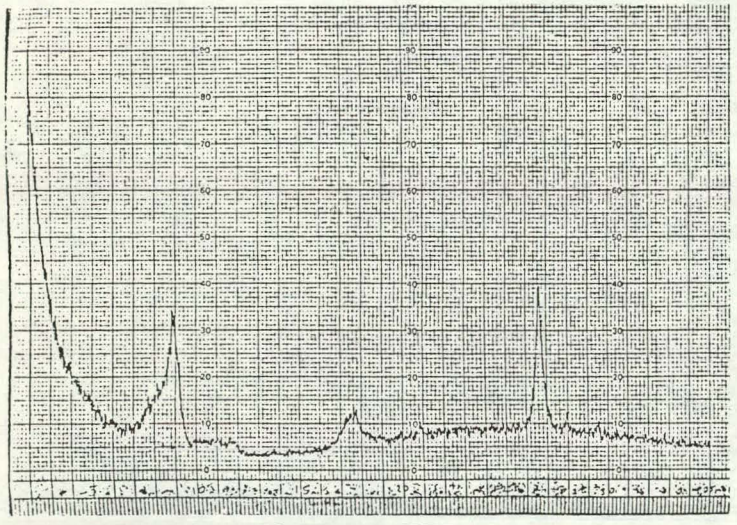

ETHYLENE GLYCOL TREATED

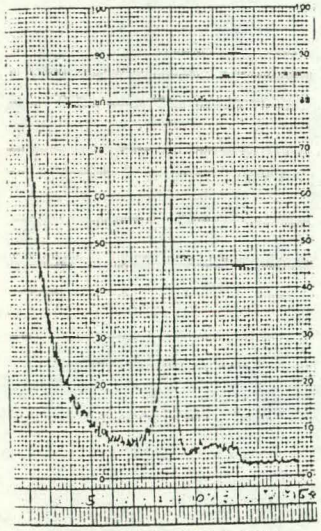

HEAT TREATED

Clays Present (Ratios):

Illite	4
Mixed-Layer Clay	6

Water Adsorption-Desorption Isotherm

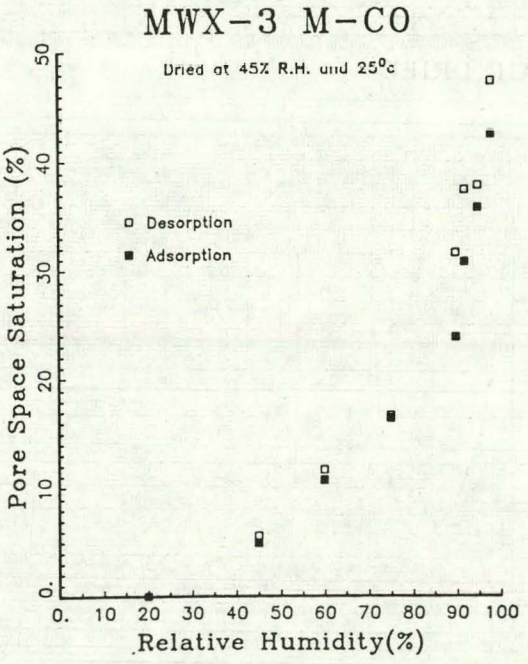

BET Surface Area of Core = 3.57 m^2/g

Figure A25. Properties related to microporosity - MWX3 M-CO.
[Depth: 6445.0-6445.8 ft.; Zone: coastal]

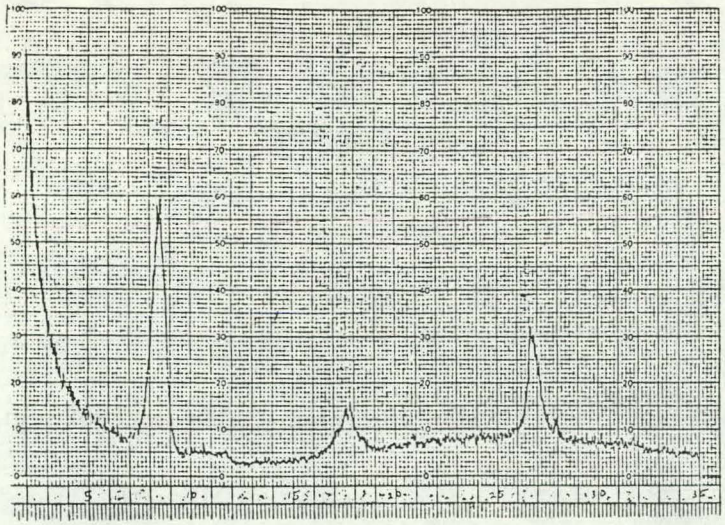

AIR DRIED

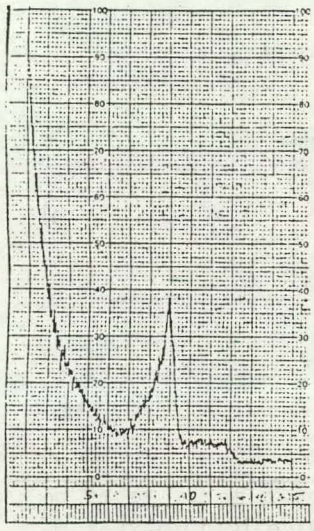

ETHYLENE GLYCOL TREATED

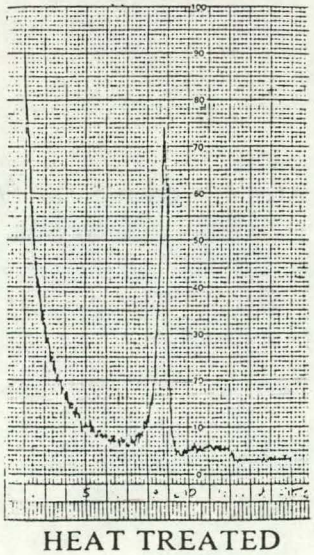

HEAT TREATED

Clays Present (Ratios):

Illite	5
Mixed-Layer Clay	5

Water Adsorption-Desorption Isotherm

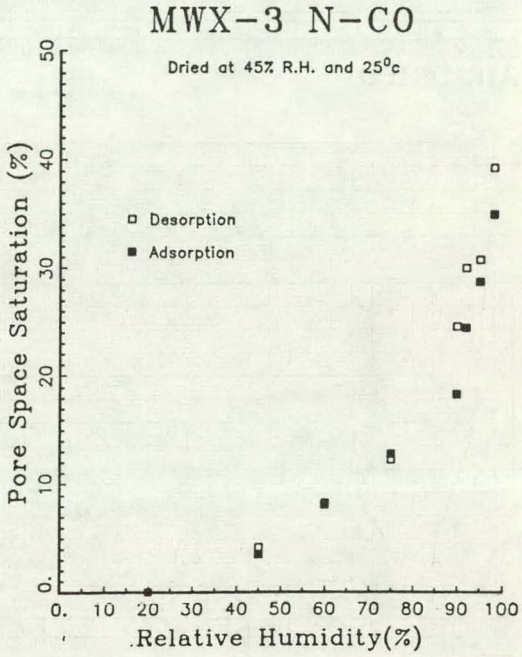

BET Surface Area of Core = 3.46 m^2/g

Figure A26. Properties related to microporosity - MWX3 N-CO.
[Depth: 6461.1-6461.8 ft.; Zone: coastal]

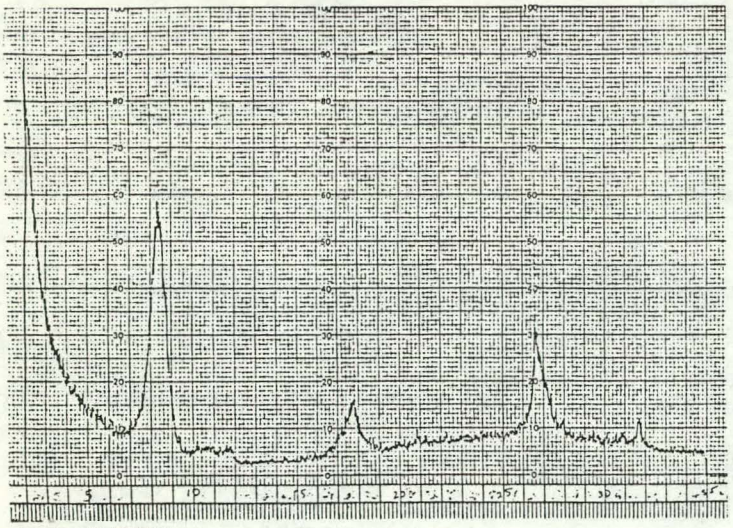

AIR DRIED

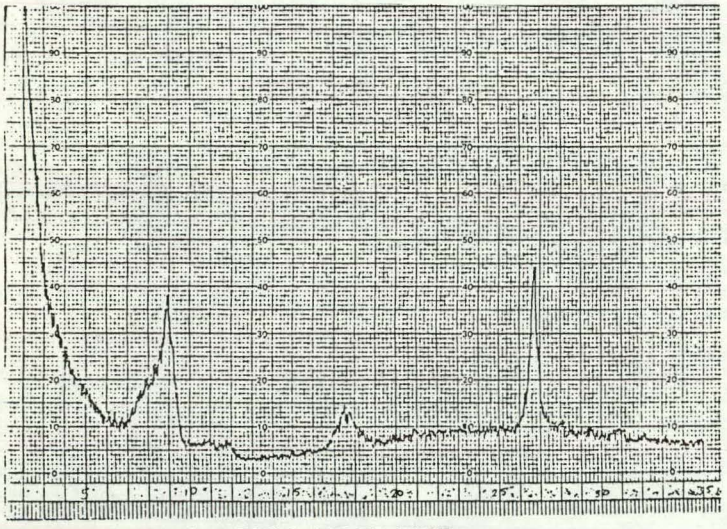

ETHYLENE GLYCOL TREATED

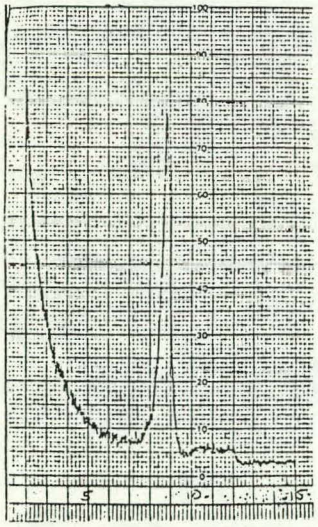

HEAT TREATED

Clays Present (Ratios):

Illite	4
Mixed-Layer Clay	6

Water Adsorption-Desorption Isotherm

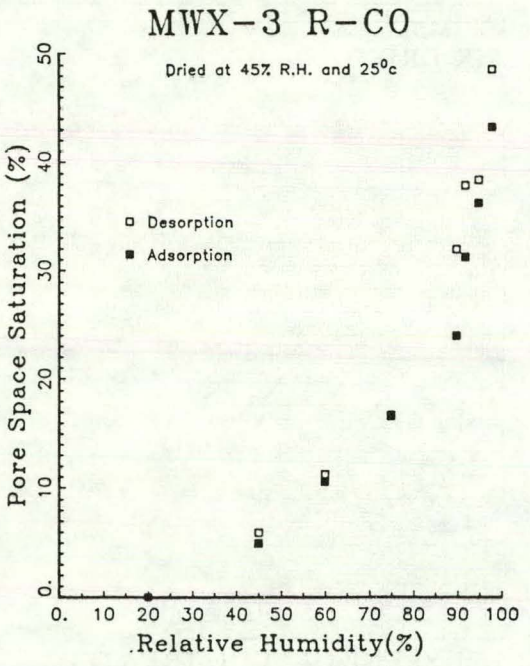

BET Surface Area of Core = 3.05 m^2/g

Figure A27. Properties related to microporosity - MWX3 R-CO.
[Depth: 6511.9-6512.4 ft.; Zone: coastal]

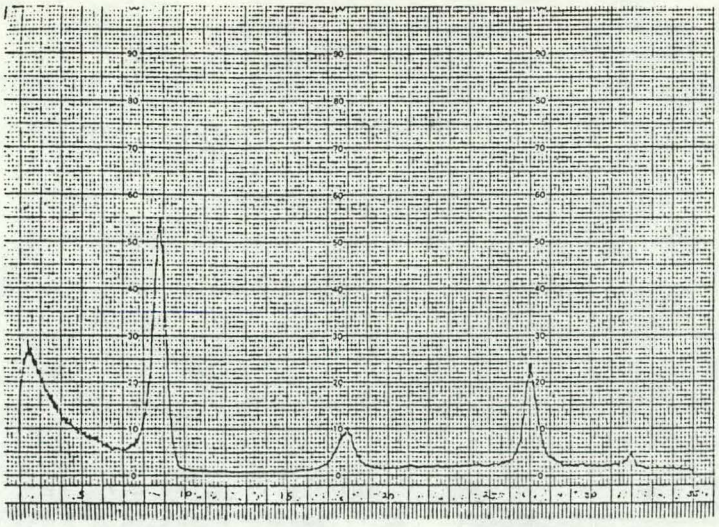

AIR DRIED

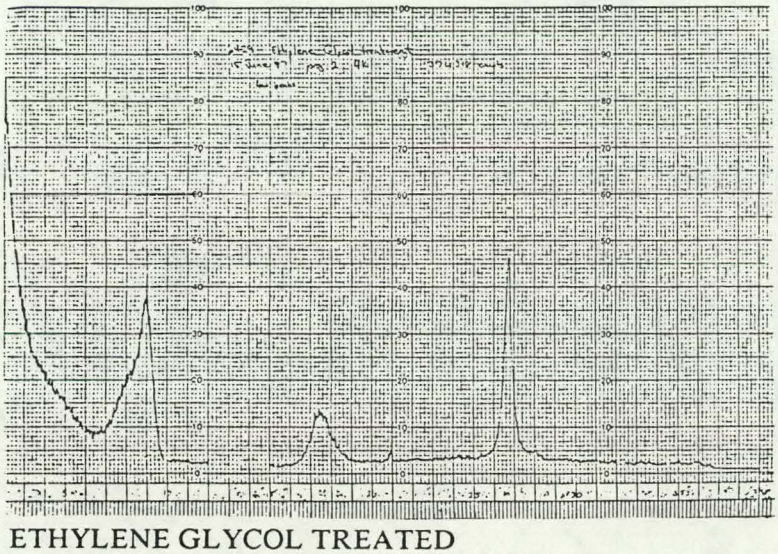

ETHYLENE GLYCOL TREATED

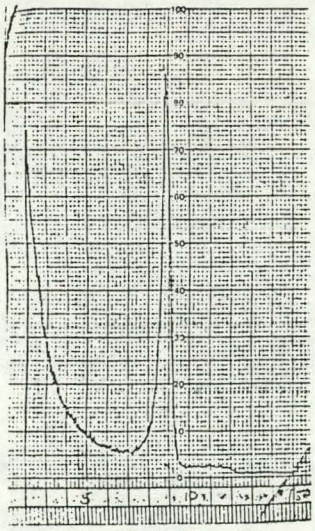

HEAT TREATED

Clays Present (Ratios):

Illite	4
Mixed-Layer Clay	6

Water Adsorption-Desorption Isotherm

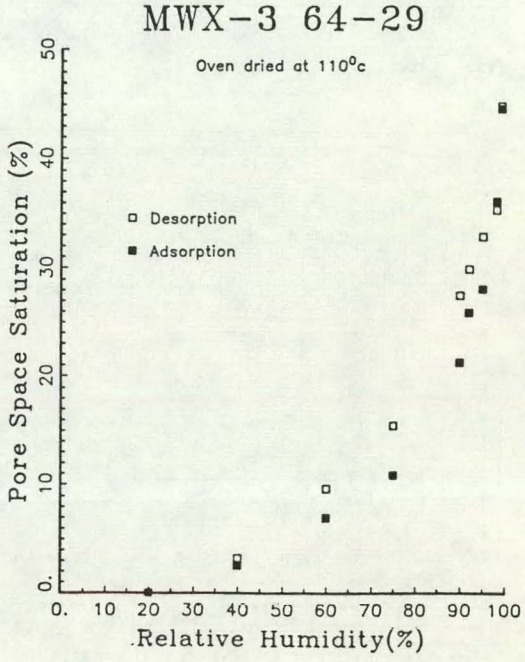

BET Surface Area of Core = 4.35 m^2/g

Figure A28. Properties related to microporosity - MWX3 64-29.
[Depth: 6464.5-6465.0 ft.; Zone: coastal]

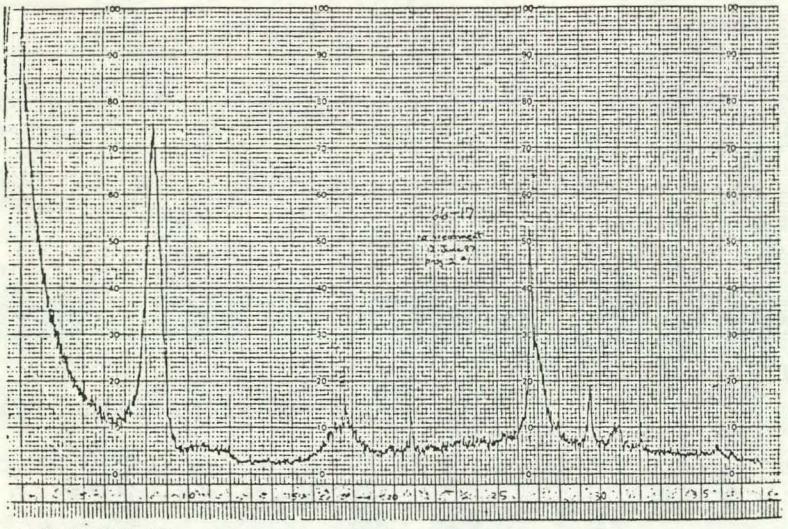

AIR DRIED

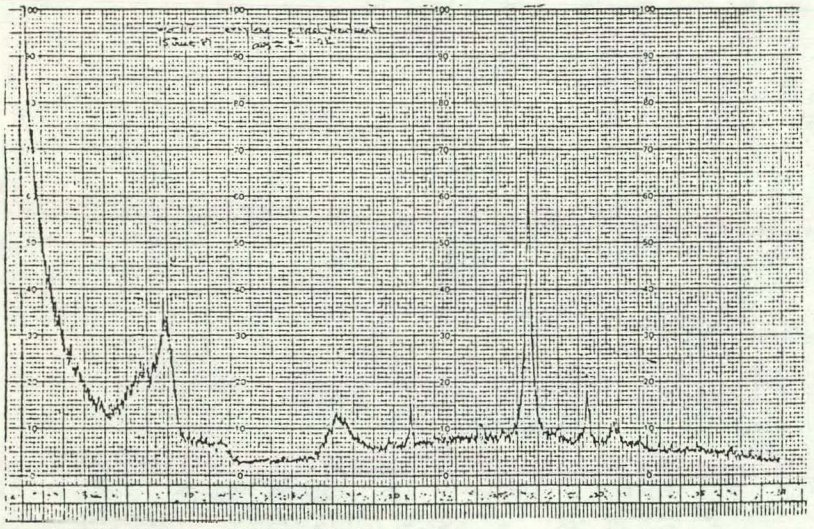

ETHYLENE GLYCOL TREATED

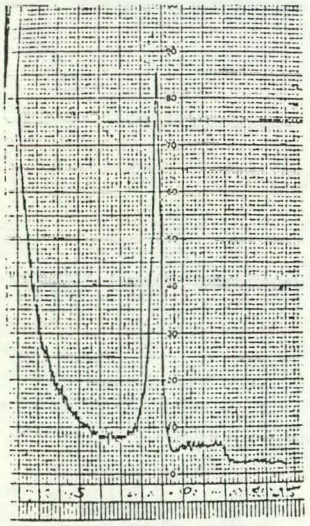

HEAT TREATED

Clays Present (Ratios):

Illite	4
Mixed-Layer Clay	6

Water Adsorption-Desorption Isotherm

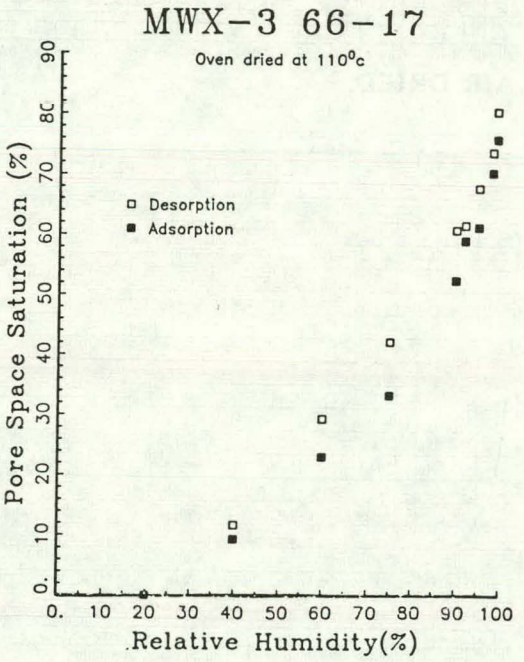

BET Surface Area of Core = 2.41 m^2/g

Figure A29. Properties related to microporosity - MWX3 66-17.
[Depth: 6893.4-6893.8 ft.; Zone: paludal]

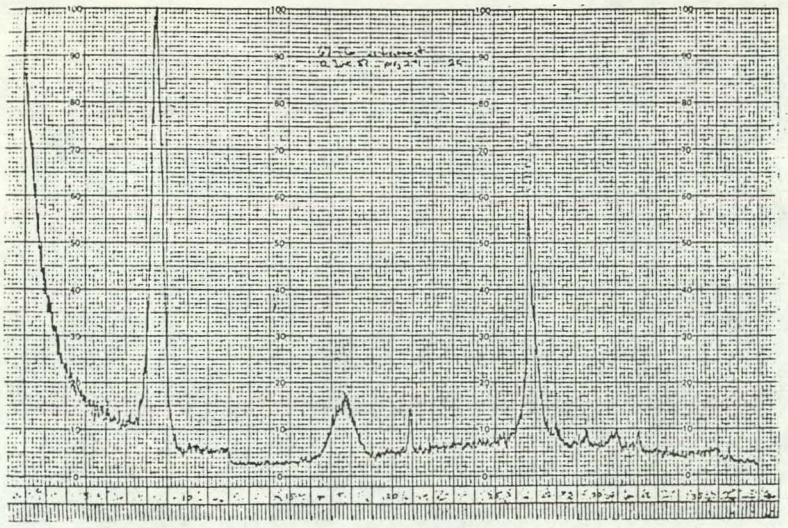

AIR DRIED

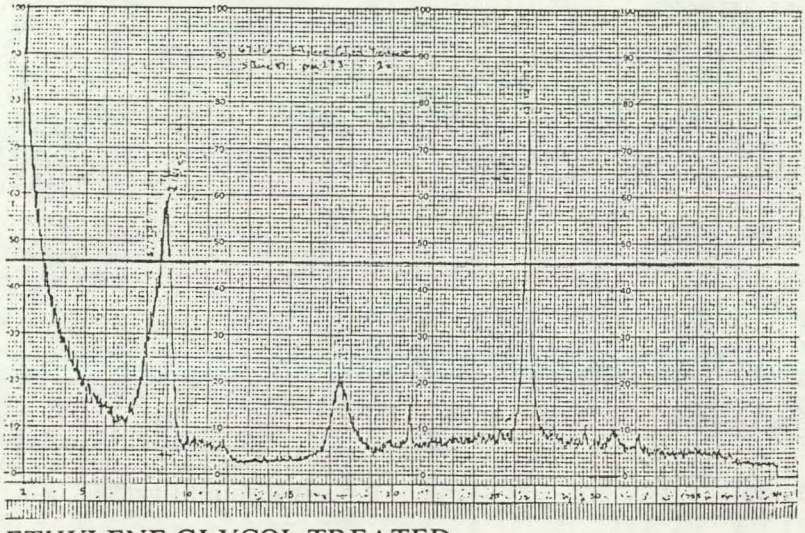

ETHYLENE GLYCOL TREATED

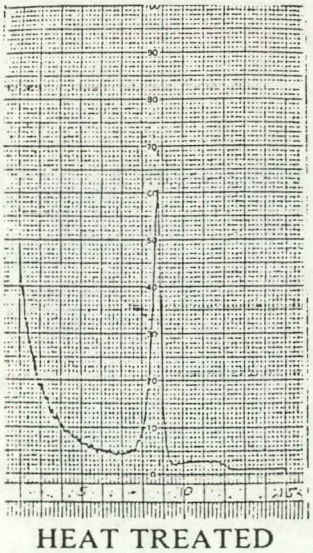

HEAT TREATED

Clays Present (Ratios):

Illite	5
Mixed-Layer Clay	5

Water Adsorption-Desorption Isotherm

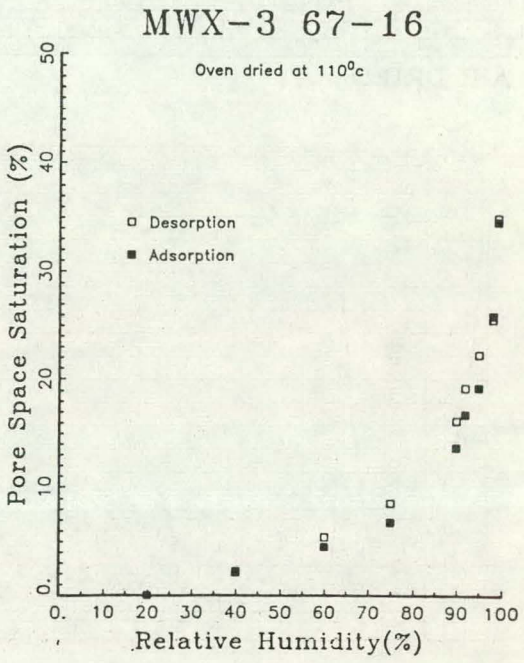

BET Surface Area of Core = 3.41 m^2/g

Figure A30. Properties related to microporosity - MWX3 67-16.
[Depth: 7096.1-7096.7 ft.; Zone: paludal]

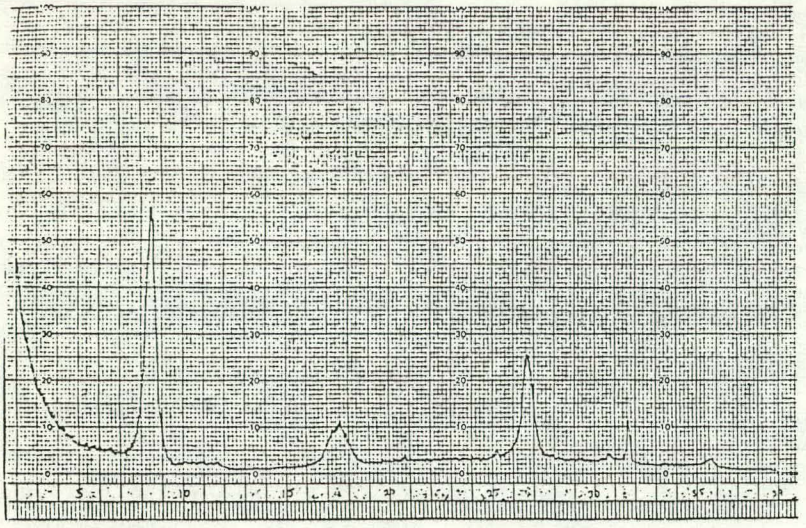

AIR DRIED

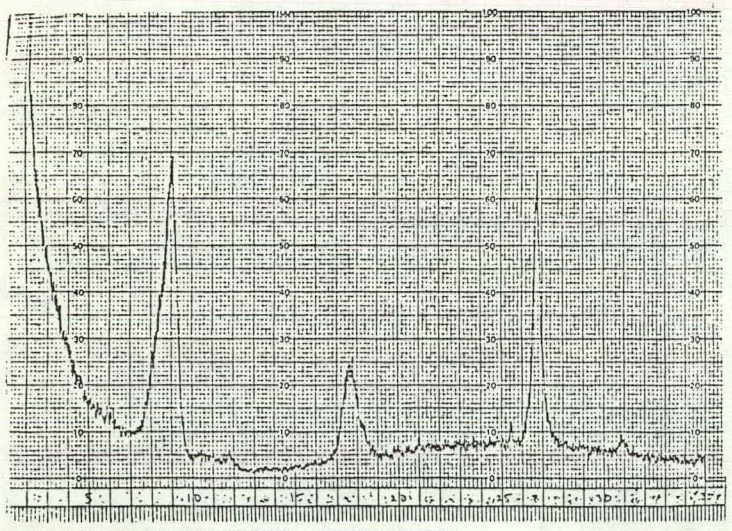

ETHYLENE GLYCOL TREATED

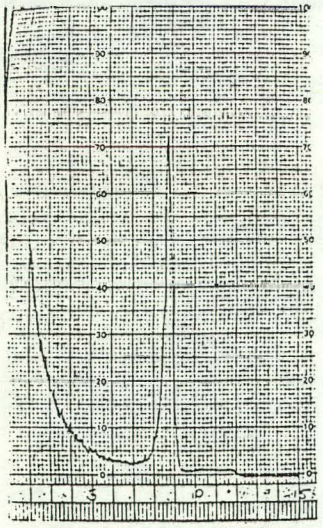

HEAT TREATED

Clays Present (Ratios):

Illite	4
Mixed-Layer Clay	6

Water Adsorption-Desorption Isotherm

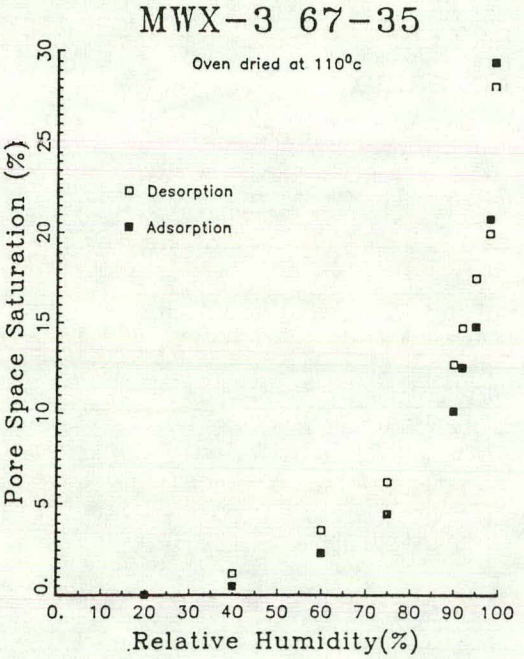

BET Surface Area of Core = 3.00 m^2/g

Figure A31. Properties related to microporosity - MWX3 67-35.
[Depth: 7134.2-7134.6 ft.; Zone: paludal]

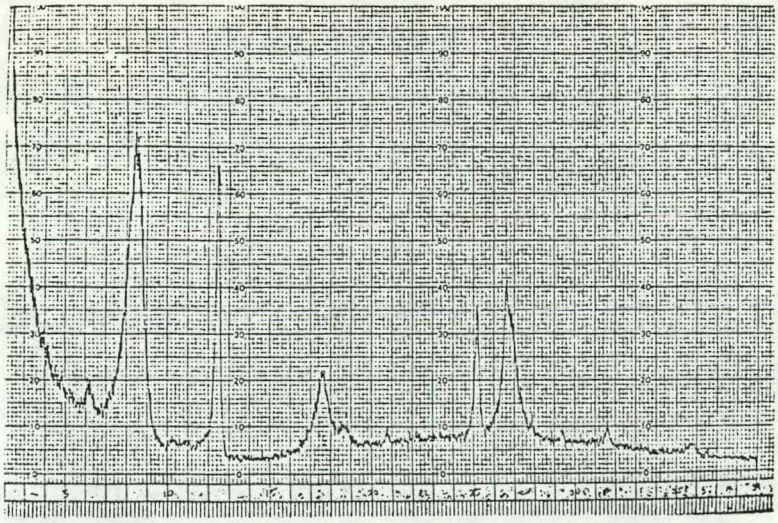

AIR DRIED

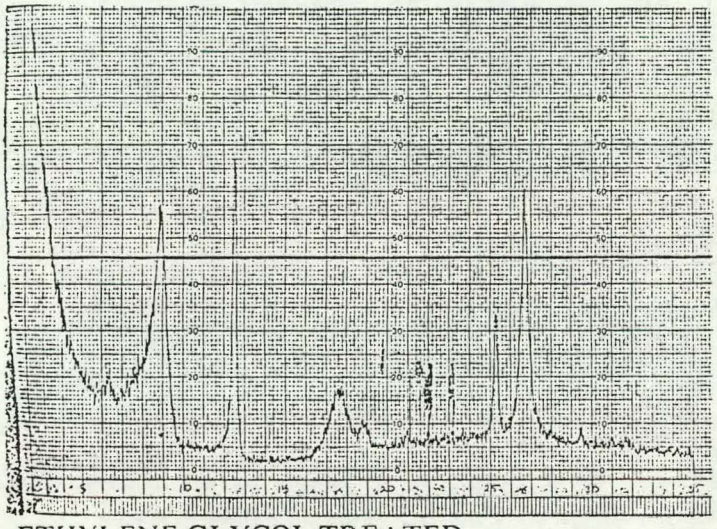

ETHYLENE GLYCOL TREATED

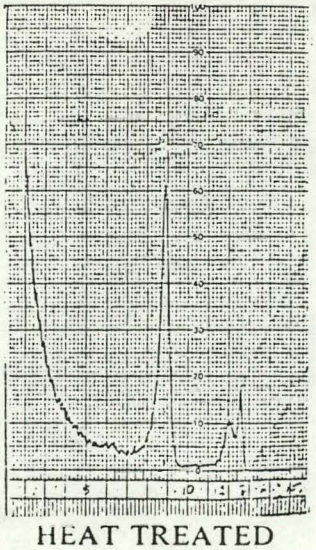

HEAT TREATED

Clays Present (Ratios):

Illite	4
Mixed-Layer Clay	5
Chlorite	1

Water Adsorption-Desorption Isotherm

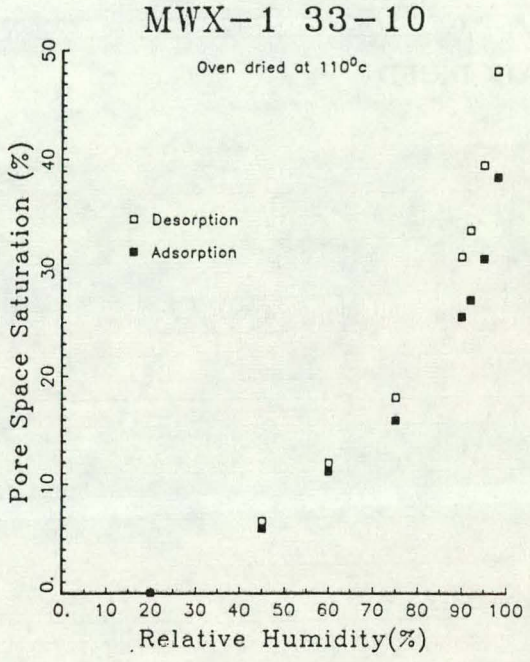

BET Surface Area of Core = 0.93 m^2/g

Figure A32. Properties related to microporosity - MWX1 33-10.
[Depth: 5962.6-5963.1 ft.; Zone: fluvial]

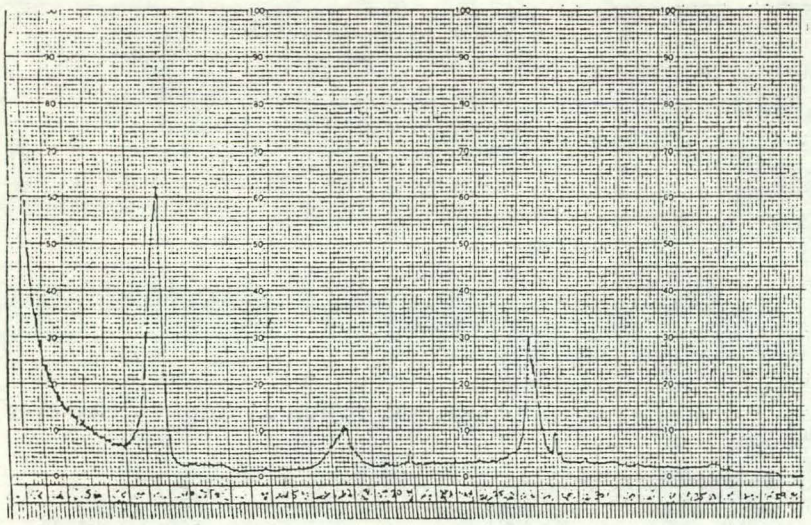

AIR DRIED

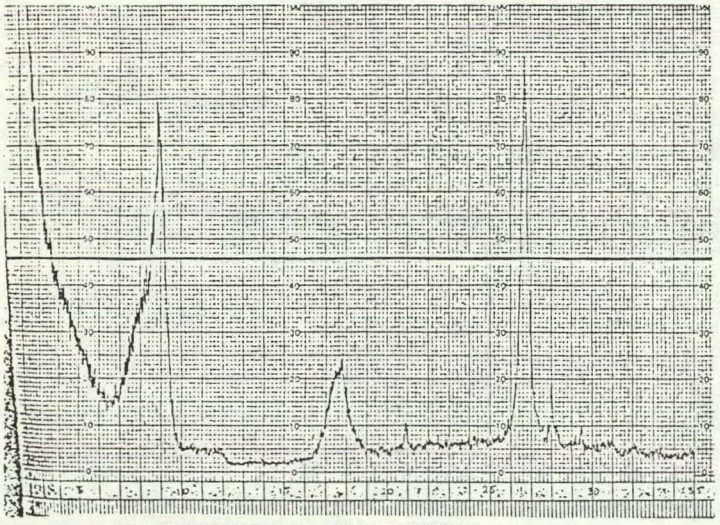

ETHYLENE GLYCOL TREATED

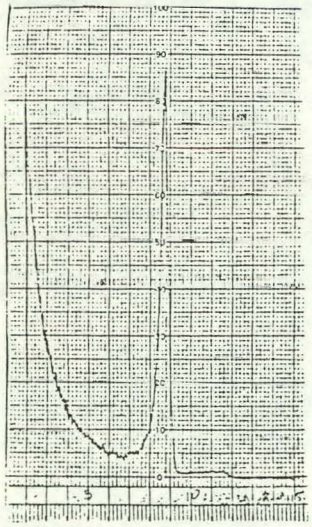

HEAT TREATED

Clays Present (Ratios):

Illite	4
Mixed-Layer Clay	6

Water Adsorption-Desorption Isotherm

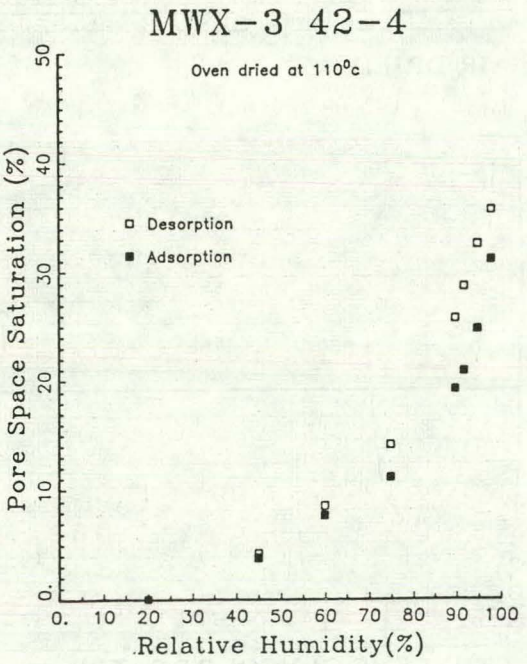

Figure A33. Properties related to microporosity - MWX3 42-4.
[Depth: 6546.5-6547.1 ft.; Zone: coastal]

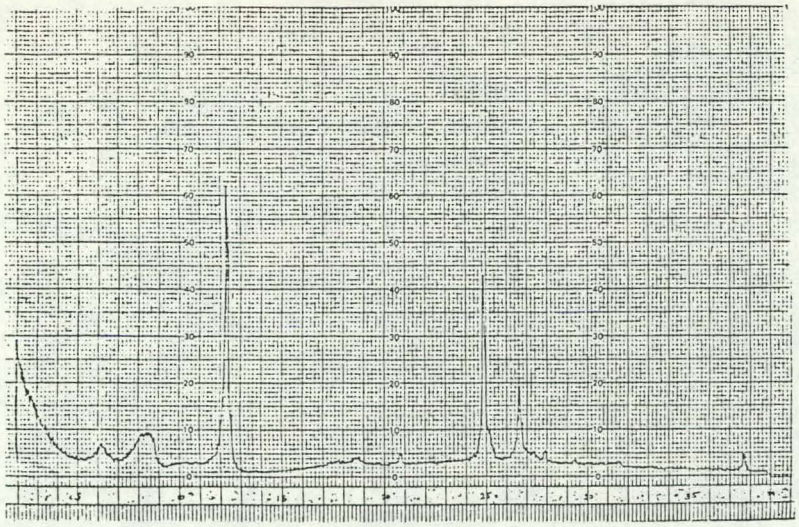

AIR DRIED

Clays Present (Ratios):

Illite	1
Mixed-Layer Clay	1
Kaolinite	8
Chlorite	Trace

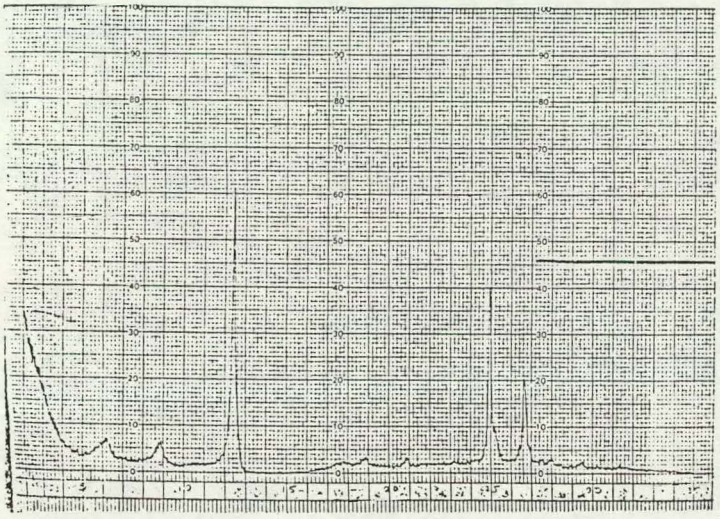

ETHYLENE GLYCOL TREATED

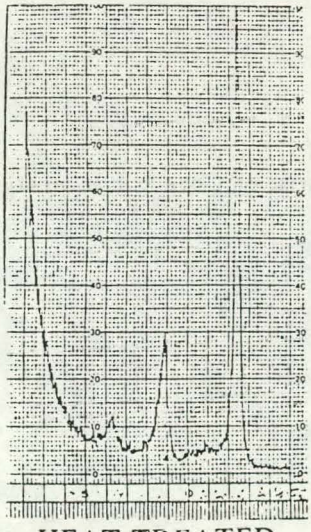

HEAT TREATED

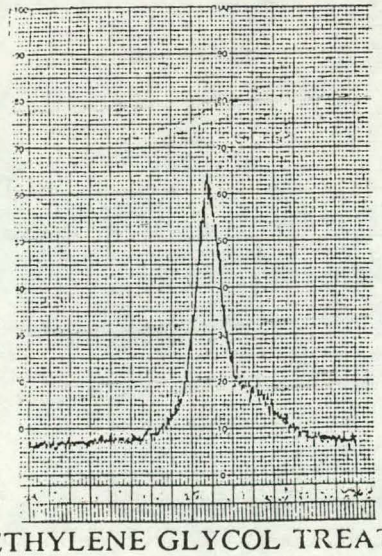

ETHYLENE GLYCOL TREATED

BET Surface Area of Core = 1.25 m^2/g

Figure A34. Properties related to microporosity - MWX1 3-11.
[Depth: 4319.4-4320.4 ft.; Zone: paralic]

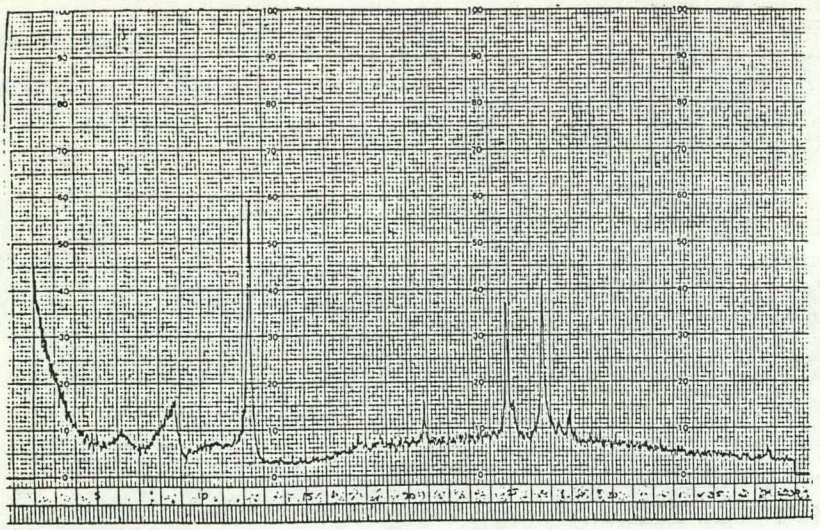

AIR DRIED

Clays Present (Ratios):

Illite	1
Mixed-Layer Clay	1
Kaolinite	7
Chlorite	Trace

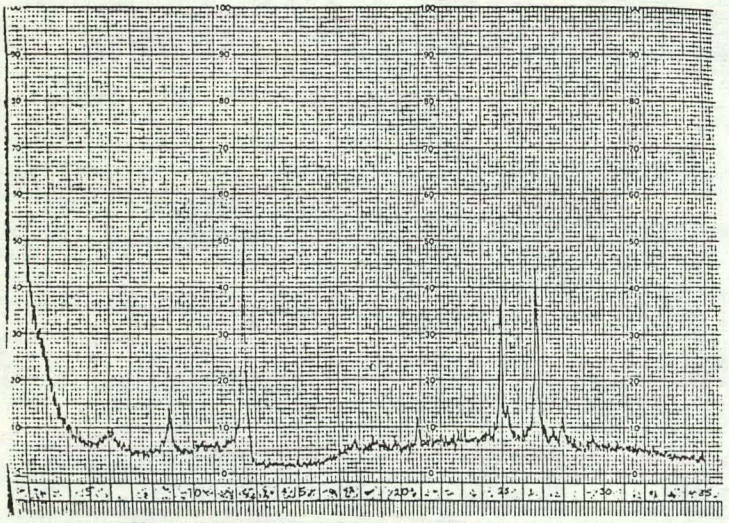

ETHYLENE GLYCOL TREATED

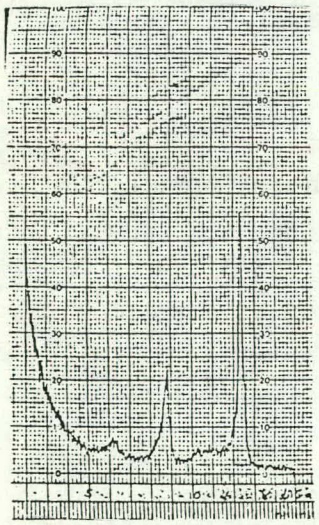

HEAT TREATED

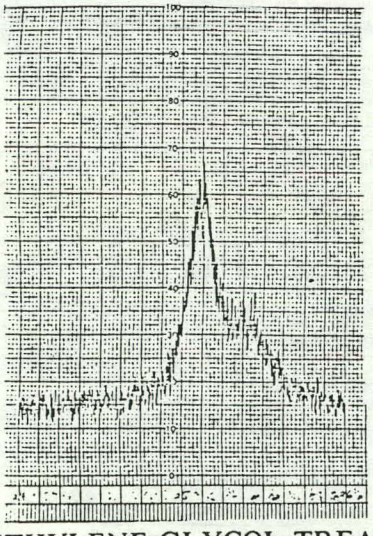

ETHYLENE GLYCOL TREATED

BET Surface Area of Core = 1.36 m^2/g

Figure A35. Properties related to microporosity - MWX1 3-21.
[Depth: 4308.3-4309.1 ft.; Zone: paralic]

☆U.S. GOVERNMENT PRINTING OFFICE: 1988-548-122/60039